NOAA Technical Memorandum

January 2004 version 1.4 – see corrections in appendix G.

Polar Orbiting Environmental Satellite Space Environment Monitor - 2: Instrument Descriptions and Archive Data Documentation

D.S. Evans
M.S. Greer

Space Environment Center
Boulder, Colorado
December, 2000

CONTENTS

Glossary of Acronyms and Terms

Archive record	A single record written to the archive CD-ROM. An archive record comprises a full 32-seconds of SEM data and corresponds to data obtained from a TIP major frame.
DPU	Data Processing Unit, a component of the SEM.
eV	electron Volt, a unit of charged particle energy.
MEPED	Medium Energy Proton and Electron Detector, a component of the SEM.
MeV	One-million electron-Volts
NESDIS	National Environmental Satellite, Data, and Information Service
NOAA	National Oceanic and Atmospheric Administration
NPOESS	National Polar-orbiting Operational Environmental Satellite System
Pitch Angle	The angle between a particle's velocity vector and the local magnetic field direction.
POES	Polar Orbiting Environmental Satellite
SEM	Space Environment Monitor
TED	Total Energy Detector, a component of the SEM
TIP	TIROS Information Processor, the POES data handling system.
TIP major frame	320 TIP minor frames comprising 32-seconds of data.
TIP minor frame	104, 8-bit data words transmitted from the POES satellite in 0.1-second. The SEM is assigned two of those data words.
TIROS	Television and InfraRed Observation Satellite

Polar Orbiting Environmental Satellite
Space Environment Monitor - 2
Instrument Descriptions and Archive Data Documentation

D.S. Evans and M.S. Greer

Abstract

Beginning with NOAA-15, an upgraded Space Environment Monitor (SEM-2) is included in the POES satellite instrument complement. This document contains the technical descriptions of the improved Total Energy Detector and upgraded Medium Energy Proton and Electron Detector. A thorough description of the content of the archive data tape and all the information required to convert the archived data to usable information is given. The description of the archive file format provides the information needed to read and unpack the data from the file. Appendices provide examples of 'C' and FORTRAN programs that read the archive file and technical information regarding the instruments and conversion of raw data to physical units.

1 Introduction

The National Oceanic and Atmospheric Administration Polar Orbiting Environmental Satellites (POES) (formerly known as TIROS for Television and InfraRed Observation Satellite) carry a suite of instruments that detect and monitor the influx of energetic ions and electrons into the atmosphere and the particle radiation environment at the altitude of the satellite. Both phenomena vary as a result of solar and geomagnetic activity. Beginning with the NOAA-15 satellite, an upgraded version of the Space Environment Monitor (SEM-2) is being flown. A number of SEM-2 instruments have been procured and it is anticipated that the SEM-2 instruments will be included on the NOAA/POES satellites until superceded by the NPOESS satellite program sometime after 2010.

Because the SEM-2 instruments differ significantly from the earlier SEM-1, there has been a complete revision to the data processing and archiving process. A number of improvements have also been included. Among these are incorporating up-to-date satellite orbit information and magnetic field models in the calculation of various magnetic coordinates, improved data quality control, and modern data storage media.

The archive data are written to CD-ROM, each disk containing 2-months of data. Copies may be obtained from:

National Oceanic and Atmospheric Administration
National Environmental Satellite, Data, and Information Service
National Geophysical Data Center E/GC2
325 Broadway
Boulder Colorado 80303, USA
Attn: Mr. Daniel Wilkinson
or: daniel.c.wilkinson@noaa.gov

This technical memorandum is designed to assist the user in reading the SEM-2 data archive files and in interpreting the information contained in the SEM-2 data. The memorandum includes a description of the instruments and their operation, information needed to convert telemetered sensor responses to physical parameters, specifications of all data channels, and a description of added information, such as orbital parameters.

2 Total Energy Detector (TED) SEM-2 Instrument Description and Operation

2.1 Instrument Description

The Total Energy Detector is designed to measure the energy flux carried by auroral particles, both positively charged ions (assumed here to be protons) and electrons, into the polar atmosphere. The magnitude and spatial extent of this energy flux are good measures of both the level of auroral activity and the atmospheric response to that energy input.

The TED in SEM-2 contains eight individual cylindrical curved-plate, electrostatic-analyzer, Channeltron charged-particle detector systems. The eight detector systems are divided into two sets of four systems, each set viewing charged particles coming from different directions so that measurements of directional energy fluxes carried by auroral particles are made at two different angles to the geomagnetic field. One set of four is mounted on the three-axis stabilized spacecraft so that the center of each detector field of view is outward along the local zenith, parallel to the Earth-center-to-satellite radial vector, which is the –X direction in spacecraft coordinates (see Figure 2.1.1). This detector set is referred to as the 0º detectors. The second set of four detectors are mounted so that each detector field of view is centered at 30° to the Earth-center-to-satellite radial vector, toward the –Z direction in spacecraft coordinates. In this document, data from the detector set that views radially outwards (0º) have names with the suffix “0” while data from the set viewing at 30° to the local zenith have names with the suffix “30”.

Of the four detector systems in each set, two are devoted to measuring protons. The electrostatic analyzer voltage in one detector system is swept to measure protons over the energy range 50 eV to 1000 eV while the analyzer voltage in the second is swept to measure protons over the energy range 1000 eV to 20,000 eV. The remaining two detector systems are devoted to measuring electrons, with one covering the energy range 50 eV to 1000 eV and the second 1000 eV to 20,000 eV.

The field of view of the electron and proton 1000-20,000 eV detector systems are 1.5° by 9°, half angles. The field of view of the 50 - 1000 eV electron detector system is 6.7° by 3.3°, half angles. The field of view of the 50 - 1000 eV proton detector system is 6.6° by 8.7°, half angles.

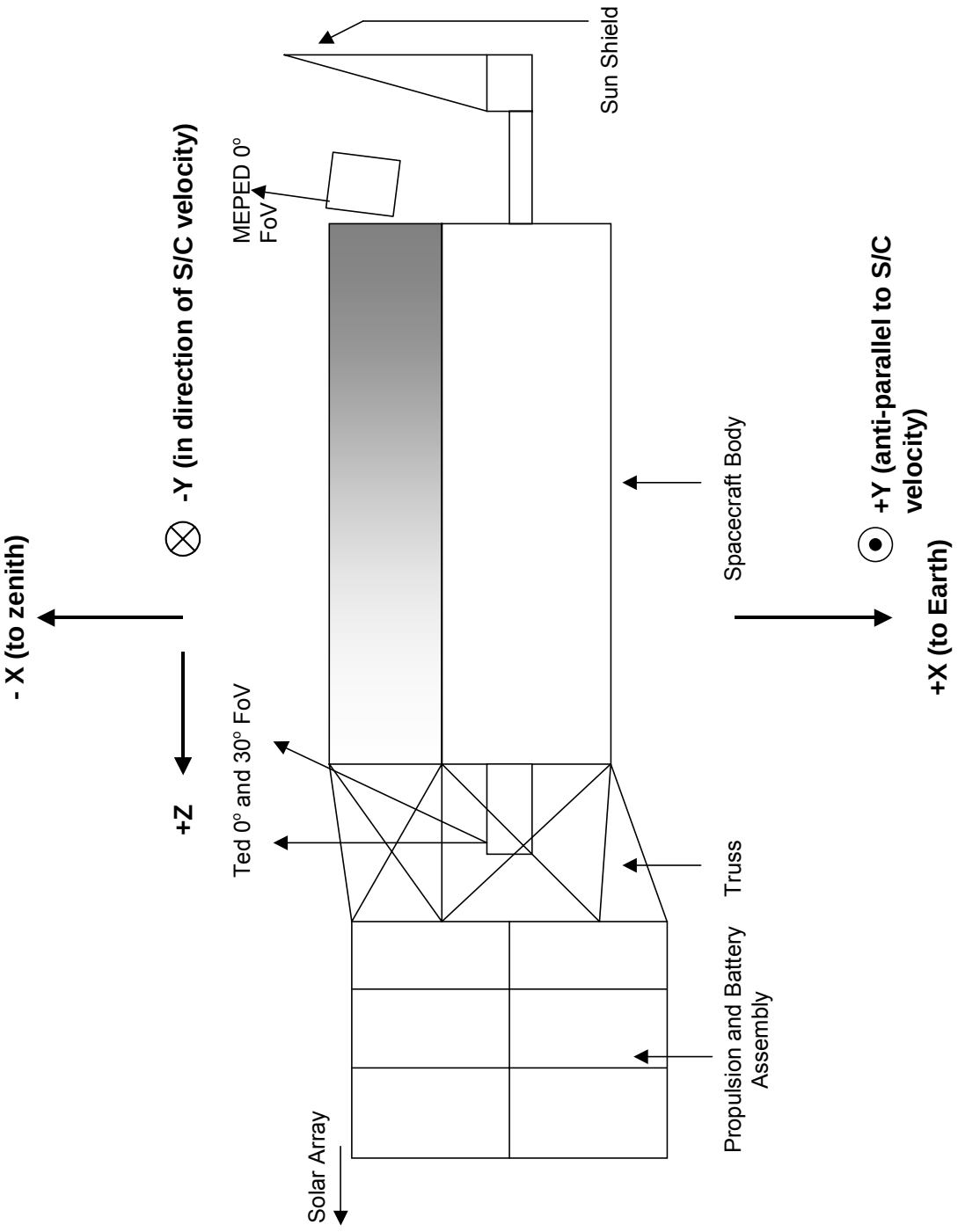
Sun Shield
MEPED 0°
FoV
-Y (in direction of S/C velocity)
- X (to zenith)
+Z
Ted 0° and 30° FoV
Spacecraft Body
+Y (anti-parallel to S/C
velocity)
+X (to Earth)
Truss
Propulsion and Battery
Assembly
Solar Array

Figure 2.1.1

The analyzer energy sweep for all eight detectors is divided into eight contiguous energy bands. The edge and center energies of each band are listed in Table 2.1.1. Energy bands 1 through 8 are for the low energy detector systems that sweep from 50 eV to 1000 eV while 9 through 16 are for the high-energy detector systems that sweep from 1000 eV to 20,000 eV.

Table 2.1.1
TED Energy Bands

Energy Band	Low-Energy Edge (eV)	Center Energy (eV)	High-Energy Edge (eV)	Total Energy Band Width (eV)
1	50	61	73	23
2	73	89	106	33
3	106	130	154	48
4	154	189	224	70
5	224	274	325	101
6	325	399	473	148
7	473	580	688	215
8	688	844	1000	312
9	1000	1227	1454	454
10	1454	1784	2115	661
11	2115	2595	3075	961
12	3075	3774	4472	1397
13	4472	5488	6503	2031
14	6503	7980	9457	2954
15	9457	11605	13753	4296
16	13753	16877	20000	6247

Within each energy band the energy sweep is stepped upward in time through eight equally spaced energy levels, but because the width of each energy band increases in a logarithmic manner the step size increases with increasing energy band.

The full energy sweep cycle time for each detector system is 2.0 seconds. The analyzer sweep over a single energy band takes 0.2 seconds so the sampling over the eight bands making up the full energy range requires 1.6 seconds. The reset of the analyzer plate voltage requires 0.2 seconds. During the remaining 0.2 seconds of an instrument cycle the analyzer plate voltages are set to electrical ground, while counts from each Channeltron particle sensor are accumulated to provide a measure of the background response of each detector system. The energy sweep, reset, and background accumulation are done simultaneously for all eight detector systems.

The on-board Data Processing Unit (DPU) compresses all TED sensor "count" data to fit the 0 to 255 dynamic range of the digital word transmitted from the NOAA/POES satellite. The software that reads the archive data record decompresses the data word according to the table in Appendix B before passing the data to a user. A unique negative value for a data word indicates the data word had been lost in the processing and a data "pad" had been inserted.

2.2 Determination of Particle Directional Energy Flux Moments

The on-board DPU accumulates the Channeltron particle detector responses (counts) from each detector system during each 0.2-second energy sweep through an energy band. At the completion of a full energy sweep, an on-board microprocessor manipulates these data to obtain the integrated auroral particle directional energy flux moment from each of the eight detector systems. (The integrated directional energy flux moment is defined as the energy flux carried by particles having energies within a defined range, originating from a differential solid angle and passing through a differential area that is oriented normal to the particle velocity vector).

The on-board data processing takes into account both the increasing energy of the particles being measured during the course of a full energy sweep, and (to first order) the dependence of the Channeltron counting efficiency upon particle energy and species. This is done by applying multiplicative weighting factors to the counts accumulated within each energy band.

Table 2.2.1 lists the weighting factors used for the TED instrument on-board NOAA-15, that is, TED instrument Serial Number 011. Similar information for the other TED instruments is included in Appendix C. The "Particle Energy" weighting factors are determined from laboratory calibrations of each instrument and represent a combination of the weight given to the particle energy and to the varying Channeltron detection efficiency. The "Detection Efficiency" weighting factors are a second order correction for any remaining difference in detector counting efficiency between the four lowest energy bands and the four highest. The "Detection Efficiency" weight factor is only applied, if at all, to the counts accumulated in the four highest energy bands in each detector system.

The microprocessor in the DPU constructs the integrated particle energy flux moment for each detector system by multiplying the sensor counts accumulated within each energy band by both of the appropriate weighting factors and then summing the eight resulting values together. The data from the 0º detector systems are in archive array *ted0* and the data from the 30º detector systems are in archive array *ted30* (see Section 4.4.1).

Table 2.2.1
TED Weighting Factors
TED Serial Number 011

0º electron low-energy band number	Particle energy weight	Detector efficiency weight	30º electron low-energy band number	Particle energy weight	Detector efficiency weight
1	1.0	1.0	1	1.0	1.0
2	1.5	1.0	2	1.5	1.0
3	2.0	1.0	3	2.0	1.0
4	3.0	1.0	4	3.0	1.0
5	4.0	1.0	5	4.0	1.0
6	6.0	1.0	6	6.0	1.0
7	8.0	1.0	7	8.0	1.0
8	12.0	1.0	8	12.0	1.0
0º electron high-energy band number	**Particle energy weight**	**Detector efficiency weight**	**30º electron high-energy band number**	**Particle energy weight**	**Detector efficiency weight**
9	1.0	1.0	9	1.0	1.0
10	1.5	1.0	10	1.5	1.0
11	3.0	1.0	11	3.0	1.0
12	4.0	1.0	12	4.0	1.0
13	8.0	0.667	13	8.0	0.667
14	16.0	0.667	14	16.0	0.667
15	24.0	0.667	15	24.0	0.667
16	48.0	0.667	16	48.0	0.667
0º proton low-energy band number	**Particle energy weight**	**Detector efficiency weight**	**30º proton low-energy band number**	**Particle energy weight**	**Detector efficiency weight**
1	1.0	1.0	1	1.0	1.0
2	1.5	1.0	2	1.5	1.0
3	2.0	1.0	3	2.0	1.0
4	2.0	1.0	4	2.0	1.0
5	3.0	1.0	5	3.0	1.5
6	4.0	1.0	6	4.0	1.5
7	6.0	1.0	7	6.0	1.5
8	8.0	1.0	8	8.0	1.5
0º proton high-energy band number	**Particle energy weight**	**Detector efficiency weight**	**30º proton high-energy band number**	**Particle energy weight**	**Detector efficiency weight**
9	3.0	1.0	9	3.0	1.0
10	4.0	1.0	10	4.0	1.0
11	4.0	1.0	11	4.0	1.0
12	6.0	1.0	12	6.0	1.0
13	8.0	1.0	13	8.0	1.0
14	12.0	1.0	14	12.0	1.0
15	12.0	1.0	15	12.0	1.0
16	16.0	1.0	16	16.0	1.0

The factors that convert the telemetered integrated energy flux moment data (after decompression using the table in Appendix B) to physical units have been determined using a combination of laboratory calibration and computer simulation of the sensor responses to model particle energy spectra. The factors that convert from decompressed data values to integrated energy flux values in units of mW m^{-2} $ster^{-1}$ for the TED instrument on NOAA-15, as integrated over the appropriate energy range, are given in Table 2.2.2. This information is listed in Appendix C for other TED instruments.

Table 2.2.2
Conversion to Integrated Directional Energy Flux Moment
TED Serial Number 011

Sensor	Energy range eV	To convert decompressed counts to mW m-2 ster-1 multiply by
0º low-energy electron	50 - 1000	1.746 x 10-6
30º low-energy electron	50 - 1000	2.322 x 10-6
0º high-energy electron	1000 - 20000	5.328 x 10-5
30º high-energy electron	1000 - 20000	5.782 x 10-5
0º low-energy proton	50 - 1000	1.030 x 10-6
30º low-energy proton	50 - 1000	8.628 x 10-7
0º high-energy proton	1000 - 20000	3.652 x 10-5
30º high-energy proton	1000 - 20000	2.602 x 10-5

It should be noted that the archive data record does not include the physical values for the directional energy flux moments, but only the compressed sensor response value as computed by the DPU and telemetered from the spacecraft. The decompressed data values are multiplied by the appropriate factors in Table 2.2.2 to obtain directional energy flux moments in physical units.

2.3 Determination of Particle Omni-directional Energy Fluxes

The principle objective of the TED instrument is to monitor the auroral particle energy deposition into the atmosphere. This physical parameter is computed from the directional energy flux observations using the procedure set down in Raben, et al. (1995) and is briefly described here.

Auroral particles measured by the TED detector systems can reach the atmosphere at 120 km altitude only if their pitch angle, □sat, at the satellite location satisfies the relation

Equation 2.3.1 $$sin^2(\alpha_{sat}) \leq \sqrt{(B_{sat}/B_{120})} = sin^2(\alpha_{mir})$$

B_{sat} is the scalar magnetic field at the satellite and B_{120} is the scalar magnetic field strength at 120 km altitude along the magnetic field line of force joining the satellite to the location where the particles would enter the atmosphere. Particles with pitch angles not satisfying this relationship will magnetically mirror and return upward along the magnetic field line before reaching the atmosphere. The particle pitch angle is, by convention, the angle between the velocity vector of a particle and the local magnetic field direction. For the TED instrument viewing directions, the corresponding particle pitch angles at the satellite will generally be $\leq 90^{o}$ in the Northern Hemisphere, and $\geq 90^{o}$ in the Southern). The parameters B_{sat} and B_{120}, together with the pitch angles of the particles being measured at the satellite by the two sets of TED detectors, are calculated using a magnetic field model. The calculation is carried out every 8 seconds along the satellite orbit and the results are included in the archive data record array *head* (see Section 4.2.2). Also included in the *head* array are the particle pitch angles transformed from their values at the satellite to 120 km altitude using the relation:

Equation 2.3.2 $$sin^2(\alpha_{120}) = sin^2(\alpha_{sat})\sqrt{(B_{120}/B_{sat})}$$

If $sin(\alpha_{120}) > 1.0$, the particles measured at the satellite do not reach the atmosphere.

The calculation of omni-directional energy flux involves evaluating the following integral.

Equation 2.3.3 $$E_F = 2\pi\int E_D(\alpha) sin\alpha cos\alpha d\alpha$$

$E_D(\alpha)$ is the pitch angle dependent integrated directional energy flux moment defined above, and α is the particle's pitch angle. If α is the pitch angle transformed to 120 km altitude using equation 2.3.2, then the integration limits for α are 0º to 90º in the Northern Hemisphere or 180º to 90º in the Southern. E_F is the energy flux through a unit area normal to the magnetic field vector carried by downward moving particles within the energy range of E_D.

Using the integrated directional energy flux moments as determined from Table 2.2.2, the omni-directional energy flux moments for electrons of energies between 50 eV and 1000 eV and between 1000 eV and 20,000 eV, and for protons of energies between 50 eV and 1000 eV and between 1000 eV and 20,000 eV can be calculated. These four calculated values constitute the first four of the seven elements in the archive record array *tedfx*.

There are three cases that must be considered in the calculation of these four omni-directional energy flux moments.

Case 1. Both sets of TED detectors view particles that reach the atmosphere. This is the case for all observations made at geographic latitudes poleward of about 30º in both the Northern and Southern Hemispheres.

The particle pitch angle that is midway between those viewed by the two sets of TED detector systems is calculated ($\alpha_{mid} = (\alpha_1+\alpha_2)/2.0$), and then the set of TED detectors that view particles with pitch angles closest to 0º (180º in the Southern Hemisphere) is identified. (There are geographic locations in the Southern Hemisphere where the detector set that is viewing 30º from the zenith is actually sensing incident particles with pitch angles closer to 180º than the set viewing the zenith). Using the superscript "1" to denote the directional energy flux moment obtained from the detector viewing closest to 0º which is assumed to be representive of the directional energy flux moments at angles between 0º and the angle given by α_{mid}, and the superscript "2" to denote the directional energy flux moment obtained from the other detector set, which is representitive for all angles between α_{mid} and 90º, Equation 2.3.3 reduces to

Equation 2.3.4 $$E_F = \pi ({}^1E_D \, sin^2(\alpha_{mid}) + {}^2E_D \, (1.–sin^2(\alpha_{mid})))$$

The calculation of E_F is executed four times, using values of ${}^1E_D$ and ${}^2E_D$ from the sensor pairs listed in Table 2.2.2, to yield integrated omni-directional energy flux moments for electrons between 50 and 1000 eV and between 1000 and 20,000 eV, and for protons between 50 and 1000 eV and between 1000 and 20,000 eV.

Case 2. Only one set of the TED detectors view particles that reach the atmosphere. This is the case for many observations made at latitudes equatorward of 30º but poleward of the equatorial regions.

Whenever one set of TED detectors is viewing particles that will magnetically mirror before reaching the atmosphere, the integrated directional energy flux moment measurements provided by the other detector are assumed to be representitive of energy fluxes at all pitch angles. In this case Equation 2.3.3 reduces to

Equation 2.3.5 $$E_F = \pi E_D$$

where E_D is provided by the detectors viewing particles that reach the atmosphere. The meaning of all elements in *tedfx* is described above.

Case 3. Neither set of TED detector systems views particles that reach the atmosphere. This is often the case for observations made in the equatorial regions. In this case the energy flux moments are set to a "pad" value.

It should be noted that the integrated omni-directional energy flux moments computed in this fashion are energy fluxes through unit areas at the top of the atmosphere that are oriented normal to the magnetic field vector. If the magnetic field vector is not perpendicular to the top of the atmosphere, these energy flux moments should be corrected by multiplying by $cos\beta$, where β is the inclination of the magnetic field to the vertical. This correction has not been made in the calculation of intergrated omni-directional energy fluxes. The angle β can be calculated from the three components of the magnetic field vector at 120 km altitude that are included in the array *head* (Section 4.2.2) and the correction made if required.

2.4 Identification of Particle "Characteristic" Energy

There is a requirement that the instrument identify for each particle species, detector system viewing direction, and energy sweep the particular energy band in the full energy range 50 to 20,000 eV that contained the maximum directional energy flux. The DPU performs this function at the completion of each energy sweep by comparing the sensor responses accumulated in each energy band and selecting the energy band with the maximum response. The comparison takes into account the particle energy and energy bandwidth associated with each band, the Channeltron detection efficiency, and additional weighting to account for differences between the 50-1000 eV and 1000-20,000 eV detector systems. The identification is made for both electrons and protons, at both the zenith and 30º viewing angles for each 2-second instrument cycle. The four identifications of the energy band containing the maximum directional energy flux and the actual sensor responses within those energy bands (see Section 2.5) are transmitted for every 2-second instrument cycle.

Simulations were of the detector system responses to Maxwellian particle energy distributions were conducted. These simulations verified that the energy band identified by the DPU as the one with the maximum energy flux was most often the energy band that actually contained the maximum in the differential energy flux, an energy twice the temperature of a Maxwellian distribution, and was never more than one energy band different from the correct one.

2.5 Particle Intensities Within Specific Energy Bands

In addition to the sensor responses within the "characteristic" energy bands that are available for every instrument cycle, actual sensor responses in four of the sixteen specific energy bands for each detector system are telemetered on a sub-commutated, low duty cycle basis. These energy bands are numbers 4 and 8 from the 50 - 1000 eV lower energy detector systems and bands 11 and 14 from the 1000 - 20,000 eV higher energy systems.

Keeping in mind that the archive record contains 32 seconds of data (16 energy sweep cycles of the TED detector systems), the sequence of data readouts is listed in Table 2.5.1.

Table 2.5.1
Sequence of the Readout of TED Sensor Responses in Specific Energy Bands

Energy Sweep Cycle	TED Sensors	Energy Bands Read Out
1, 5, 9, and 13	0º electron sensors	4, 8, 11, and 14
2, 6, 10, and 14	30º electron sensors	4, 8, 11, and 14
3, 7, and 11	0º proton sensors	4, 8, 11, and 14
4, 8, and 12	30º proton sensors	4, 8, 11, and 14

Proton sensor energy band response data from sweep cycles 15 and 16 are missing because accumulated background responses from the eight individual detector systems are telemetered instead.

These telemetered and decompressed sensor responses may be converted to physical units: either the particle directional energy flux contained in that energy band (in units of mW m^{-2} $ster^{-1}$) using the multiplicative factors in Table 2.5.2, or differential-directional particle number flux (in units of particles m^{-2} sec^{-1} $ster^{-1}$ eV^{-1}) using the multiplicative factors in Table 2.5.3.

Table 2.5.2
Multiplicative Factors to Convert Actual Counts Within an Energy Band to Directional Energy Flux Contained Within that Energy Band

TED S/N 011 Electron Detector System

Energy band	Band center energy (eV)	0º electron sensor to convert counts to mW m^{-2} $ster^{-1}$	30º electron sensor to convert counts to mW m^{-2} $ster^{-1}$
1	61	1.363×10^{-6}	1.821×10^{-6}
2	89	2.126×10^{-6}	2.824×10^{-6}
3	130	3.147×10^{-6}	4.151×10^{-6}
4	189	4.633×10^{-6}	6.179×10^{-6}
5	274	6.834×10^{-6}	9.105×10^{-6}
6	399	9.901×10^{-6}	1.313×10^{-5}
7	580	1.451×10^{-5}	1.931×10^{-5}
8	844	2.113×10^{-5}	2.809×10^{-5}
9	1227	4.948×10^{-5}	5.296×10^{-5}
10	1784	8.045×10^{-5}	8.668×10^{-5}
11	2595	1.310×10^{-4}	1.414×10^{-4}
12	3774	2.126×10^{-4}	2.298×10^{-4}
13	5488	3.438×10^{-4}	3.722×10^{-4}
14	7980	5.527×10^{-4}	5.998×10^{-4}
15	11605	8.793×10^{-4}	9.562×10^{-4}
16	16877	1.378×10^{-3}	1.502×10^{-3}

TED S/N 011 Proton Detector System

Energy band	Band center energy (eV)	0º proton sensor to convert counts to mW m^{-2} $ster^{-1}$	30º proton sensor to convert counts to mW m^{-2} $ster^{-1}$
1	61	7.511×10^{-7}	8.123×10^{-7}
2	89	1.160×10^{-6}	1.233×10^{-6}
3	130	1.614×10^{-6}	1.769×10^{-6}
4	189	2.265×10^{-6}	2.554×10^{-6}
5	274	3.141×10^{-6}	3.674×10^{-6}
6	399	4.325×10^{-6}	5.185×10^{-6}
7	580	6.004×10^{-6}	7.420×10^{-6}
8	844	8.304×10^{-6}	1.055×10^{-5}
9	1227	9.307×10^{-5}	7.056×10^{-5}
10	1784	1.231×10^{-4}	9.196×10^{-5}
11	2595	1.623×10^{-4}	1.199×10^{-4}
12	3774	2.131×10^{-4}	1.554×10^{-4}
13	5488	2.800×10^{-4}	2.012×10^{-4}
14	7980	3.664×10^{-4}	2.590×10^{-4}
15	11605	4.772×10^{-4}	3.298×10^{-4}
16	16877	6.149×10^{-4}	4.135×10^{-4}

Table 2.5.3
Multiplicative Factors to Convert From Actual Counts Within an Energy Band to Directional Number Flux at the Center Energy of that Band

TED S/N 011 Electron Detector System

Energy band	Band center energy (eV)	0º electron sensor convert counts to particles m^{-2} sec^{-1} eV^{-1} $ster^{-1}$	30º electron sensor convert counts to particles m^{-2} sec^{-1} eV^{-1} $ster^{-1}$
1	61	6.015×10^{6}	8.036×10^{6}
2	89	4.398×10^{6}	5.842×10^{6}
3	130	3.108×10^{6}	4.101×10^{6}
4	189	2.167×10^{6}	2.890×10^{6}
5	274	1.511×10^{6}	2.012×10^{6}
6	399	1.050×10^{6}	1.393×10^{6}
7	580	7.260×10^{5}	9.665×10^{5}
8	844	5.013×10^{5}	6.665×10^{5}
9	1227	5.543×10^{5}	5.932×10^{5}
10	1784	4.277×10^{5}	4.608×10^{5}
11	2595	3.305×10^{5}	3.565×10^{5}
12	3774	2.551×10^{5}	2.758×10^{5}
13	5488	1.971×10^{5}	2.134×10^{5}
14	7980	1.521×10^{5}	1.650×10^{5}
15	11605	1.171×10^{5}	1.272×10^{5}
16	16877	8.968×10^{4}	9.764×10^{4}

TED S/N 011 Proton Detector System

Energy band	Band center energy (eV)	0º proton sensor convert counts to particles m^{-2} sec^{-1} eV^{-1} $ster^{-1}$	30º proton sensor convert counts to particles m^{-2} sec^{-1} eV^{-1} $ster^{-1}$
1	61	3.314×10^{6}	3.583×10^{6}
2	89	2.400×10^{6}	2.552×10^{6}
3	130	1.595×10^{6}	1.748×10^{6}
4	189	1.060×10^{6}	1.195×10^{6}
5	274	6.948×10^{5}	8.124×10^{5}
6	399	4.590×10^{5}	5.502×10^{5}
7	580	3.006×10^{5}	3.714×10^{5}
8	844	1.971×10^{5}	2.504×10^{5}
9	1227	1.043×10^{6}	7.910×10^{5}
10	1784	6.532×10^{5}	4.879×10^{5}
11	2595	4.064×10^{5}	3.006×10^{5}
12	3774	2.524×10^{5}	1.844×10^{5}
13	5488	1.571×10^{5}	1.134×10^{5}
14	7980	9.763×10^{4}	6.976×10^{4}
15	11605	6.062×10^{4}	4.282×10^{4}
16	16877	3.748×10^{4}	2.619×10^{4}

2.6 TED Sensor Background Responses

The final 0.2 seconds of each TED instrument cycle is devoted to obtaining the Channeltron sensor background measurement. Counts from each Channeltron are accumulated during this 0.2 seconds for 16 consecutive instrument cycles for a total integration time of 3.2 seconds. The background data from each of the eight Channeltron particle detectors is telemetered once every 32 seconds, instead of the proton energy bands 4, 8, 11, and 14 responses, during energy sweeps 15 and 16 (see Section 2.5).

2.7 TED Correction for High Background

There are portions of the POES orbit where a significant contribution to the TED sensor responses is from very energetic particles that penetrate the instrument shielding and reach the Channeltron particle detectors. Such intervals are identified by unusually high count rates in the sensor background channels. When the background rates are elevated, the TED sensor responses are corrected for the penetrating radiation, and the energy flux moments calculated using the corrected responses. While the calculated energy flux moments in the archive data file are corrected values, the sensor responses stored in the archive data record are the uncorrected data as telemetered from the satellite. Whenever a correction for high background has been made to the energy flux moment, a flag is set in the array *qual*.

2.8 TED Data Quality Control

The TED sensor data are subjected to two tests for internal consistency. The first is a comparison of the sensor responses in energy bands 3, 7, 10, and 13, whenever available from a given detector system, with that system's sensor response in the energy band identified as containing the maximum in the particle directional energy flux. A sensor response in any of those four energy bands that convert to a directional energy flux greater than the identified maximum is an indication of questionable data. A flag is set in the array *qual* to indicate that fact (Section 4.5.1).

The second test is a comparison of the directional energy flux contained in the energy band identified as being the maximum, to the total directional energy flux integrated over the full energy range of that sensor. If the directional energy flux within that single energy band exceeds the directional energy flux integrated over the full range, there is likely an error in data transmission and a flag is set in the array *qual* (Section 4.5.1).

2.9 Timing of TED Data Acquisition Relative to Time Tag

The time tag provided in the archive record is the time tag assigned at the beginning of a 2-second interval, when data that are transferred from the SEM-2 DPU to the POES data handling system are introduced into the POES data format. That time is not the time the actual measurement was made by the SEM-2. The archive record provides data time tags every 8 seconds (every fourth 2-second cycle of the TED instrument) and that time refers to the first of the four cycles. It is implicit that the times associated with the second, third, and fourth cycles are incremented by 2-seconds each.

The timing of the actual data acquisition in the TED instrument relative to time T, the time tag given the individual data point in the archive record, are given in Table 2.9.1

Table 2.9.1
Timing of TED Functions Relative to Data Time Tag

TED function	Time interval relative to T
Full energy sweep	– 1.2 s to + 0.4 s
Accumulation in energy bands 1 and 9	– 1.2 s to + 1.0 s
Accumulation in energy bands 2 and 10	– 1.0 s to – 0.8 s
Accumulation in energy bands 3 and 11	– 0.8 s to – 0.6 s
Accumulation in energy bands 4 and 12	– 0.6 s to – 0.4 s
Accumulation in energy bands 5 and 13	– 0.4 s to – 0.2 s
Accumulation in energy bands 6 and 14	– 0.2 s to 0.0 s
Accumulation in energy bands 7 and 15	0.0 s to + 0.2 s
Accumulation in energy bands 8 and 16	+ 0.2 s to + 0.4 s
Plate voltage reset	+ 0.4 s to + 0.6 s
Accumulation of background data	+ 0.6 s to + 0.8 s

Background data are telemetered once every 32 seconds and represent responses accumulated during the background dwell period for 16 consecutive 2-second instrument cycles. Given a time T, referring to the time tag at the start of a 32 second archive record, the first of the 16 accumulation periods is between T – 5.4 and T – 5.2 seconds while the last accumulation period is between T + 26.6 and T + 26.8 seconds.

2.10 TED In-Flight Calibration

The TED instrument performance is periodically checked by means of an in-flight calibration (IFC) procedure; this procedure has two phases. The first involves feeding all eight Channeltron pulse amplifier and pulse height discriminator chains with pulses of varying amplitude from an on-board pulse generator. This is done while cycling the pulse height discriminator thresholds through four levels and verifying that those thresholds trip at the appropriate input pulse amplitudes. This phase of the IFC lasts 32-seconds and a flag is set in the SEM-2 status data to indicate that an IFC is in progress.

The second phase of the IFC involves continuous cycling of all pulse height discriminator thresholds through the four levels, while the TED continues normal operation without any artificial pulse stimulus. This phase continues for approximately one orbit of the satellite or about 100 minutes. The purpose of this phase of the IFC is to determine whether the cycling of the threshold levels has a significant effect on the overall sensor responses during times when auroral particle fluxes are significant. If there is a significant reduction in sensor responses as the pulse height discriminator thresholds increase, it indicates degradation in the Channeltron particle sensors. Increasing the Channeltron operating voltage by ground command compensates the gain degradation. The TED IFC flag continues to be set until the completion of the second phase of the IFC.

Archive data taken during the first phase of the IFC must be discarded, and the data during the second phase should be treated with caution.

3 MEPED Instrument Description

3.1 Overview

In addition to the TED, the SEM-2 includes a set of solid-state energetic particle detectors that monitor the intensities of protons and electrons over a range extending from 30 keV to more than 200 MeV. Particles having those energies include the radiation belt (Van Allen belt) populations, the particles in energetic solar particle events (solar proton events), and the low energy portion of the galactic cosmic ray population. Enhanced fluxes of these particles entering the atmosphere can produce significant and widespread degradation in short-wave radio propagation; in extreme cases even radio blackouts. The energetic particles also contribute to astronaut radiation exposure, especially on high inclination orbit missions during energetic solar particle events.

In order to monitor the particle fluxes over this wide range of energy and for both protons and electrons, the MEPED includes eight separate particle detector systems. Two are proton solid-state detector telescopes that monitor the intensity of protons in six energy bands over the range 30 keV to 6,900 keV. Two are electron solid-state detector telescopes that monitor the intensity of electrons in three energy bands in the range 30 keV to 2,500 keV. The remaining four detector systems are “dome” or “omni-directional” detector systems designed to be sensitive to very energetic protons incident on a solid-state detector over a wide range of angles. Metal absorbers set the specific proton energy thresholds for the “dome” detectors over the detector.

The following sections describe each detector system in more detail.

3.2 Proton Solid State Detector Telescope

Figure 3.2.1 is a cross-section schematic of the proton solid-state detector telescope. A magnetic field of approximately 0.2 Tesla is applied across the entrance aperture and collimator structure to prevent electrons entering the aperture with energies less than about 1,000 keV from reaching the solid-state detectors. With the exception of the entrance aperture, the detectors are surrounded by a combination of aluminum and tungsten shielding to prevent electrons of energies less than 6,000 keV or protons of energies less than 90 MeV from penetrating the structure walls and reaching the detectors.

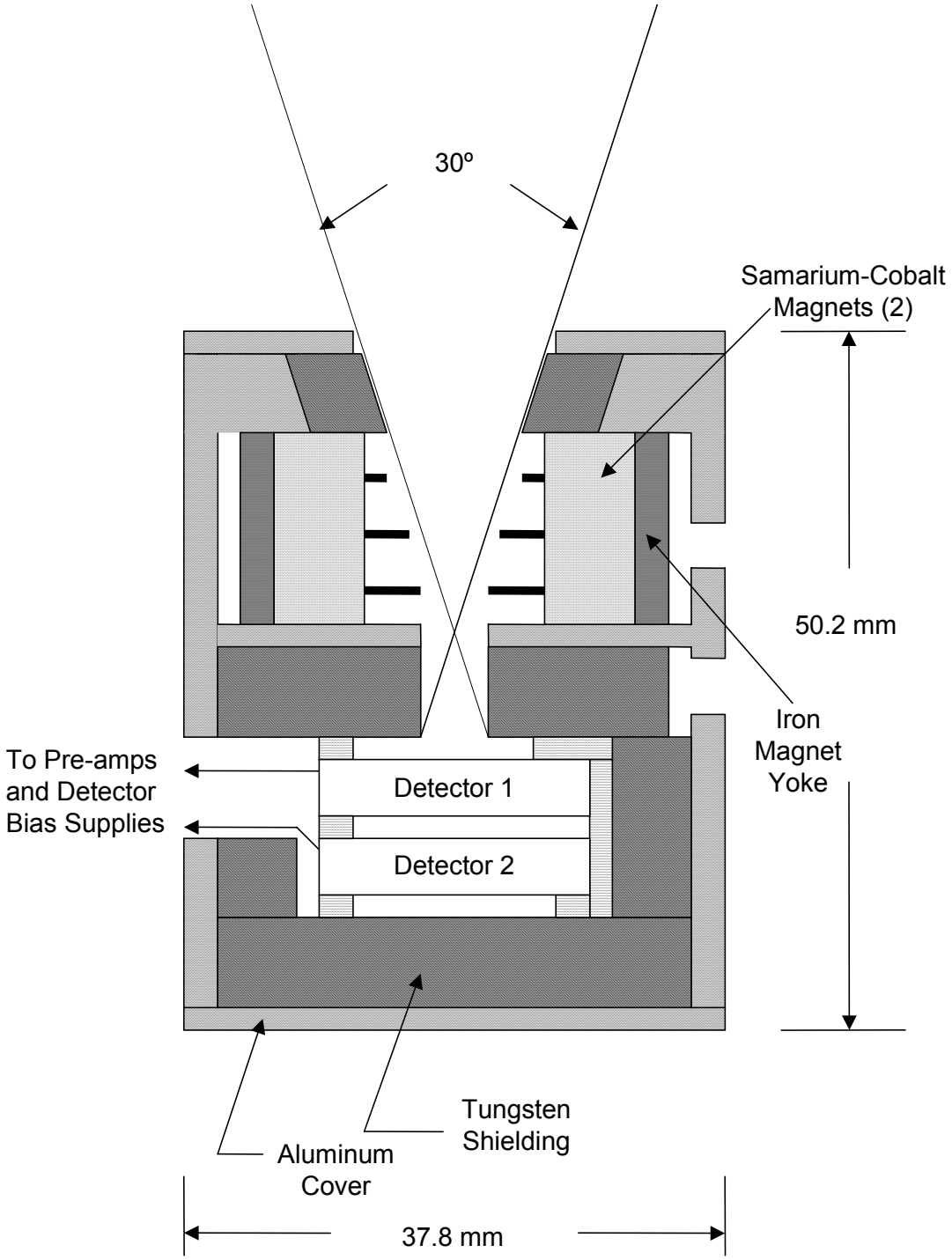
30º
Samarium-Cobalt
Magnets (2)
50.2 mm
Iron
Magnet
Yoke
To Pre-amps
and Detector
Bias Supplies
Detector 1
Detector 2
Tungsten
Shielding
Aluminum
Cover
37.8 mm

Figure 3.2.1

Both solid-state detectors are totally depleted silicon surface barrier detectors, each 200 microns thick. The front detector, D1, has a sensitive area of 25 mm^2 while the back detector, D2, has a sensitive area of 50 mm^2. The front surface of each detector is covered with an aluminum film 20 $\mu g\ cm^{-2}$ thick to reduce light sensitivity and provide an electrical contact.

Protons that enter through the collimator structure and are stopped by the first detector (no coincidence with a response in the back detector) are sorted according to their energy loss in the detector, determined by electronic pulse height analysis, into one of five proton energy ranges. A sixth proton energy band is established when a proton passes through the front detector and is stopped by the back detector, producing coincident responses in both detectors.

Two identical proton solid-state detector telescopes are included in the SEM-2. One (the 0º telescope) is oriented so that the central axis of the field of view is rotated in the XZ plane 9º from the –X direction toward the –Z direction (see Figure 1). The second (the 90º telescope) is oriented so that the center axis of the field of view is rotated 9º in the YZ plane from the +Y direction (anti-parallel to the satellite's velocity vector) also toward the –Z direction. These rotations ensure a clear field of view.

The proton energies, which take into account the energy lost in passing though the 20 $\mu g\ cm^{-2}$ aluminum layer, together with the detector pulse height logic to select those energies, are given in Table 3.2.1. The pulse height levels, L1 through L5 refer to particle energy loss thresholds in the front detector, and L6 refers to the particle energy loss threshold in the back detector.

Table 3.2.1
MEPED Proton Energy Bands and Pulse Height Logic

Channel Identification	Electron Energy Range	Pulse Height Level Logic	
0/90 P1	30 keV to 80 keV	L1 on	but not L2 or L6
0/90 P2	80 keV to 240 keV	L1 and L2 on	but not L3 or L6
0/90 P3	240 keV to 800 keV	L1 and L3 on	but not L4 or L6
0/90 P4	800 keV to 2500 keV	L1 and L4 on	but not L5 or L6
0/90 P5	2500 keV to 6900 keV	L1 and L5 on	
0/90 P6	>6900 keV	L1 and L6 on	but not L5

Data from each proton telescope are accumulated for 1.0 second but the accumulation electronics are shared between the two detectors so that a full data set from both requires 2.0 seconds to acquire.

The nominal geometric factor for the proton solid-state detector telescopes is .01 cm^2 ster. To obtain the proton directional number flux within a given proton energy channel the count rate, in counts per second, should be multiplied by 100. The resulting flux is in units of protons cm^{-2} sec^{-1} $ster^{-1}$.

Experience has shown that the front silicon solid-state detector in the proton telescope suffers radiation damage that becomes significant after two to three years of operation. The effect of the radiation damage is to reduce the fraction of free charge produced in the detector by incident particles that is collected within the 85 nsec integration time set by the charge-sensitive amplifier. This reduction, in turn, can effectively raise the energy thresholds to values well above those listed above. For this reason, some care should be used in interpreting data obtained by the proton detector telescopes after three years of operation.

3.3 Electron Solid State Detector Telescope

Figure 3.3.1 is a cross-section schematic of the electron solid-state detector telescope. With the exception of the entrance aperture, the detectors are surrounded by a combination of aluminum and tungsten shielding to prevent electrons of energies less than 6,000 keV or protons of energies less than 90 MeV from penetrating the structure walls and reaching the detector. The final aperture in the collimator structure is covered by a 76 micron thick nickel foil (678 μg cm^{-2}) to reduce light sensitivity and stop low energy protons from reaching the solid-state detector.

The solid-state detector in the electron detector telescope is a totally depleted silicon surface barrier detector, 700 microns thick with a sensitive area of 25 mm^2. The front surface of the detector is covered with an aluminum film 20 μg cm^{-2} thick to further reduce light sensitivity and provide an electrical contact.

The energy deposited in the detector by particles incident on the detector is pulse height analyzed. One discriminator amplitude level (L4) is set to an equivalent particle energy loss of 2,500 keV, and is used in anti-coincidence with the other discriminator levels to exclude sensor responses to particles depositing more than 2,500 keV energy in the detector.

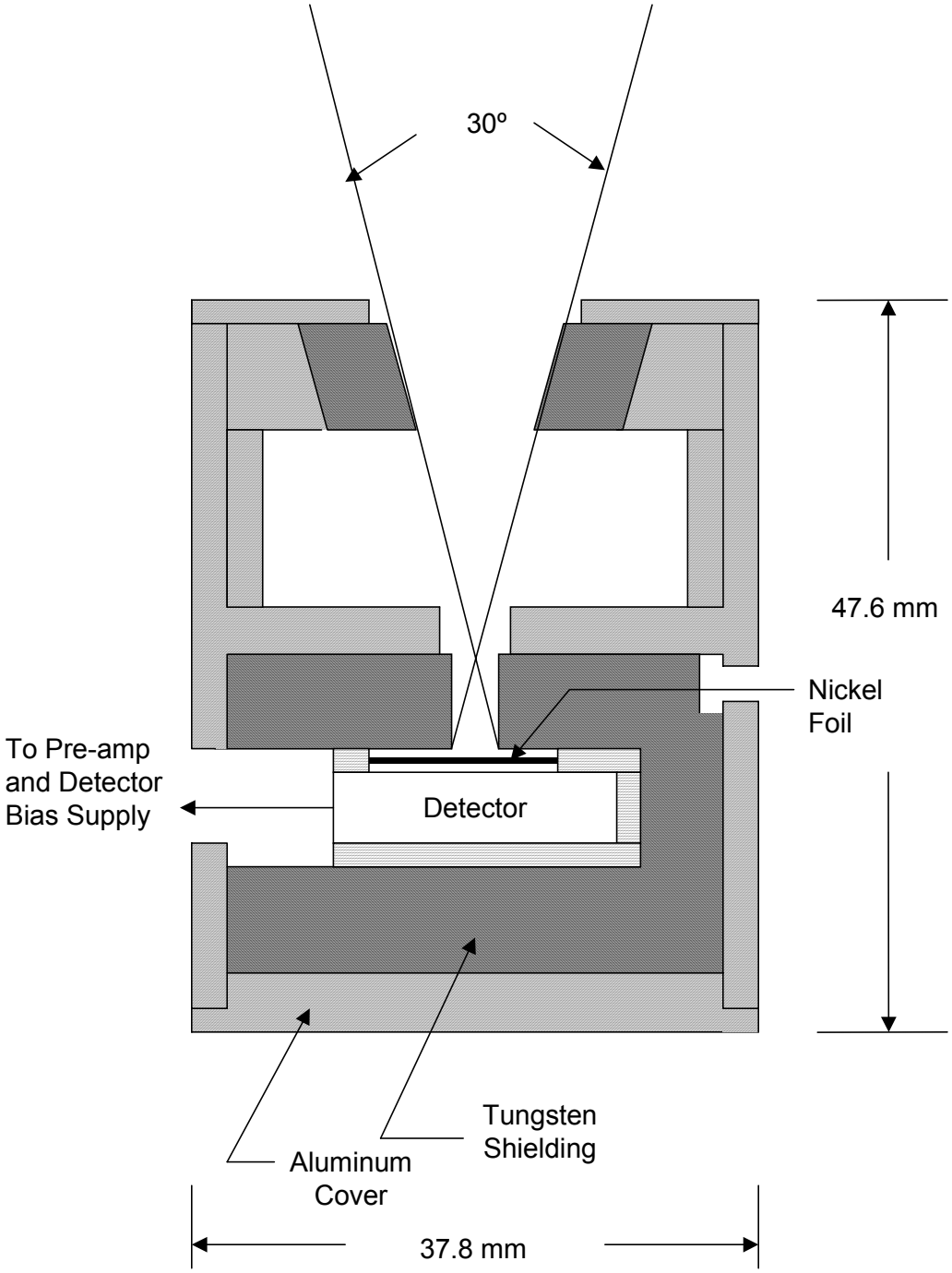
30º
47.6 mm
Nickel
Foil
To Pre-amp
and Detector
Bias Supply
Detector
Tungsten
Shielding
Aluminum
Cover
37.8 mm

Figure 3.3.1

Two identical electron solid-state detector telescopes are included in SEM-2. One, the 0º telescope, is oriented so that the central axis of the field of view is rotated in the XZ plane 9º from the –X direction toward the –Z direction (see Figure 2.1.1). The second, the 90º telescope, is oriented so that the center axis of the field of view is rotated 9º in the YZ plane from the +Y direction (anti-parallel to the satellite velocity vector) also toward the –Z direction. These rotations ensure a clear field of view.

Table 3.3.1 gives the electron energies, taking into account the energy lost in passing though the nickel foil and aluminum layer, together with the detector pulse height logic used to select those energies.

Table 3.3.1
MEPED Electron Energy Bands and Pulse Height Logic

Channel Identification	Electron Energy Range	Pulse Height Level Logic	
0/90 E1	30 keV to 2500 keV	L1 on	but not L2 or L4
0/90 E2	100 keV to 2500 keV	L1 and L2 on	but not L3 or L4
0/90 E3	300 keV to 2500 keV	L1 and L3 on	but not L4

The electron detector telescopes are also sensitive to protons entering through the collimator with enough energy to pass through the nickel foil and into the detector. The proton energies, taking into account energy loss in passing through the foil that will produce responses in the three electron energy channels are given below.

Table 3.3.2
MEPED Electron Detector Sensitivity to Protons

Channel Identification	Sensitive to Protons Having Energies
0/90 E1	210 keV to 2700 keV
0/90 E2	280 keV to 2700 keV
0/90 E3	440 keV to 2700 keV

In principle, the contribution of protons to the total electron telescope sensor response can be determined from the proton detector telescope observations, but the effects of radiation damage to the silicon detectors in the proton detector system can make this correction uncertain. Care should be taken in interpreting observations from the electron detector telescope at times when the proton telescope sensor response indicates large fluxes of protons in the >200 keV energy range.

Data from each electron detector telescope are accumulated for 1.0 second but the accumulation electronics are shared between the two detectors so that a full data set from both requires 2.0 seconds to acquire.

The nominal geometric factor for the electron solid-state detector telescopes is .01 cm^2 ster. To obtain the electron directional number flux within a given electron energy channel, the count rate, in counts per second, should be multiplied by 100. The resulting flux is in units of electrons cm^{-2} sec^{-1} $ster^{-1}$.

The electron telescope sensor responses are checked to make certain that the responses in the >30 keV channel are always greater than or equal to the responses in the >100 keV channels. The responses in the >100 keV channel should always be greater than or equal to the responses in the >300 keV channel. If this is not the case, it indicates that a bit error is present and the appropriate flag is set in array *qual* (see Section 4.5.1).

3.4 Omni-directional (Dome) Solid State Detectors

Four separate omni-directional solid-state detectors are included in the SEM-2 in order to monitor the high energy proton fluxes associated with energetic solar particle events. The basic design of all four sensors is identical (see Figures 3.4.1 and 3.4.2).

Each omni-directional sensor contains a silicon surface-barrier, solid-state detector, 3 mm thick, with a 50 mm^2 sensitive area – a circle 8 mm in diameter. The detector is located under a nearly hemispheric metal shell or moderator. The thickness of the shell and the shell material determine the minimum proton energy required to both penetrate the shell and deposit 2.5 MeV of energy in the detector, the threshold for generating a detector count.

The omni-directional detectors are mounted to view radially outwards from the earth with the central axis of each detector oriented 9º from the –X direction toward the –Z direction (see Figure 2.1.1) parallel to the viewing axis of the 0º MEPED proton and electron detector telescope units.

With the exception of the field of view subtended by the hemispheric shell, the detector assembly is surrounded by tungsten shielding to reduce the detector response to energetic particles incident from directions other than through the dome.

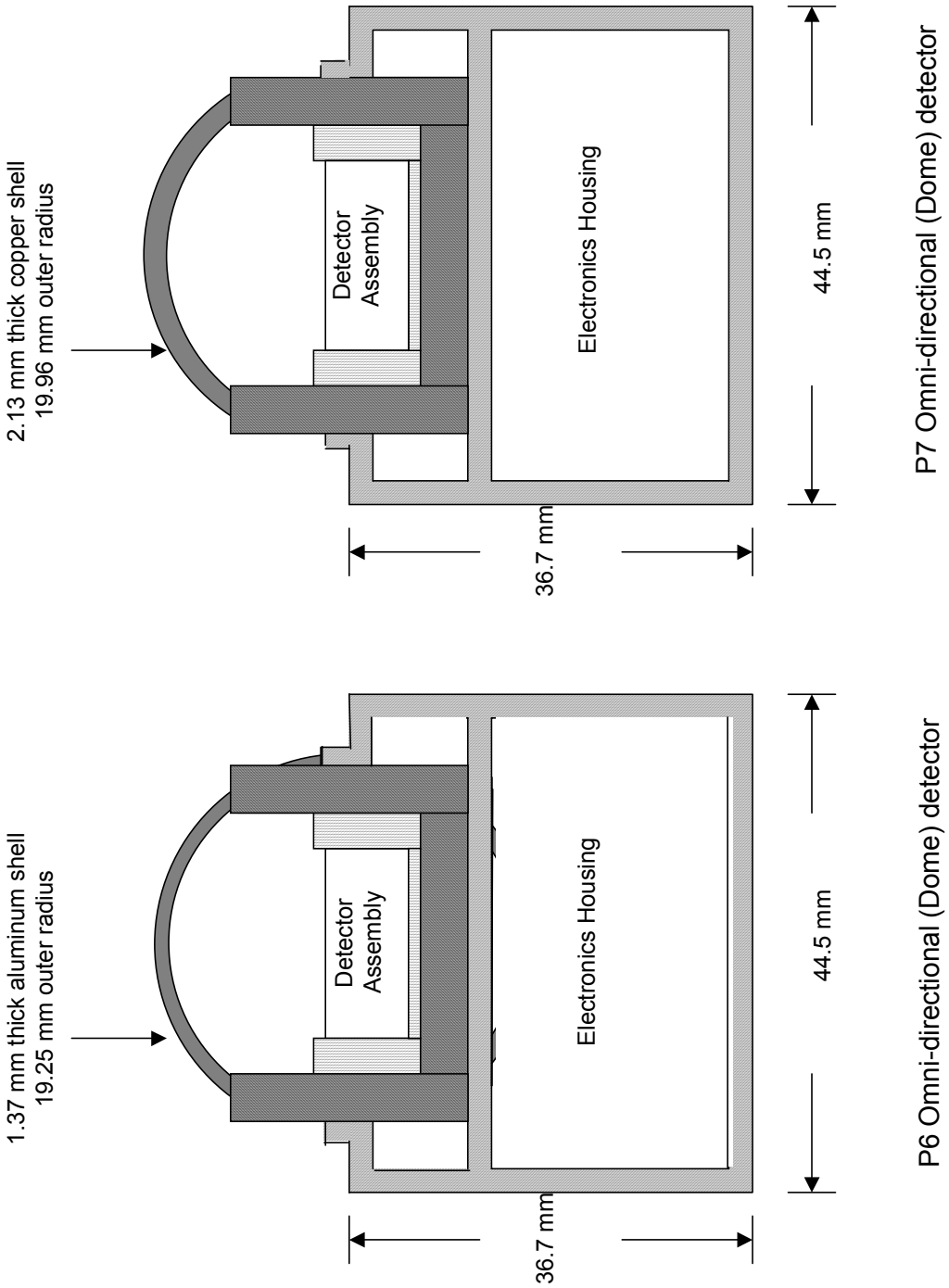
2.13 mm thick copper shell
19.96 mm outer radius
Detector Assembly
Electronics Housing
44.5 mm
36.7 mm
P7 Omni-directional (Dome) detector
1.37 mm thick aluminum shell
19.25 mm outer radius
Detector Assembly
Electronics Housing
44.5 mm
36.7 mm
P6 Omni-directional (Dome) detector

Figure 3.4.1

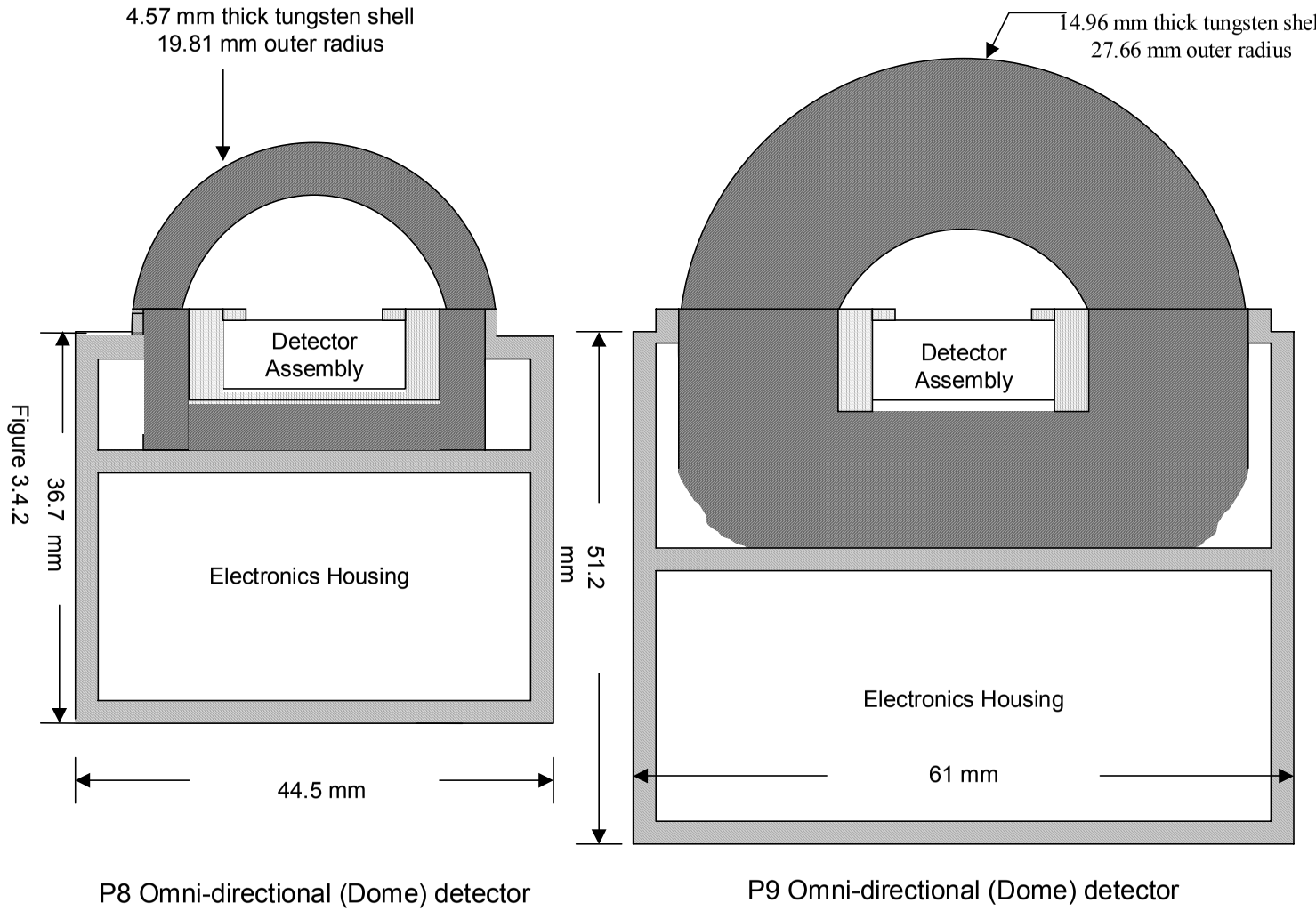

Figure 3.4.2

P8 Omni-directional (Dome) detector

P9 Omni-directional (Dome) detector

The absorber shell for detectors P6 and P7 encompass about a 120º field as viewed from the solid-state detector (see Figure 3.4.1) while the absorber shell for detectors P8 and P9 encompass about a 180º field, that is a full hemisphere, as viewed from the solid-state detector (Figure 3.4.2). It should be also noted that the tungsten shielding surrounding the solid-state detectors in P8 and P9 is the same thickness as the tungsten dome so that, unlike P6 and P7, the proton energy required to reach the detector is independent of the direction of arrival, neglecting the presence of the spacecraft structure and additional absorbing material.

Table 3.4.1 lists the detector designation, shell thickness, shell material, and minimum proton energy required to penetrate the shell or the tungsten shielding and produce a detector response.

Table 3.4.1
Minimum Detectable Proton Energies

Detector	Shell Material	Thickness (mm)	Minimum Energy to Penetrate the Shell and be Detected	Minimum Energy to Penetrate the Shielding and be Detected
P6	Aluminum	1.37	16 MeV	70 MeV
P7	Copper	2.13	35 MeV	70 MeV
P8	Tungsten	4.57	70 MeV	70 MeV
P9	Tungsten	14.96	140 MeV	140 MeV

(*Note* that there is an ambiguity between the *omni-directional* detector P6 and the highest energy channel, P6, in the proton detector *telescope* system. The ambiguity is removed, since the proton detector telescope channels always have a prefix “0” or “90”).

The maximum proton energy sensed by the omni-directional detectors is determined by the requirement that the protons, after passing through all the absorbing material, lose 2.5 MeV of energy in the solid-state detector in order to be counted. The energy of the proton entering the solid-state detector, even after passing through the various absorbing materials, is usually sufficient for it to pass entirely through the detector, and the energy actually deposited in the detector decreases with increasing proton energy. As the particle energy increases, the energy lost in the silicon detector eventually becomes less than 2.5 MeV, and that proton is not longer counted. The proton path length through the detector is variable, however, and can range from as long as 10 mm for a proton that enters the detector obliquely, to as short as 3 mm for a proton that enters normal to the detector face. This variation in path lengths and corresponding energy loss in the detector leads to a wide variation in the maximum proton energy that will be detected. Table 3.4.2 lists the maximum

proton energies detectable by each of the four omni-directional detectors under four conditions; for a proton incident through the shell directly along the central axis of the detector, for a proton entering through the shell but at 60º to the central axis and passing obliquely through the solid-state detector, for a proton penetrating the tungsten shielding from below the detector on a path along the central axis, and for a proton penetrating the tungsten shielding at an angle of 120º to the central axis. Note that for detectors P8 and P9 the first two cases are identical to the last two.

While there is a wide variation in the maximum detectable proton energy as a function of the particle angle of incidence, a reasonable assumption for the maximum energy, valid for all four omni-directional detectors and all angles of incidence, is about 500 MeV.

Table 3.4.2
Maximum Detectable Proton Energies

Detector	0º Incidence Through Shell	60º Incidence Through Shell	180º Incidence Through Shielding	120º Incidence Through Shielding
P6	215 MeV	1100 MeV	235 MeV	1110 MeV
P7	220 MeV	1100 MeV	235 MeV	1110 MeV
P8	235 MeV	1110 MeV	235 MeV	1110 MeV
P9	275 MeV	1130 MeV	275 MeV	1130 MeV

The geometric factors (transfer functions) needed to convert the omni-directional solid-state detector responses to proton flux values are not uniquely defined, being very dependent upon proton energy and the angular distribution of the proton population. Appendix F outlines procedures for recovering proton number fluxes from the omni-directional sensor responses for two angular distributions of particles that are typically encountered.

3.5 Timing of MEPED Data Accumulation Relative to Time Tag

Table 3.5.1 lists the accumulation periods for each of the 22 MEPED sensor channels and the accumulation start and end times relative to the data point time tag in the archive data record.

Table 3.5.1

Detector Channel Identification	Accumulation Period (sec)	Accumulation Interval Relative to Archive Record Time Tag
0 E1	1.0	– 1.80 s to – 0.80 s
0 E2	1.0	– 1.80 s to – 0.80 s
0 E3	1.0	– 1.80 s to – 0.80 s
0 P1	1.0	– 1.80 s to – 0.80 s
0 P2	1.0	– 1.80 s to – 0.80 s
0 P3	1.0	– 1.80 s to – 0.80 s
0 P4	1.0	– 1.80 s to – 0.80 s
0 P5	1.0	– 1.80 s to – 0.80 s
0 P6	1.0	– 1.80 s to – 0.80 s
90 E1	1.0	– 0.80 s to + 0.20 s
90 E2	1.0	– 0.80 s to + 0.20 s
90 E3	1.0	– 0.80 s to + 0.20 s
90 P1	1.0	– 0.80 s to + 0.20 s
90 P2	1.0	– 0.80 s to + 0.20 s
90 P3	1.0	– 0.80 s to + 0.20 s
90 P4	1.0	– 0.80 s to + 0.20 s
90 P5	1.0	– 0.80 s to + 0.20 s
90 P6	1.0	– 0.80 s to + 0.20 s
Omni-directional P6	2.0	– 1.80 s to + 0.20 s
Omni-directional P7	2.0	– 1.80 s to + 0.20 s
Omni-directional P8	4.0	– 3.80 s to + 0.20 s
Omni-directional P9	4.0	– 3.80 s to + 0.20 s

3.6 MEPED In-Flight Calibration

The MEPED instrument undergoes a weekly in-flight calibration procedure. This procedure involves stimulating each of the MEPED sensor charge-sensitive-amplifier, threshold-discriminator chain with pulses whose amplitudes increase linearly with time. By noting the time when the output of each sensor energy channel begins to respond to this stimulus, the threshold discriminator level and corresponding energy in keV is checked. By observing the change in the stimulus pulse amplitude required to completely "turn on" the lowest energy level of each sensor, the noise level of that solid-state detector is also determined.

An in-flight calibration lasts for 384 seconds and while it is in progress an appropriate status flag is set. During that time MEPED data should be ignored.

Procedures and software to analyze the in-flight calibration data from the MEPED suite of sensors have been developed at SEC and the reduced calibration data are included in the history of the instrument performance.

4 Polar Orbiting Environmental Satellite (POES) Archive Data File

This section describes the data contained in the archive record. An archive record comprises 32 seconds of data, including a full set of orbital parameters provided every 8 seconds (sub-satellite latitude and longitude every 2 seconds), 16 full data collection cycles from the TED, the MEPED electron and proton telescope instruments, the P6 and P7 omni-directional detector sensors, and 4 full cycles of the P8 and P9 omni-directional detector sensors. A full set of background data from the 8 TED detector systems is included once in the 32 second archive record. Finally, a selected portion of the SEM-2 instrument status, temperature, and system health data as well as data quality and ancillary information are included.

Appendix D provides a C language program and Appendix E a FORTRAN language program that can be used to access the archive data. In this document, two dimensional arrays will be referred to as (i,j) for FORTRAN and as [j] [i] for C. The i and j values differ in position because of the difference in the way C and FORTRAN deal with column/row majority in two dimensional arrays. With the exception of the array *tedback*, described in Section 2.4.4, the 'j' dimension in a two dimensional array is either 4 or 16; 4 for arrays that contain values for every 8 seconds, and 16 for arrays that have values for every 2 seconds of data. In both cases the arrays contain data spanning 32 seconds. In this section of the document, Tables number the dimension 'i' beginning with 1. In 'C' the index would start from 0.

In general, the data in the archive record can be divided into five types: instrument status and health information, time and orbit parameter information, MEPED sensor data, TED data, and data quality and ancillary information.

The data in each of these five categories that are returned by the program that reads the archive record are described in detail.

4.1 Instrument Status and Health

Instrument status and health information is returned from the read program in two arrays. The first array is named *status*, which contains 10 elements, and the second is named *analog* and contains 17 elements.

4.1.1 *status* Array

The contents of the *status* array are summarized in Table 4.1.1. This array occurs once per archive record and is applicable to the entire 32 seconds of data. (See Appendix G: *Further errata as of January 6, 2004* concerning the use of Table 4.1.1)

Table 4.1.1
Contents of the *status* Array

Array Element	Descriptor	Range of Data Value	Interpretation
1	MEPED On-Off	0 or 1	0 for MEPED off, 1 for MEPED on
2	TED On-Off	0 or 1	0 for TED off, 1 for TED on
3	MEPED IFC	0 or 1	1 if MEPED in-flight calibration in progress, 0 if in-flight calibration not in progress
4	TED IFC	0 or 1	1 if TED in-flight calibration in progress, 0 if in-flight calibration not in progress
5	TED electron discriminator level	0 to 3	see below
6	TED proton discriminator level	0 to 3	see below
7	TED electron HV supply	0 to 7	see below
8	TED proton HV supply	0 to 7	see below
9	μ processor in use	0 or 1	0 if micro-processor A is on 1 if micro-processor B is on
10	μ processor error flag	0 or 1	0 if no processor error detected 1 if a processor error detected

The pulse-height discriminator levels for the TED electron and TED proton detector systems can be independently changed to one of four values by ground command. This was done in case electronic noise produced spurious counts that a higher pulse height discrimination level would suppress. Normally the pulse height discriminator levels for both the electron and proton detector systems are set to the lowest level (zero).

The high voltage applied to the Channeltron particle detectors in the TED electron and proton detector systems can be independently changed to one of eight levels by ground command. This is done to compensate for gain degradation in the Channeltron particle detectors. This degradation can, over time, be severe enough that the pulse outputs from these detectors would fall below the threshold set by the pulse height discriminators. Increasing the high voltage on the Channeltron detectors increases their gain to overcome any degradation. The Channeltron high voltages for both the electron and proton detector systems are initially set to the lowest voltage state.

4.1.2 *analog* Array

The contents of the *analog* array are summarized in Table 4.1.2. This array occurs once per archive record and is applicable to the entire 32 seconds of data.

Table 4.1.2
Contents of the *analog* Array

Array Element	Descriptor	Nominal Value	Interpretation
1	TED +5 V monitor	+ 5.0 V	TED electronics +5 V monitor
2	TED electron Channeltron high voltage monitor	+ 2600 V	Voltage monitor dependent upon commandable high voltage setting
3	TED proton Channeltron high voltage monitor	+ 1700 V	Voltage monitor dependent upon commandable high voltage setting
4	TED sweep voltage monitor	variable 0 to + 500 V	Electrostatic analyzer plate voltage monitor
5	TED temperature	variable –20 to + 20 ºC	TED instrument temperature
6	MEPED +5 V monitor	+ 5.0 V	MEPED electronics +5 V monitor
7	MEPED circuit temperature	variable –20 to + 20 ºC	MEPED circuit board temperature
8	MEPED omni-directional detector bias voltage	+ 650 V	Omni-directional solid-state detector bias voltage
9	MEPED proton telescope detector bias voltage	+ 60 V	Proton telescope solid-state detector bias voltage
10	MEPED electron telescope detector bias voltage	+ 150 V	Electron telescope solid-state detector bias voltage
11	MEPED proton telescope detector temperature	variable –20 to + 20 ºC nominal 0 ºC	Proton telescope, solid-state detector temperature
12	MEPED electron telescope detector temperature	variable –20 to + 20 ºC nominal 0 ºC	Electron telescope solid-state detector temperature
13	MEPED omni-directional detector temperature	variable –20 to + 20 ºC nominal 0 ºC	Omni-directional solid-state detector temperature
14	DPU + 5 V monitor	+ 5.0 V	Data Processing Unit +5 V monitor
15	□processor A +5 V monitor	+ 5.0 V	□processor A monitor + 5 V if processor A is on
16	□processor B +5 V monitor	0.0 V	□processor B monitor 0 V if processor B is off
17	DPU temperature	variable –20 to + 20 ºC	Data processing unit temperature

4.2 Timing and Orbital Information

Timing and orbital information are returned from the read program in three arrays. The first is called ihd, which contains 6 elements, and the second is named head, and contains 27 elements. Both ihd and head are returned four times for each 32-second archive record or every 8 seconds. The third array is called ssLoc, and has 2 elements; it is returned sixteen times for each 32 second record or every 2 seconds.

4.2.1 ihd Array, dimensioned (6,4) in FORTRAN, [4][6] in 'C'

The contents of the ihd array are summarized in Table 4.2.1. The entries are for the first 2 seconds of each 8-second iteration of 'j'.

Table 4.2.1
Contents of the jth iteration of the ihd Array

i	Descriptor	Nominal Value	Interpretation
1	satellite ID	Satellite Dependent	NOAA-15 has ID of 4 NOAA-16 has ID of 2
2	year	>1998	The 4 digit year
3	day of year	1 to 366	The 3 digit day of the year
4	millisecond of day	0 to 86399000	Milliseconds of the UT day at the start of the 8 second data block
5	satellite altitude	850	satellite altitude in km
6	orbit number	up to 65335	orbit number incremented at northbound equator crossing

4.2.2 head Array, dimensioned (27,4) in FORTRAN, [4][27] in 'C'

The contents of the head array are summarized in Table 4.2.2. The entries are for the first 2 seconds of each 8-second iteration of 'j'.

The majority of the entries in head are calculated from a magnetic field model using knowledge of both the orbit and the three-axis stabilized orientation of the satellite. For the NOAA/POES satellite data processing these calculations are done using a current International Geomagnetic Reference Field (IGRF) model for the epoch midway through the year the data were acquired. For example, all magnetic orbital data during the year 2000 were calculated using the IGRF 2000.5 model. The geocentric radius of the satellite orbit is also updated once a year using the ephemeris from January 1 of that year. For NOAA-15 in 2000, the geocentric distance to the satellite varied between 7188 and 7204 km. For

purposes of the magnetic calculations the orbit was assumed circular around the earth center with a radius of 7195 km. It is planned that the magnetic calculations will be updated once a year using the new IGRF model and satellite orbit information.

The determination of the "foot-of-the-field-line" (*fofl*) location – the geographic point where the magnetic field line threading the satellite intersects 120 km in altitude above the earth, where precipitating auroral particles detected at the satellite actually enter the atmosphere – is done by tracing in 1 km steps (using a program kindly provided by Joseph Cain, private communication, 1983) along the magnetic field direction calculated from the IGRF model until the 120 km altitude is reached. The hemisphere, northern or southern, for the *fofl* location is based upon whether the satellite is north or south of the geomagnetic equator.

The IGRF model is also used to calculate the three components (positive eastward, positive southward, and positive radially outward) of the magnetic field vector at the satellite. The magnetic field direction, together with knowledge of the viewing directions of the SEM-2 sensors relative to the orientation of the three-axis stabilized spacecraft, permits calculation of the angle between the central axis of each sensor field of view and the magnetic field. This angle is converted to the magnetic pitch angle of the charged particles sensed by the various detectors, the convention being that the pitch angle is the angle between the particle velocity vector and the magnetic field direction.

The magnetic field vector at the *fofl* location is also calculated using the IGRF model. The pitch angles (p/a) of the particles detected at the satellite are transformed to their values at the *fofl* location using the ratio of magnetic field strength at the satellite to that at the *fofl*. If the particles detected at the satellite magnetically mirror above the atmosphere, the *fofl* pitch angle is set to a "pad" value (see Table 4.2.2).

The McIlwain *L*-value at the satellite location is calculated from the INVAR FORTRAN program that is available from the National Space Science Data Center at the Goddard Space Flight Center in Greenbelt, MD. INVAR uses the IGRF model and the *L*-value calculations are updated once a year with the updated IGRF model. If the calculated *L*-value is greater than 20.0, the *L*-value is set to a "pad" value (see Table 4.2.2).

The dipole magnetic latitude and magnetic longitude at the *fofl* location are calculated using the position of the north magnetic pole that is returned by the INVAR routine. This position is updated once a year for the archive data processing.

The corrected magnetic latitude at the *fofl* location is computed using the routine written by Papitashvili and Papitashvili following the procedure given by *Gustafsson, et al.* (1992). This routine also uses the IGRF magnetic field model, and the corrected magnetic latitude calculations are updated once a year.

The eccentric magnetic local time at the *fofl* location is calculated following the procedures set down by *Cole*, (1963) and *Fraser-Smith*, (1987). The calculation is updated once a year using the current IGRF model field. The eccentric magnetic local time is returned as an angle from 0º to 360º, with 0º being magnetic midnight, and the angle incremented by 15º per hour magnetic local time.

The local time is calculated at the sub-satellite location by assuming the local time is the Universal Time incremented by one hour for every 15º east of the Greenwich meridian. The equation of time is not used in the calculation, so this variable is only approximately the true local solar time at the sub-satellite point. The local time is also returned as an angle from 0º to 360º with 0º being midnight.

The calculations that involve the magnetic field are not performed in full for each data point in the archive processing; instead a table is created once a year with all the magnetically controlled orbital parameters calculated for a grid of geographic latitudes and longitudes. A cubic interpolation is then used to compute orbital parameters for each data point, given the sub-satellite location along the orbit. The errors introduced by this procedure are negligible.

Table 4.2.2
Contents of the j^{th} iteration of the the *head* Array

i	Descriptor	Nominal Value Or Range	Comment
1	satellite inclination	98.6º	
2	sub-satellite latitude	–90.º to +90.º	
3	sub-satellite longitude	0.º to 360.º	
4	radial component of ***B*** at the satellite	–50000. to +50000.	nanoTesla
5	east component of ***B*** at the satellite	–50000. to +50000.	nanoTesla
6	south component of ***B*** at the satellite	–50000. to +50000.	nanoTesla
7	scalar value of *B* at the satellite	+50000.	nanoTesla
8	0º TED p/a at the satellite	0º to +180º	
9	30º TED p/a at the satellite	0º to +180º	
10	0º MEPED p/a at the satellite	0º to +180º	
11	90º MEPED p/a at the satellite	0º to +180º	
12	radial component of ***B*** at the *fofl*	–50000. to +50000.	nanoTesla
13	east component of ***B*** at the *fofl*	–50000. to +50000.	nanoTesla
14	south component of ***B*** at the *fofl*	–50000. to +50000.	nanoTesla
15	scalar value of *B* at the *fofl*	+60000.	nanoTesla
16	0º TED p/a at the *fofl*	0º to +180º	–999.0 if particles mirror above atmosphere
17	30º TED p/a at the *fofl*	0º to +180º	set to –999.0 if particles mirror above atmosphere
18	0º MEPED p/a at the *fofl*	0º to +180º	set to –999.0 if particles mirror above atmosphere
19	90º MEPED p/a at the *fofl*	0º to +180º	set to –999.0 if particles mirror above atmosphere
20	*fofl* geographic latitude	–90.º to +90.º	
21	*fofl* geographic longitude	0.º to 360.º	
22	*fofl* geomagnetic latitude	–90.º to +90.º	
23	*fofl* geomagnetic longitude	0.º to 360.º	
24	McIlwain *L*-value	0.9 to 20.0	set to –999.0 if *L* > 20.0
25	corrected magnetic latitude	–90.º to +90.º	
26	sub-satellite local time	0.º to 360.º	
27	fofl magnetic local time	0.º to 360.º	

4.2.3 *ssLoc* Array, dimensioned (2,16) in FORTAN, [16][2] in 'C'

The contents of the array called *ssLoc* are summarized in Table 4.2.3. The higher temporal resolution, 2-second orbital data are included to assist in interpolating the lower resolution orbital data in the *head* array should it be required.

Table 4.2.3
Contents of the j^{th} iteration of the Array *ssLoc*

i	Descriptor	Nominal Value or Range
1	sub-satellite latitude	–90.º to +90.º
2	sub-satellite longitude	0.º to 360.º

4.3 MEPED Sensor Data

The MEPED sensor data are contained in 3 arrays returned from the archive record, providing data with a 2-second time resolution. The first array is called *mep0* and contains data from both the 0º proton and 0º electron telescopes. The next array is called *mep90* and contains data from both the 90º proton and 90º electron telescopes, and the third array is named *mepOmni* and contains data from the four omni-directional solid-state detectors.

4.3.1 *mep0* and *mep90* Arrays, dimensioned (9,16) in FORTRAN, [16][9] in 'C'

The contents of the *mep0* and *mep90* arrays are summarized in Tables 4.3.1a and 4.3.1b.

Table 4.3.1a
Contents of the j^{th} iteration of the Array *mep0*

i	Descriptor	Valid Range	Comment
1	0P1	0. to 1998848.0	set to –999.0 for missing data
2	0P2	0. to 1998848.0	set to –999.0 for missing data
3	0P3	0. to 1998848.0	set to –999.0 for missing data
4	0P4	0. to 1998848.0	set to –999.0 for missing data
5	0P5	0. to 1998848.0	set to –999.0 for missing data
6	0P6	0. to 1998848.0	set to –999.0 for missing data
7	0E1	0. to 1998848.0	set to –999.0 for missing data
8	0E2	0. to 1998848.0	set to –999.0 for missing data
9	0E3	0. to 1998848.0	set to –999.0 for missing data

Table 4.3.1b
Contents of the j^{th} iteration of the Array *mep90*

i	Descriptor	Valid Range	Comment
1	90P1	0. to 1998848.0	set to –999.0 for missing data
2	90P2	0. to 1998848.0	set to –999.0 for missing data
3	90P3	0. to 1998848.0	set to –999.0 for missing data
4	90P4	0. to 1998848.0	set to –999.0 for missing data
5	90P5	0. to 1998848.0	set to –999.0 for missing data
6	90P6	0. to 1998848.0	set to –999.0 for missing data
7	90E1	0. to 1998848.0	set to –999.0 for missing data
8	90E2	0. to 1998848.0	set to –999.0 for missing data
9	90E3	0. to 1998848.0	set to –999.0 for missing data

4.3.2 *mepOmni* Array, dimensioned (4,16) in FORTRAN, [16][4] in 'C'

The contents of the *mepOmni* array are summarized in Table 4.3.2. Note that the P8 and P9 sensor data are sub-commutated and valid data for each are contained only in alternate 2-second repetitions of *mepOmni.*

Table 4.3.2
Contents of the j^{th} iteration of the Array *mepOmni*

i	Descriptor	Valid Range	Comment
1	P6	0. to 1998848.0	set to –999.0 for missing data
2	P7	0. to 1998848.0	set to –999.0 for missing data
3	P8	0. to 1998848.0	set to –999.0 for missing data data valid only for 1^{st}, 3^{rd}, 5^{th}, 7^{th}, 9^{th}, 11^{th}, 13^{th}, and 15^{th} 2-second intervals
4	P9	0. to 1998848.0	set to –999.0 for missing data data valid only for 2^{nd}, 4^{th}, 6^{th}, 8^{th}, 10^{th}, 12^{th}, 14^{th}, and 16^{th} 2-second intervals

4.4 TED Sensor Data

The TED sensor data are contained in six arrays returned from the 32-second archive record. Two arrays, called *ted0* and *ted30*, contain full data sets from both the 0º TED and 30º TED sensors that are gathered during every 2-second instrument cycle. The arrays called *ted0s* and *ted30s* contain the sensor observations that are obtained in selected energy bands on a lower duty cycle (see Section 2.5). The fifth array, named *tedfx*, contains the various energy flux moments calculated from the data every 2-seconds, and the sixth array, called*tedback*, contains the TED sensor background data.

4.4.1 *ted0* and *ted30* Arrays, dimensioned (8,16) in FORTRAN, [16][8] in 'C'

The contents of the *ted0* and *ted30* arrays are summarized in Tables 4.4.1a and 4.4.1b. An explanation of the elements in these two arrays is in Sections 2.2 and 2.4.

Table 4.4.1a
Contents of the j^{th} iteration of the Array *ted0*

i	Descriptor	Valid Range	Comment
1	0º, 50 – 1000 eV electron integrated energy flux	0. to 1998848.0	set to –999.0 for missing data
2	0º, 50 – 1000 eV proton integrated energy flux	0. to 1998848.0	set to –999.0 for missing data
3	0º, 1000 – 20000 eV electron integrated energy flux	0. to 1998848.0	set to –999.0 for missing data
4	0º, 1000 – 20000 eV proton integrated energy flux	0. to 1998848.0	set to –999.0 for missing data
5	energy band containing maximum in 0º electron flux	1 to 16	set to –999.0 for missing data
6	energy band containing maximum in 0º proton flux	1 to 16	set to –999.0 for missing data
7	0º electron sensor response in the "maximum" energy band	0. to 1998848.0	set to –999.0 for missing data
8	0º proton sensor response in the "maximum" energy band	0. to 1998848.0	set to –999.0 for missing data

Table 4.4.1b
Contents of the j^{th} iteration of the Array *ted30*

i	Descriptor	Valid Range	Comment
1	30º, 50 – 1000 eV electron integrated energy flux	0. to 1998848.0	set to –999.0 for missing data
2	30º, 50 – 1000 eV proton integrated energy flux	0. to 1998848.0	set to –999.0 for missing data
3	30º, 1000 – 20000 eV electron integrated energy flux	0. to 1998848.0	set to –999.0 for missing data
4	30º, 1000 – 20000 eV proton integrated energy flux	0. to 1998848.0	set to –999.0 for missing data
5	energy band containing maximum in 30º electron flux	1 to 16	set to –999.0 for missing data
6	energy band containing maximum in 30º proton flux	1 to 16	set to –999.0 for missing data
7	30º electron sensor response in the “maximum” energy band	0. to 1998848.0	set to –999.0 for missing data
8	30º proton sensor response in the “maximum” energy band	0. to 1998848.0	set to –999.0 for missing data

4.4.2 *ted0s* and *ted30s* Arrays, dimensioned (8,4) in FORTRAN, [4][8] in ‘C’

The contents of the arrays *ted0s* and *ted30s* are summarized in Tables 4.4.2a and 4.4.2b. These arrays contain the sensor responses in the four preselected energy bands that are returned from the TED instrument on a lower duty cycle than the 2-second instrument cycle time. An explanation of the elements in these two arrays is in Section 2.5. If an element has missing data, the value returned from the archive record is set to a “pad” value. Note that 0º and 30º proton data are not taken during the fifteenth or sixteenth 2-second interval in the 32-second record, as sensor background data are telemetered instead.

Table 4.4.2a
Contents of the j^{th} iteration of the Array *ted0s*

i	Descriptor	Valid Range	Comment
1	0º electron sensor response energy band 4	0. to 1998848.0	data taken in 1st, 5th, 9th, and 13th 2-second interval
2	0º electron sensor response energy band 8	0. to 1998848.0	data taken in 1st, 5th, 9th, and 13th 2-second interval
3	0º electron sensor response energy band 11	0. to 1998848.0	data taken in 1st, 5th, 9th, and 13th 2-second interval
4	0º electron sensor response energy band 14	0. to 1998848.0	data taken in 1st, 5th, 9th, and 13th 2-second interval
5	0º proton sensor response energy band 4	0. to 1998848.0	data taken in 3rd, 7th, and 11th 2-second interval
6	0º proton sensor response energy band 8	0. to 1998848.0	data taken in 3rd, 7th, and 11th 2-second interval
7	0º proton sensor response energy band 11	0. to 1998848.0	data taken in 3rd, 7th, and 11th 2-second interval
8	0º proton sensor response energy band 14	0. to 1998848.0	data taken in 3rd, 7th, and 11th 2-second interval

Table 4.4.2b
Contents of the j^{th} iteration of the Array *ted30s*

i	Descriptor	Valid Range	Comment
1	30º electron sensor response energy band 4	0. to 1998848.0	data taken in 2nd, 6th, 10th, and 14th 2-second interval
2	30º electron sensor response energy band 8	0. to 1998848.0	data taken in 2nd, 6th, 10th, and 14th 2-second interval
3	30º electron sensor response energy band 11	0. to 1998848.0	data taken in 2nd, 6th, 10th, and 14th 2-second interval
4	30º electron sensor response energy band 14	0. to 1998848.0	data taken in 2nd, 6th, 10th, and 14th 2-second interval
5	30º proton sensor response energy band 4	0. to 1998848.0	data taken in 4th, 8th, and 12th 2-second interval
6	30º proton sensor response energy band 8	0. to 1998848.0	data taken in 4th, 8th, and 12th 2-second interval
7	30º proton sensor response energy band 11	0. to 1998848.0	data taken in 4th, 8th, and 12th 2-second interval
8	30º proton sensor response energy band 14	0. to 1998848.0	data taken in 4th, 8th, and 12th 2-second interval

4.4.3 *tedfx* Array, dimensioned (7,16) in FORTRAN, [16][7] in 'C'

The contents of the array named *tedfx* is summarized in Table 4.4.3. The numerical values in *tedfx* are calculated from the telemetered electron and proton energy flux information found in the arrays *ted0* and *ted30*, using the laboratory calibrations of the instrument sensitivities and the procedures outlined in Section 2.3. Valid omni-directional energy fluxes may range from 0.0 to as high 600.0 ergs cm^{-2} sec^{-1} (equivalent to units of mW m^{-2}), with default values as noted in the table.

Table 4.4.3
Contents of the j^{th} iteration of the Array *tedfx*

i	Meaning of element units of mW m^{-2}	Assigned value in the case of missing data	Assigned value in the case of no TED sensor viewing particles entering the atmosphere
1	50-1000 eV electron omni-directional flux	-990.	-996.
2	1000-20000 eV electron omni-directional flux	-991.	-996.
3	50-1000 eV proton omni-directional flux	-992.	-996.
4	1000-20000 eV proton omni-directional flux	-993.	-996.
5	50-20000 eV electron omni-directional flux	-994.	-996.
6	50-20000 eV proton omni-directional flux	-995.	-996.
7	50-20000 eV proton plus electron omni-directional flux	-997.	-996.

4.4.4 *tedback* Array, dimensioned (2,4) in FORTRAN, [4][2] in 'C'

The contents of the array named *tedback* is summarized in Table 4.4.4. The index, i, that runs from 1 to 2 signifies whether the sensor background information is for the 0º TED detectors (index equal to 1) or for the 30º TED detectors (index equal to 2). The index, j, that runs from 1 to 4 references one of the four TED sensors at that orientation. The *tedback* array is returned once for each 32-second archive record.

Table 4.4.4
Contents of the Array *tedback*

i, j	Descriptor	Valid Range	Assigned value in the case of missing data
1,1	0º, high energy electron sensor background	0. to 1998848.0	-999.0
1,2	0º, low energy electron sensor background	0. to 1998848.0	-999.0
1,3	0º, high energy proton sensor background	0. to 1998848.0	-999.0
1,4	0º, low energy proton sensor background	0. to 1998848.0	-999.0
2,1	30º, high energy electron sensor background	0. to 1998848.0	-999.0
2,2	30º, low energy electron sensor background	0. to 1998848.0	-999.0
2,3	30º, high energy proton sensor background	0. to 1998848.0	-999.0
2,4	30º, low energy proton sensor background	0. to 1998848.0	-999.0

4.5 Data Quality and Ancillary Information

Data quality and ancillary information for each 32-second archive record are contained in the arrays called *qual*, *minor*, and *mdf*, and in three scalar numbers named; *cSum*, *cSumFlag*, and *major*.

The variable *cSum* refers to a checksum that is calculated by the DPU in the SEM-2 and inserted into the telemetry stream once each 32-seconds. The checksum telemetered from the satellite once each 32-seconds is the sum, modulo 256, of the values of the 640 SEM-2 data words that the DPU processed and passed into the Tiros Information Processor (TIP) data stream during the immediately previous 32-second major frame of data. This allows a cross check between the sum, modulo 256, of the 640 data words actually received and the sum calculated by the DPU. A disagreement between the sum calculated on the ground and that calculated by the DPU indicates that there is one or more telemetry bit errors in the 32-second TIP major frame received on the ground. The value of *cSum* is the checksum as received on the ground.

The variable *cSumFlag* indicates whether the checksum as calculated in the archive processing from the data words received on the ground agrees with the checksum value in the telemetry stream. If there is a data gap, the telemetered checksum calculated for the last 32-second major frame of data received will be missing and the comparison cannot be made. The value of *cSumFlag* may be 0, 1, or 2 with the following meaning.

cSumFlag=0, telemetered and calculated check sums agree, no bit errors present,

cSumFlag=1, telemetered and calculated check sums agree, bit errors likely,

cSumFlag=2, a comparison could not be made because the necessary telemetered check sum had a missing data flag. The data in this 32-second record may be valid but should be treated with caution.

cSumFlag=3, a comparison could not be made because a subsequent data gap meant the necessary telemetered check sum was not available. The data in this 32-second record may be valid but should be treated with caution.

The value of *major* is a major frame number that can range from 0 to 7. The major frame number is introduced into the TIP data stream by the satellite data handling system. The major frame number is necessary for decoding certain housekeeping data that are highly subcommutated. The major frame number is not required for the intepretation and the use of any SEM-2 sensor data.

4.5.1 *qual* Array

The array *qual* contains sixteen 2-byte integer elements for each 32-second archive record, and each entry provides data quality information about the data in the corresponding 2-second dataset. Individual bits in each entry of *qual* are set to either 0 or 1 to indicate the result of various data quality tests imposed on the data contained in each 2-second set. Only the 8 least significant bits of each integer word are used. Table 4.5.1 lists the meaning of each of the least significant bits.

Table 4.5.1
Contents of Array *qual*

Bit Location	Binary Value	Meaning
0 (lsb)	1	Not used
1	2	Not used
2	4	Not used
3	8	TED energy fluxes corrected for background (Sect. 2.7)
4	16	MEPED electron data not sensible (Sect. 3.3)
5	32	Inconsistency in TED 4-spectrum data (Sect. 2.8)

Bit Location	Binary Value	Meaning
6	64	Inconsistency in TED energy flux moment (Sect. 2.8)
7 (msb)	128	Some data missing within the 2-second record

4.5.2 *minor* Array

The array called *minor* contains 16 values of the minor frame count that is introduced into the telemetered data stream from the satellite by the TIP. A TIP minor frame is 0.1 seconds long. There are 20 TIP minor frames making up a SEM-2 2-second dataset and 320 minor frames in a 32-second archive record that corresponds to a TIP major frame. The *minor* array contains the minor frame value at the start of each of the sixteen 2-second datasets making up an archive record. The sequence of values in *minor* should **always** be 000, 020, 040, 060, 080, 100, 120, 140, 160, 180, 200, 220, 240, 260, 280, and 300.

The data in minor are not absolutely required for the interpretation and use of any SEM-2 sensor data. These data are useful, however, to confirm the proper ordering of the MEPED omni-directional P8 and P9 data that are subcommutated. Data from the P8 sensor are read out during minor frame numbers 000, 040, 080, 120, 160, 200, 240, and 280, while data from the P9 sensor occur at minor frame numbers 020, 060, 100, 140, 180, 220, 260, and 300.

4.5.3 *mdf* Array, dimensioned (40,16) in FORTRAN, [16][40] in 'C'

The processing of data downlinked from the POES satellite can occasionally suffer the loss of bit synchronization when the signal is poor. When this occurs the data processing software inserts pad values into the SEM-2 data stream. The numerical value of the inserted pad value is ambiguous because that value may also normally appear in the data stream. To remove this ambiguity, the processing software sets a flag indicating whether or not a pad value was inserted in each data word in the SEM-2 data stream that is passed to the Space Environment Center. The SEM-2 instrument was allocated two digital words in the POES TIP minor frame format. The minor frame cadence is one minor frame every 0.1-second, or 40 digital data words every 2-seconds. The array *mdf* has 40 elements, corresponding to each of those 40 data words, and is repeated sixteen times for a 32-second archive record. Each element has been cross-referenced to the appropriate SEM-2 data channel. Both the C language and FORTRAN language programs that read the archive record check the contents of the *mdf* array and, if an element in that array is set to 1 (indicating that a pad value had been inserted) the software will set the appropriate data element to the default missing data value which is –999.0.

Acknowledgements

The contribution to the SEM-2 project by Dr. Robert Bushnell, The SEM-2 Program Manager from 1989 until 1997 and Mr. Alexander (Bob) Muckle, the Program Manager since 1997 is gratefully acknowledged. The support of Mr. Richard Grubb, who has contributed in countless ways to the Space Environment Monitors that are included in both the GOES and POES satellites over the past three decades, is also acknowledged with pleasure. The contributions of Mr. William Barrett, Mr. Kelvin Fedrick, and Mr. Paul Packard to the assimilation of the SEM-2 data stream provided from the central processing facility at NESDIS were very important as were Mr. Barrett's oversight of the SEM-2 DPU design. Ms. Susan Sahm contributed significantly to the SEM-2 data processing program that created the archive file. Mr. Lawrence Puga did a masterful job of editing this document. Finally, the Space Environment Center would like to thank the technical and management staff at Panametrics, Inc., for the high quality design, construction, and testing of the SEM-2 instruments that was so critical to the success of the program.

References

Raben, V.J., D.S. Evans, H.H. Sauer, S.R. Sahm, and M. Huynh, TIROS/NOAA Satellite Space Environment Monitor Data Archive Documentation: 1995 Update, NOAA Technical Memorandum ERL SEL-86, February, 1995.

Cole, K.D., Eccentric Dipole Coodinates, Aust. J. Phys. **16**, 423-429, 1963.

Fraser-Smith, A.C., Centered and Eccentric Geomagnetic Dipoles and Their Poles, 1600-1985, Rev. Geophys., **25**, 1-16, 1987.

Gustafsson, G., N.E. Papitashvili, and V.O. Papitashvili, A Revised Corrected Geomagnetic Coordinate System for Epochs 1985 and 1990, J. Atmos. Terr. Phys., **54**, 1609-1631, 1992.

Appendix A. ARCHIVE RECORD

The POES archive record comprises 32 seconds of SEM-2 data together with all added orbital, quality, and ancillary data. It consists of a single record of 2544 bytes. Various data parameters occur in this string as 1-, 2-, or 4-byte integer entities. Depending on the parameter, once it is unpacked from the archive record, the entity is either left unaltered, is expanded using a lookup table, or is converted to physical units using an appropriate conversion factor. The result of the unpacking is the data arrays, both integer and non-integer ("float" in 'C', "real" in FORTRAN) that have been described above. The following table shows the characteristics and treatment of the parameters that result in the 32-second data set. Sample programs for unpacking the archive record are provided in Appendix D ('C' language) and Appendix E (FORTRAN).

The following table identifies each entity in the packed archive record and the corresponding parameter in each of the unpacked data arrays. The table uses FORTRAN indexing notation. In 'C' the indices would start with 0, and multi-dimensional arrays would have their dimensions reversed.

The decimal conversion factors listed in the right hand column are the multiplicative factors used to convert from the integer-type entity to a decimal value of a parameter in proper physical units. Conversion factors labled "table" refer to the lookup table in Appendix B that is used to convert sensor responses telemetered from the POES satellite to "decompressed" sensor counts.

The Archive Record as a Byte Array

Packed		Unpacked Parameter	Range	Units	Conversion Factor
Byte Number	Len				
0	4	*cSumFlag*	0 = good data 1 = checksum does not match, bad data 2 = checksum not available for comparison	N/A	none
4	4	*cSum*	0-255	N/A	none
8	2	*major*	0-7	N/A	none
10	1	*status*(1)	0 or 1	N/A	none
11	1	*status*(2)	0 or 1	N/A	none
12	1	*status*(3)	0 or 1	N/A	none
13	1	*status*(4)	0 or 1	N/A	none
14	1	*status*(5)	0 to 3		
15	1	*status*(6)	0 to 3		
16	1	*status*(7)	0 to 7		
17	1	*status*(8)	0 to 7		
18	1	*status*(9)	0 or 1		
19	1	*status*(10)	0 or 1		
20	4	*analog*(1)			0.0001
24	4	*analog*(2)			0.0001
28	4	*analog*(3)			0.0001
32	4	*analog*(4)			0.0001
36	4	*analog*(5)			0.0001
40	4	*analog*(6)			0.0001
44	4	*analog*(7)			0.0001
48	4	*analog*(8)			0.0001
52	4	*analog*(9)			0.0001
56	4	*analog*(10)			0.0001
60	4	*analog*(11)			0.0001
64	4	*analog*(12)			0.0001
68	4	*analog*(13)			0.0001
72	4	*analog*(14)			0.0001
76	4	*analog*(15)			0.0001
80	4	*analog*(16)			0.0001
84	4	*analog*(17)			0.0001
88	4	*ssLoc*(1, 1), *head*(2,1)	+90.0 to -90.0	degrees	0.0001
92	4	*ssLoc*(1, 2)	+90.0 to -90.0	degrees	0.0001
96	4	*ssLoc*(1, 3)	+90.0 to -90.0	degrees	0.0001
100	4	*ssLoc*(1, 4)	+90.0 to -90.0	degrees	0.0001
104	4	*ssLoc*(2, 1), *head*(3,1)	0.0 to 360.0	degrees	0.0001
108	4	*ssLoc*(2, 2)	0.0 to 360.0	degrees	0.0001
112	4	*ssLoc*(2, 3)	0.0 to 360.0	degrees	0.0001
116	4	*ssLoc*(2, 4)	0.0 to 360.0	degrees	0.0001
120	4	*ssLoc*(1, 5), *head*(2,2)	+90.0 to -90.0	degrees	0.0001
124	4	*ssLoc*(1, 6)	+90.0 to -90.0	degrees	0.0001
128	4	*ssLoc*(1, 7)	+90.0 to -90.0	degrees	0.0001
132	4	*ssLoc*(1, 8)	+90.0 to -90.0	degrees	0.0001
136	4	*ssLoc*(2, 5), *head*(3,2)	0.0 to 360.0	degrees	0.0001

Packed		Unpacked Parameter	Range	Units	Conversion Factor
Byte Number	Len				
140	4	*ssLoc*(2, 6)	0.0 to 360.0	degrees	0.0001
144	4	*ssLoc*(2, 7)	0.0 to 360.0	degrees	0.0001
148	4	*ssLoc*(2, 8)	0.0 to 360.0	degrees	0.0001
152	4	*ssLoc*(1, 9), *head*(2,3)	+90.0 to -90.0	degrees	0.0001
156	4	*ssLoc*(1,10)	+90.0 to -90.0	degrees	0.0001
160	4	*ssLoc*(1,11)	+90.0 to -90.0	degrees	0.0001
164	4	*ssLoc*(1,12)	+90.0 to -90.0	degrees	0.0001
168	4	*ssLoc*(2, 9), *head*(3,3)	0.0 to 360.0	degrees	0.0001
172	4	*ssLoc*(2,10)	0.0 to 360.0	degrees	0.0001
176	4	*ssLoc*(2,11)	0.0 to 360.0	degrees	0.0001
180	4	*ssLoc*(2,12)	0.0 to 360.0	degrees	0.0001
184	4	*ssLoc*(1,13), *head*(2,4)	+90.0 to -90.0	degrees	0.0001
188	4	*ssLoc*(1,14)	+90.0 to -90.0	degrees	0.0001
192	4	*ssLoc*(1,15)	+90.0 to -90.0	degrees	0.0001
196	4	*ssLoc*(1,16)	+90.0 to -90.0	degrees	0.0001
200	4	*ssLoc*(2,13), *head*(3,4)	0.0 to 360.0	degrees	0.0001
204	4	*ssLoc*(2,14)	0.0 to 360.0	degrees	0.0001
208	4	*ssLoc*(2,15)	0.0 to 360.0	degrees	0.0001
212	4	*ssLoc*(2,16)	0.0 to 360.0	degrees	0.0001
216	4	*ihd*(1,1)	NOAA-15 is 4	N/A	none
220	4	*ihd*(2,1)	1998 -	None	none
224	4	*ihd*(3,1)	1 to 366	Day No	none
228	4	*ihd*(4,1)	0 to 86400000	msec	none
232	4	*ihd*(5,1)		Km	none
236	4	*head*(1,1)	nominal 98.6	degrees	0.0001
240	4	*ihd*(6,1)	1 to 65535	N/A	none
244	2	*qual*(1)	*	N/A	none
246	2	*qual*(2)	*	N/A	none
248	2	*qual*(3)	*	N/A	none
250	2	*qual*(4)	*	N/A	none
252	2	*minor*(1)	0	N/A	none
254	2	*minor*(2)	020	N/A	none
256	2	*minor*(3)	040	N/A	none
258	2	*minor*(4)	060	N/A	none
260	40	*mdf*(1 to 40, 1)	0 or 1	N/A	none
300	40	*mdf*(1 to 40, 2)	0 or 1	N/A	none
340	40	*mdf*(1 to 40, 3)	0 or 1	N/A	none
380	40	*mdf*(1 to 40, 4)	0 or 1	N/A	none
420	4	*ihd*(1,2)	NOAA-15 is 4	N/A	none
424	4	*ihd*(2,2)	1998 -	None	none
428	4	*ihd*(3,2)	1 to 366	Day No	none
432	4	*ihd*(4,2)	0-86400000	msec	none
436	4	*ihd*(5,2)		Km	none
440	4	*head*(1,2)	nominal 98.6	degrees	0.0001
444	4	*ihd*(6,2)	1 to 65535	N/A	none
448	2	*qual*(5)	*	N/A	none
450	2	*qual*(6)	*	N/A	none
452	2	*qual*[7)	*	N/A	none
454	2	*qual*(8)	*	N/A	none
456	2	*minor*(5)	080	N/A	none

Packed		Unpacked Parameter	Range	Units	Conversion Factor
Byte Number	Len				
458	2	*minor*(6)	100	N/A	none
460	2	*minor*(7)	120	N/A	none
462	2	*minor*(8)	140	N/A	none
464	40	*mdf*(1 to 40, 5)	0 or 1	N/A	none
504	40	*mdf*(1 to 40, 6)	0 or 1	N/A	none
544	40	*mdf*(1 to 40, 7)	0 or 1	N/A	none
584	40	*mdf*(1 to 40, 8)	0 or 1	N/A	none
624	4	*ihd*(1,3)	NOAA-15 is 4	N/A	none
628	4	*ihd*(2,3)	1998 -	None	none
632	4	*ihd*(3,3)	1 to 366	Day No	none
636	4	*ihd*(4,3)	0-86400000	msec	none
640	4	*ihd*(5,3)		Km	none
644	4	*head*(1,3)	nominal 98.6	degrees	0.0001
648	4	*ihd*(6,3)	1 to 65535	N/A	none
652	2	*qual*(9)	*	N/A	none
654	2	*qual*(10)	*	N/A	none
656	2	*qual*(11)	*	N/A	none
658	2	*qual*(12)	*	N/A	none
660	2	*minor*(9)	160	N/A	none
662	2	*minor*(10)	180	N/A	none
664	2	*minor*(11)	200	N/A	none
666	2	*minor*(12)	220	N/A	none
668	40	*mdf*(1 to 40, 9)	0 or 1	N/A	none
708	40	*mdf*(1 to 40,10)	0 or 1	N/A	none
748	40	*mdf*(1 to 40,11)	0 or 1	N/A	none
788	40	*mdf*(1 to 40,12)	0 or 1	N/A	none
828	4	*ihd*(1,4)	NOAA-15 is 4	N/A	none
832	4	*ihd*(2,4)	1998 -	None	none
836	4	*ihd*(3,4)	1 to 366	Day No	none
840	4	*ihd*(4,4)	0-86400000	msec	none
844	4	*ihd*(5,4)		Km	none
848	4	*head*(1,4)	nominal 98.6	degrees	0.0001
852	4	*ihd*(6,4)	1 to 65535	N/A	none
856	2	*qual*(13)	*	N/A	none
858	2	*qual*(14)	*	N/A	none
860	2	*qual*(15)	*	N/A	none
862	2	*qual*(16)	*	N/A	none
864	2	*minor*(13)	240	N/A	none
866	2	*minor*(14)	260	N/A	none
868	2	*minor*(15)	280	N/A	none
870	2	*minor*(16)	300	N/A	none
872	40	*mdf*(1 to 40,13)	0 or 1	N/A	none
912	40	*mdf*(1 to 40,14)	0 or 1	N/A	none
952	40	*mdf*(1 to 40,15)	0 or 1	N/A	none
992	40	*mdf*(1 to 40,16)	0 or 1	N/A	none
1032	1	*mep0*(1, 1)	0 to 255	counts	table
1033	1	*mep0*(2, 1)	0 to 255	counts	table
1034	1	*mep0*(3, 1)	0 to 255	counts	table
1035	1	*mep0*(4, 1)	0 to 255	counts	table
1036	1	*mep0*(5, 1)	0 to 255	counts	table

Packed		Unpacked Parameter	Range	Units	Conversion Factor
Byte Number	Len				
1037	1	*mep0*(6, 1)	0 to 255	counts	table
1038	1	*mep0*(7, 1)	0 to 255	counts	table
1039	1	*mep0*(8, 1)	0 to 255	counts	table
1040	1	*mep0*(9, 1)	0 to 255	counts	table
1041	1	*mep0*(1, 2)	0 to 255	counts	table
1042	1	*mep0*(2, 2)	0 to 255	counts	table
1043	1	*mep0*(3, 2)	0 to 255	counts	table
1044	1	*mep0*(4, 2)	0 to 255	counts	table
1045	1	*mep0*(5, 2)	0 to 255	counts	table
1046	1	*mep0*(6, 2)	0 to 255	counts	table
1047	1	*mep0*(7, 2)	0 to 255	counts	table
1048	1	*mep0*(8, 2)	0 to 255	counts	table
1049	1	*mep0*(9, 2)	0 to 255	counts	table
1050	1	*mep0*(1, 3)	0 to 255	counts	table
1051	1	*mep0*(2, 3)	0 to 255	counts	table
1052	1	*mep0*(3, 3)	0 to 255	counts	table
1053	1	*mep0*(4, 3)	0 to 255	counts	table
1054	1	*mep0*(5, 3)	0 to 255	counts	table
1055	1	*mep0*(6, 3)	0 to 255	counts	table
1056	1	*mep0*(7, 3)	0 to 255	counts	table
1057	1	*mep0*(8, 3)	0 to 255	counts	table
1058	1	*mep0*(9, 3)	0 to 255	counts	table
1059	1	*mep0*(1, 4)	0 to 255	counts	table
1060	1	*mep0*(2, 4)	0 to 255	counts	table
1061	1	*mep0*(3, 4)	0 to 255	counts	table
1062	1	*mep0*(4, 4)	0 to 255	counts	table
1063	1	*mep0*(5, 4)	0 to 255	counts	table
1064	1	*mep0*(6, 4)	0 to 255	counts	table
1065	1	*mep0*(7, 4)	0 to 255	counts	table
1066	1	*mep0*(8, 4)	0 to 255	counts	table
1067	1	*mep0*(9, 4)	0 to 255	counts	table
1068	1	*mep90*(1, 1)	0 to 255	counts	table
1069	1	*mep90*(2, 1)	0 to 255	counts	table
1070	1	*mep90*(3, 1)	0 to 255	counts	table
1071	1	*mep90*(4, 1)	0 to 255	counts	table
1072	1	*mep90*(5, 1)	0 to 255	counts	table
1073	1	*mep90*(6, 1)	0 to 255	counts	table
1074	1	*mep90*(7, 1)	0 to 255	counts	table
1075	1	*mep90*(8, 1)	0 to 255	counts	table
1076	1	*mep90*(9, 1)	0 to 255	counts	table
1077	1	*mep90*(1, 2)	0 to 255	counts	table
1078	1	*mep90*(2, 2)	0 to 255	counts	table
1079	1	*mep90*(3, 2)	0 to 255	counts	table
1080	1	*mep90*(4, 2)	0 to 255	counts	table
1081	1	*mep90*(5, 2)	0 to 255	counts	table
1082	1	*mep90*(6, 2)	0 to 255	counts	table
1083	1	*mep90*(7, 2)	0 to 255	counts	table
1084	1	*mep90*(8, 2)	0 to 255	counts	table
1085	1	*mep90*(9, 2)	0 to 255	counts	table
1086	1	*mep90*(1, 3)	0 to 255	counts	table

Packed		Unpacked Parameter	Range	Units	Conversion Factor
Byte Number	Len				
1087	1	*mep90*(2, 3)	0 to 255	counts	table
1088	1	*mep90*(3, 3)	0 to 255	counts	table
1089	1	*mep90*(4, 3)	0 to 255	counts	table
1090	1	*mep90*(5, 3)	0 to 255	counts	table
1091	1	*mep90*(6, 3)	0 to 255	counts	table
1092	1	*mep90*(7, 3)	0 to 255	counts	table
1093	1	*mep90*(8, 3)	0 to 255	counts	table
1094	1	*mep90*(9, 3)	0 to 255	counts	table
1095	1	*mep90*(1, 4)	0 to 255	counts	table
1096	1	*mep90*(2, 4)	0 to 255	counts	table
1097	1	*mep90*(3, 4)	0 to 255	counts	table
1098	1	*mep90*(4, 4)	0 to 255	counts	table
1099	1	*mep90*(5, 4)	0 to 255	counts	table
1100	1	*mep90*(6, 4)	0 to 255	counts	table
1101	1	*mep90*(7, 4)	0 to 255	counts	table
1102	1	*mep90*(8, 4)	0 to 255	counts	table
1103	1	*mep90*(9, 4)	0 to 255	counts	table
1104	1	*mepOmni*(1, 1)	0 to 255	counts	table
1105	1	*mepOmni*(2, 1)	0 to 255	counts	table
1106	1	*mepOmni*(3, 1)	0 to 255	counts	table
1107	1	ignore entry			
1108	1	*mepOmni*(1, 2)	0 to 255	counts	table
1109	1	*mepOmni*(2, 2)	0 to 255	counts	table
1110	1	ignore entry			
1111	1	*mepOmni*(4, 2)	0 to 255	counts	table
1112	1	*mepOmni*(1, 3)	0 to 255	counts	table
1113	1	*mepOmni*(2, 3)	0 to 255	counts	table
1114	1	*mepOmni*(3, 3)	0 to 255	counts	table
1115	1	ignore entry			
1116	1	*mepOmni*(1, 4)	0 to 255	counts	table
1117	1	*mepOmni*(2, 4)	0 to 255	counts	table
1118	1	ignore entry			
1119	1	*mepOmni*(4, 4)	0 to 255	counts	table
1120	1	*ted0*(1, 1)	0 to 255	counts	table
1121	1	*ted0*(2, 1)	0 to 255	counts	table
1122	1	*ted0*(3, 1)	0 to 255	counts	table
1123	1	*ted0*(4, 1)	0 to 255	counts	table
1124	1	*ted0*(1, 2)	0 to 255	counts	table
1125	1	*ted0*(2, 2)	0 to 255	counts	table
1126	1	*ted0*(3, 2)	0 to 255	counts	table
1127	1	*ted0*(4, 2)	0 to 255	counts	table
1128	1	*ted0*(1, 3)	0 to 255	counts	table
1129	1	*ted0*(2, 3)	0 to 255	counts	table
1130	1	*ted0*(3, 3)	0 to 255	counts	table
1131	1	*ted0*(4, 3)	0 to 255	counts	table
1132	1	*ted0*(1, 4)	0 to 255	counts	table
1133	1	*ted0*(2, 4)	0 to 255	counts	table
1134	1	*ted0*(3, 4)	0 to 255	counts	table
1135	1	*ted0*(4, 4)	0 to 255	counts	table
1136	1	*ted0*(5, 1)	0 to 15	N/A	none

Packed		Unpacked Parameter	Range	Units	Conversion Factor
Byte Number	Len				
1137	1	*ted0*(6, 1)	0 to 15	N/A	table
1138	1	*ted0*(7, 1)	0 to 255	counts	table
1139	1	*ted0*(8, 1)	0 to 255	counts	table
1140	1	*ted0*(5, 2)	0 to 15	N/A	table
1141	1	*ted0*(6, 2)	0 to 15	N/A	table
1142	1	*ted0*(7, 2)	0 to 255	counts	table
1143	1	*ted0*(8, 2)	0 to 255	counts	table
1144	1	*ted0*(5, 3)	0 to 15	N/A	table
1145	1	*ted0*(6, 3)	0 to 15	N/A	table
1146	1	*ted0*(7, 3)	0 to 255	counts	table
1147	1	*ted0*(8, 3)	0 to 255	counts	table
1148	1	*ted0*(5, 4)	0 to 15	N/A	none
1149	1	*ted0*(6, 4)	0 to 15	N/A	none
1150	1	*ted0*(7, 4)	0 to 255	counts	table
1151	1	*ted0*(8, 4)	0 to 255	counts	table
1152	1	*ted30*(1, 1)	0 to 255	counts	table
1153	1	*ted30*(2, 1)	0 to 255	counts	table
1154	1	*ted30*(3, 1)	0 to 255	counts	table
1155	1	*ted30*(4, 1)	0 to 255	counts	table
1156	1	*ted30*(1, 2)	0 to 255	counts	table
1157	1	*ted30*(2, 2)	0 to 255	counts	table
1158	1	*ted30*(3, 2)	0 to 255	counts	table
1159	1	*ted30*(4, 2)	0 to 255	counts	table
1160	1	*ted30*(1, 3)	0 to 255	counts	table
1161	1	*ted30*(2, 3)	0 to 255	counts	table
1162	1	*ted30*(3, 3)	0 to 255	counts	table
1163	1	*ted30*(4, 3)	0 to 255	counts	table
1164	1	*ted30*(1, 4)	0 to 255	counts	table
1165	1	*ted30*(2, 4)	0 to 255	counts	table
1166	1	*ted30*(3, 4)	0 to 255	counts	table
1167	1	*ted30*(4, 4)	0 to 255	counts	table
1168	1	*ted30*(5, 1)	0 to 15	N/A	none
1169	1	*ted30*(6, 1)	0 to 15	N/A	none
1170	1	*ted30*(7, 1)	0 to 255	counts	table
1171	1	*ted30*(8, 1)	0 to 255	counts	table
1172	1	*ted30*(5, 2)	0 to 15	N/A	none
1173	1	*ted30*(6, 2)	0 to 15	N/A	none
1174	1	*ted30*(7, 2)	0 to 255	counts	table
1175	1	*ted30*(8, 2)	0 to 255	counts	table
1176	1	*ted30*(5, 3)	0 to 15	N/A	none
1177	1	*ted30*(6, 3)	0 to 15	N/A	none
1178	1	*ted30*(7, 3)	0 to 255	counts	table
1179	1	*ted30*(8, 3)	0 to 255	counts	table
1180	1	*ted30*(5, 4)	0 to 15	N/A	none
1181	1	*ted30*(6, 4)	0 to 15	N/A	none
1182	1	*ted30*(7, 4)	0 to 255	counts	table
1183	1	*ted30*(8, 4)	0 to 255	counts	table
1184	1	*mep0*(1, 5)	0 to 255	counts	table
1185	1	*mep0*(2, 5)	0 to 255	counts	table
1186	1	*mep0*(3, 5)	0 to 255	counts	table

Packed		Unpacked Parameter	Range	Units	Conversion Factor
Byte Number	Len				
1187	1	*mep0*(4, 5)	0 to 255	counts	table
1188	1	*mep0*(5, 5)	0 to 255	counts	table
1189	1	*mep0*(6, 5)	0 to 255	counts	table
1190	1	*mep0*(7, 5)	0 to 255	counts	table
1191	1	*mep0*(8, 5)	0 to 255	counts	table
1192	1	*mep0*(9, 5)	0 to 255	counts	table
1193	1	*mep0*(1, 6)	0 to 255	counts	table
1194	1	*mep0*(2, 6)	0 to 255	counts	table
1195	1	*mep0*(3, 6)	0 to 255	counts	table
1196	1	*mep0*(4, 6)	0 to 255	counts	table
1197	1	*mep0*(5, 6)	0 to 255	counts	table
1198	1	*mep0*(6, 6)	0 to 255	counts	table
1199	1	*mep0*(7, 6)	0 to 255	counts	table
1200	1	*mep0*(8, 6)	0 to 255	counts	table
1201	1	*mep0*(9, 6)	0 to 255	counts	table
1202	1	*mep0*(1, 7)	0 to 255	counts	table
1203	1	*mep0*(2, 7)	0 to 255	counts	table
1204	1	*mep0*(3, 7)	0 to 255	counts	table
1205	1	*mep0*(4, 7)	0 to 255	counts	table
1206	1	*mep0*(5, 7)	0 to 255	counts	table
1207	1	*mep0*(6, 7)	0 to 255	counts	table
1208	1	*mep0*(7, 7)	0 to 255	counts	table
1209	1	*mep0*(8, 7)	0 to 255	counts	table
1210	1	*mep0*(9, 7)	0 to 255	counts	table
1211	1	*mep0*(1, 8)	0 to 255	counts	table
1212	1	*mep0*(2, 8)	0 to 255	counts	table
1213	1	*mep0*(3, 8)	0 to 255	counts	table
1214	1	*mep0*(4, 8)	0 to 255	counts	table
1215	1	*mep0*(5, 8)	0 to 255	counts	table
1216	1	*mep0*(6, 8)	0 to 255	counts	table
1217	1	*mep0*(7, 8)	0 to 255	counts	table
1218	1	*mep0*(8, 8)	0 to 255	counts	table
1219	1	*mep0*(9, 8)	0 to 255	counts	table
1220	1	*mep90*(1, 5)	0 to 255	counts	table
1221	1	*mep90*(2, 5)	0 to 255	counts	table
1222	1	*mep90*(3, 5)	0 to 255	counts	table
1223	1	*mep90*(4, 5)	0 to 255	counts	table
1224	1	*mep90*(5, 5)	0 to 255	counts	table
1225	1	*mep90*(6, 5)	0 to 255	counts	table
1226	1	*mep90*(7, 5)	0 to 255	counts	table
1227	1	*mep90*(8, 5)	0 to 255	counts	table
1228	1	*mep90*(9, 5)	0 to 255	counts	table
1229	1	*mep90*(1, 6)	0 to 255	counts	table
1230	1	*mep90*(2, 6)	0 to 255	counts	table
1231	1	*mep90*(3, 6)	0 to 255	counts	table
1232	1	*mep90*(4, 6)	0 to 255	counts	table
1233	1	*mep90*(5, 6)	0 to 255	counts	table
1234	1	*mep90*(6, 6)	0 to 255	counts	table
1235	1	*mep90*(7, 6)	0 to 255	counts	table
1236	1	*mep90*(8, 6)	0 to 255	counts	table

Packed		Unpacked Parameter	Range	Units	Conversion Factor
Byte Number	Len				
1237	1	*mep90*(9, 6)	0 to 255	counts	table
1238	1	*mep90*(1, 7)	0 to 255	counts	table
1239	1	*mep90*(2, 7)	0 to 255	counts	table
1240	1	*mep90*(3, 7)	0 to 255	counts	table
1241	1	*mep90*(4, 7)	0 to 255	counts	table
1242	1	*mep90*(5, 7)	0 to 255	counts	table
1243	1	*mep90*(6, 7)	0 to 255	counts	table
1244	1	*mep90*(7, 7)	0 to 255	counts	table
1245	1	*mep90*(8, 7)	0 to 255	counts	table
1246	1	*mep90*(9, 7)	0 to 255	counts	table
1247	1	*mep90*(1, 8)	0 to 255	counts	table
1248	1	*mep90*(2, 8)	0 to 255	counts	table
1249	1	*mep90*(3, 8)	0 to 255	counts	table
1250	1	*mep90*(4, 8)	0 to 255	counts	table
1251	1	*mep90*(5, 8)	0 to 255	counts	table
1252	1	*mep90*(6, 8)	0 to 255	counts	table
1253	1	*mep90*(7, 8)	0 to 255	counts	table
1254	1	*mep90*(8, 8)	0 to 255	counts	table
1255	1	*mep90*(9, 8)	0 to 255	counts	table
1256	1	*mepOmni*(1, 5)	0 to 255	counts	table
1257	1	*mepOmni*(2, 5)	0 to 255	counts	table
1258	1	*mepOmni*(3, 5)	0 to 255	counts	table
1259	1	ignore entry			
1260	1	*mepOmni*(1, 6)	0 to 255	counts	table
1261	1	*mepOmni*(2, 6)	0 to 255	counts	table
1262	1	ignore entry			
1263	1	*mepOmni*(4, 6)	0 to 255	counts	table
1264	1	*mepOmni*(1, 7)	0 to 255	counts	table
1265	1	*mepOmni*(2, 7)	0 to 255	counts	table
1266	1	*mepOmni*(3, 7)	0 to 255	counts	table
1267	1	ignore entry			
1268	1	*mepOmni*(1, 8)	0 to 255	counts	table
1269	1	*mepOmni*(2, 8)	0 to 255	counts	table
1270	1	ignore entry			
1271	1	*mepOmni*(4, 8)	0 to 255	counts	table
1272	1	*ted0*(1, 5)	0 to 255	counts	table
1273	1	*ted0*(2, 5)	0 to 255	counts	table
1274	1	*ted0*(3, 5)	0 to 255	counts	table
1275	1	*ted0*(4, 5)	0 to 255	counts	table
1276	1	*ted0*(1, 6)	0 to 255	counts	table
1277	1	*ted0*(2, 6)	0 to 255	counts	table
1278	1	*ted0*(3, 6)	0 to 255	counts	table
1279	1	*ted0*(4, 6)	0 to 255	counts	table
1280	1	*ted0*(1, 7)	0 to 255	counts	table
1281	1	*ted0*(2, 7)	0 to 255	counts	table
1282	1	*ted0*(3, 7)	0 to 255	counts	table
1283	1	*ted0*(4, 7)	0 to 255	counts	table
1284	1	*ted0*(1, 8)	0 to 255	counts	table
1285	1	*ted0*(2, 8)	0 to 255	counts	table
1286	1	*ted0*(3, 8)	0 to 255	counts	table

Packed		Unpacked Parameter	Range	Units	Conversion Factor
Byte Number	Len				
1287	1	*ted0*(4, 8)	0 to 255	counts	table
1288	1	*ted0*(5, 5)	0 to 15	N/A	none
1289	1	*ted0*(6, 5)	0 to 15	N/A	none
1290	1	*ted0*(7, 5)	0 to 255	counts	table
1291	1	*ted0*(8, 5)	0 to 255	counts	table
1292	1	*ted0*(5, 6)	0 to 15	N/A	none
1293	1	*ted0*(6, 6)	0 to 15	N/A	none
1294	1	*ted0*(7, 6)	0 to 255	counts	table
1295	1	*ted0*(8, 6)	0 to 255	counts	table
1296	1	*ted0*(5, 7)	0 to 15	N/A	none
1297	1	*ted0*(6, 7)	0 to 15	N/A	none
1298	1	*ted0*(7, 7)	0 to 255	counts	table
1299	1	*ted0*(8, 7)	0 to 255	counts	table
1300	1	*ted0*(5, 8)	0 to 15	N/A	none
1301	1	*ted0*(6, 8)	0 to 15	N/A	none
1302	1	*ted0*(7, 8)	0 to 255	counts	table
1303	1	*ted0*(8, 8)	0 to 255	counts	table
1304	1	*ted30*(1, 5)	0 to 255	counts	table
1305	1	*ted30*(2, 5)	0 to 255	counts	table
1306	1	*ted30*(3, 5)	0 to 255	counts	table
1307	1	*ted30*(4, 5)	0 to 255	counts	table
1308	1	*ted30*(1, 6)	0 to 255	counts	table
1309	1	*ted30*(2, 6)	0 to 255	counts	table
1310	1	*ted30*(3, 6)	0 to 255	counts	table
1311	1	*ted30*(4, 6)	0 to 255	counts	table
1312	1	*ted30*(1, 7)	0 to 255	counts	table
1313	1	*ted30*(2, 7)	0 to 255	counts	table
1314	1	*ted30*(3, 7)	0 to 255	counts	table
1315	1	*ted30*(4, 7)	0 to 255	counts	table
1316	1	*ted30*(1, 8)	0 to 255	counts	table
1317	1	*ted30*(2, 8)	0 to 255	counts	table
1318	1	*ted30*(3, 8)	0 to 255	counts	table
1319	1	*ted30*(4, 8)	0 to 255	counts	table
1320	1	*ted30*(5, 5)	0 to 15	N/A	none
1321	1	*ted30*(6, 5)	0 to 15	N/A	none
1322	1	*ted30*(7, 5)	0 to 255	counts	table
1323	1	*ted30*(8, 5)	0 to 255	counts	table
1324	1	*ted30*(5, 6)	0 to 15	N/A	none
1325	1	*ted30*(6, 6)	0 to 15	N/A	none
1326	1	*ted30*(7, 6)	0 to 255	counts	table
1327	1	*ted30*(8, 6)	0 to 255	counts	table
1328	1	*ted30*(5, 7)	0 to 15	N/A	none
1329	1	*ted30*(6, 7)	0 to 15	N/A	none
1330	1	*ted30*(7, 7)	0 to 255	counts	table
1331	1	*ted30*(8, 7)	0 to 255	counts	table
1332	1	*ted30*(5, 8)	0 to 15	N/A	none
1333	1	*ted30*(6, 8)	0 to 15	N/A	none
1334	1	*ted30*(7, 8)	0 to 255	counts	table
1335	1	*ted30*(8, 8)	0 to 255	counts	table
1336	1	*mep0*(1, 9)	0 to 255	counts	table

Packed		Unpacked Parameter	Range	Units	Conversion Factor
Byte Number	Len				
1337	1	*mep0*(2, 9)	0 to 255	counts	table
1338	1	*mep0*(3, 9)	0 to 255	counts	table
1339	1	*mep0*(4, 9)	0 to 255	counts	table
1340	1	*mep0*(5, 9)	0 to 255	counts	table
1341	1	*mep0*(6, 9)	0 to 255	counts	table
1342	1	*mep0*(7, 9)	0 to 255	counts	table
1343	1	*mep0*(8, 9)	0 to 255	counts	table
1344	1	*mep0*(9, 9)	0 to 255	counts	table
1345	1	*mep0*(1,10)	0 to 255	counts	table
1346	1	*mep0*(2,10)	0 to 255	counts	table
1347	1	*mep0*(3,10)	0 to 255	counts	table
1348	1	*mep0*(4,10)	0 to 255	counts	table
1349	1	*mep0*(5,10)	0 to 255	counts	table
1350	1	*mep0*(6,10)	0 to 255	counts	table
1351	1	*mep0*(7,10)	0 to 255	counts	table
1352	1	*mep0*(8,10)	0 to 255	counts	table
1353	1	*mep0*(9,10)	0 to 255	counts	table
1354	1	*mep0*(1,11)	0 to 255	counts	table
1355	1	*mep0*(2,11)	0 to 255	counts	table
1356	1	*mep0*(3,11)	0 to 255	counts	table
1357	1	*mep0*(4,11)	0 to 255	counts	table
1358	1	*mep0*(5,11)	0 to 255	counts	table
1359	1	*mep0*(6,11)	0 to 255	counts	table
1360	1	*mep0*(7,11)	0 to 255	counts	table
1361	1	*mep0*(8,11)	0 to 255	counts	table
1362	1	*mep0*(9,11)	0 to 255	counts	table
1363	1	*mep0*(1,12)	0 to 255	counts	table
1364	1	*mep0*(2,12)	0 to 255	counts	table
1365	1	*mep0*(3,12)	0 to 255	counts	table
1366	1	*mep0*(4,12)	0 to 255	counts	table
1367	1	*mep0*(5,12)	0 to 255	counts	table
1368	1	*mep0*(6,12)	0 to 255	counts	table
1369	1	*mep0*(7,12)	0 to 255	counts	table
1370	1	*mep0*(8,12)	0 to 255	counts	table
1371	1	*mep0*(9,12)	0 to 255	counts	table
1372	1	*mep90*(1, 9)	0 to 255	counts	table
1373	1	*mep90*(2, 9)	0 to 255	counts	table
1374	1	*mep90*(3, 9)	0 to 255	counts	table
1375	1	*mep90*(4, 9)	0 to 255	counts	table
1376	1	*mep90*(5, 9)	0 to 255	counts	table
1377	1	*mep90*(6, 9)	0 to 255	counts	table
1378	1	*mep90*(7, 9)	0 to 255	counts	table
1379	1	*mep90*(8, 9)	0 to 255	counts	table
1380	1	*mep90*(9, 9)	0 to 255	counts	table
1381	1	*mep90*(1,10)	0 to 255	counts	table
1382	1	*mep90*(2,10)	0 to 255	counts	table
1383	1	*mep90*(3,10)	0 to 255	counts	table
1384	1	*mep90*(4,10)	0 to 255	counts	table
1385	1	*mep90*(5,10)	0 to 255	counts	table
1386	1	*mep90*(6,10)	0 to 255	counts	table

Packed		Unpacked Parameter	Range	Units	Conversion Factor
Byte Number	Len				
1387	1	*mep90*(7,10)	0 to 255	counts	table
1388	1	*mep90*(8,10)	0 to 255	counts	table
1389	1	*mep90*(9,10)	0 to 255	counts	table
1390	1	*mep90*(1,11)	0 to 255	counts	table
1391	1	*mep90*(2,11)	0 to 255	counts	table
1392	1	*mep90*(3,11)	0 to 255	counts	table
1393	1	*mep90*(4,11)	0 to 255	counts	table
1394	1	*mep90*(5,11)	0 to 255	counts	table
1395	1	*mep90*(6,11)	0 to 255	counts	table
1396	1	*mep90*(7,11)	0 to 255	counts	table
1397	1	*mep90*(8,11)	0 to 255	counts	table
1398	1	*mep90*(9,11)	0 to 255	counts	table
1399	1	*mep90*(1,12)	0 to 255	counts	table
1400	1	*mep90*(2,12)	0 to 255	counts	table
1401	1	*mep90*(3,12)	0 to 255	counts	table
1402	1	*mep90*(4,12)	0 to 255	counts	table
1403	1	*mep90*(5,12)	0 to 255	counts	table
1404	1	*mep90*(6,12)	0 to 255	counts	table
1405	1	*mep90*(7,12)	0 to 255	counts	table
1406	1	*mep90*(8,12)	0 to 255	counts	table
1407	1	*mep90*(9,12)	0 to 255	counts	table
1408	1	*mepOmni*(1, 9)	0 to 255	counts	table
1409	1	*mepOmni*(2, 9)	0 to 255	counts	table
1410	1	*mepOmni*(3, 9)	0 to 255	counts	table
1411	1	ignore entry			
1412	1	*mepOmni*(1,10)	0 to 255	counts	table
1413	1	*mepOmni*(2,10)	0 to 255	counts	table
1414	1	ignore entry			
1415	1	*mepOmni*(4,10)	0 to 255	counts	table
1416	1	*mepOmni*(1,11)	0 to 255	counts	table
1417	1	*mepOmni*(2,11)	0 to 255	counts	table
1418	1	*mepOmni*(3,11)	0 to 255	counts	table
1419	1	ignore entry			
1420	1	*mepOmni*(1,12)	0 to 255	counts	table
1421	1	*mepOmni*(2,12)	0 to 255	counts	table
1422	1	ignore entry			
1423	1	*mepOmni*(4,12)	0 to 255	counts	table
1424	1	*ted0*(1, 9)	0 to 255	counts	table
1425	1	*ted0*(2, 9)	0 to 255	counts	table
1426	1	*ted0*(3, 9)	0 to 255	counts	table
1427	1	*ted0*(4, 9)	0 to 255	counts	table
1428	1	*ted0*(1,10)	0 to 255	counts	table
1429	1	*ted0*(2,10)	0 to 255	counts	table
1430	1	*ted0*(3,10)	0 to 255	counts	table
1431	1	*ted0*(4,10)	0 to 255	counts	table
1432	1	*ted0*(1,11)	0 to 255	counts	table
1433	1	*ted0*(2,11)	0 to 255	counts	table
1434	1	*ted0*(3,11)	0 to 255	counts	table
1435	1	*ted0*(4,11)	0 to 255	counts	table
1436	1	*ted0*(1,12)	0 to 255	counts	table

Packed		Unpacked Parameter	Range	Units	Conversion Factor
Byte Number	Len				
1437	1	*ted0*(2,12)	0 to 255	counts	table
1438	1	*ted0*(3,12)	0 to 255	counts	table
1439	1	*ted0*(4,12)	0 to 255	counts	table
1440	1	*ted0*(5, 9)	0 to 15	N/A	none
1441	1	*ted0*(6, 9)	0 to 15	N/A	none
1442	1	*ted0*(7, 9)	0 to 255	counts	table
1443	1	*ted0*(8, 9)	0 to 255	counts	table
1444	1	*ted0*(5,10)	0 to 15	N/A	none
1445	1	*ted0*(6,10)	0 to 15	N/A	none
1446	1	*ted0*(7,10)	0 to 255	counts	table
1447	1	*ted0*(8,10)	0 to 255	counts	table
1448	1	*ted0*(5,11)	0 to 15	N/A	none
1449	1	*ted0*(6,11)	0 to 15	N/A	none
1450	1	*ted0*(7,11)	0 to 255	counts	table
1451	1	*ted0*(8,11)	0 to 255	counts	table
1452	1	*ted0*(5,12)	0 to 15	N/A	none
1453	1	*ted0*(6,12)	0 to 15	N/A	none
1454	1	*ted0*(7,12)	0 to 255	counts	table
1455	1	*ted0*(8,12)	0 to 255	counts	table
1456	1	*ted30*(1, 9)	0 to 255	counts	table
1457	1	*ted30*(2, 9)	0 to 255	counts	table
1458	1	*ted30*(3, 9)	0 to 255	counts	table
1459	1	*ted30*(4, 9)	0 to 255	counts	table
1460	1	*ted30*(1,10)	0 to 255	counts	table
1461	1	*ted30*(2,10)	0 to 255	counts	table
1462	1	*ted30*(3,10)	0 to 255	counts	table
1463	1	*ted30*(4,10)	0 to 255	counts	table
1464	1	*ted30*(1,11)	0 to 255	counts	table
1465	1	*ted30*(2,11)	0 to 255	counts	table
1466	1	*ted30*(3,11)	0 to 255	counts	table
1467	1	*ted30*(4,11)	0 to 255	counts	table
1468	1	*ted30*(1,12)	0 to 255	counts	table
1469	1	*ted30*(2,12)	0 to 255	counts	table
1470	1	*ted30*(3,12)	0 to 255	counts	table
1471	1	*ted30*(4,12)	0 to 255	counts	table
1472	1	*ted30*(5, 9)	0 to 15	N/A	none
1473	1	*ted30*(6, 9)	0 to 15	N/A	none
1474	1	*ted30*(7, 9)	0 to 255	counts	table
1475	1	*ted30*(8, 9)	0 to 255	counts	table
1476	1	*ted30*(5,10)	0 to 15	N/A	none
1477	1	*ted30*(6,10)	0 to 15	N/A	none
1478	1	*ted30*(7,10)	0 to 255	counts	table
1479	1	*ted30*(8,10)	0 to 255	counts	table
1480	1	*ted30*(5,11)	0 to 15	N/A	none
1481	1	*ted30*(6,11)	0 to 15	N/A	none
1482	1	*ted30*(7,11)	0 to 255	counts	table
1483	1	*ted30*(8,11)	0 to 255	counts	table
1484	1	*ted30*(5,12)	0 to 15	N/A	none
1485	1	*ted30*(6,12)	0 to 15	N/A	none
1486	1	*ted30*(7,12)	0 to 255	counts	table

Packed		Unpacked Parameter	Range	Units	Conversion Factor
Byte Number	Len				
1487	1	*ted30*(8,12)	0 to 255	counts	table
1488	1	*mep0*(1,13)	0 to 255	counts	table
1489	1	*mep0*(2,13)	0 to 255	counts	table
1490	1	*mep0*(3,13)	0 to 255	counts	table
1491	1	*mep0*(4,13)	0 to 255	counts	table
1492	1	*mep0*(5,13)	0 to 255	counts	table
1493	1	*mep0*(6,13)	0 to 255	counts	table
1494	1	*mep0*(7,13)	0 to 255	counts	table
1495	1	*mep0*(8,13)	0 to 255	counts	table
1496	1	*mep0*(9,13)	0 to 255	counts	table
1497	1	*mep0*(1,14)	0 to 255	counts	table
1498	1	*mep0*(2,14)	0 to 255	counts	table
1499	1	*mep0*(3,14)	0 to 255	counts	table
1500	1	*mep0*(4,14)	0 to 255	counts	table
1501	1	*mep0*(5,14)	0 to 255	counts	table
1502	1	*mep0*(6,14)	0 to 255	counts	table
1503	1	*mep0*(7,14)	0 to 255	counts	table
1504	1	*mep0*(8,14)	0 to 255	counts	table
1505	1	*mep0*(9,14)	0 to 255	counts	table
1506	1	*mep0*(1,15)	0 to 255	counts	table
1507	1	*mep0*(2,15)	0 to 255	counts	table
1508	1	*mep0*(3,15)	0 to 255	counts	table
1509	1	*mep0*(4,15)	0 to 255	counts	table
1510	1	*mep0*(5,15)	0 to 255	counts	table
1511	1	*mep0*(6,15)	0 to 255	counts	table
1512	1	*mep0*(7,15)	0 to 255	counts	table
1513	1	*mep0*(8,15)	0 to 255	counts	table
1514	1	*mep0*(9,15)	0 to 255	counts	table
1515	1	*mep0*(1,16)	0 to 255	counts	table
1516	1	*mep0*(2,16)	0 to 255	counts	table
1517	1	*mep0*(3,16)	0 to 255	counts	table
1518	1	*mep0*(4,16)	0 to 255	counts	table
1519	1	*mep0*(5,16)	0 to 255	counts	table
1520	1	*mep0*(6,16)	0 to 255	counts	table
1521	1	*mep0*(7,16)	0 to 255	counts	table
1522	1	*mep0*(8,16)	0 to 255	counts	table
1523	1	*mep0*(9,16)	0 to 255	counts	table
1524	1	*mep90*(1,13)	0 to 255	counts	table
1525	1	*mep90*(2,13)	0 to 255	counts	table
1526	1	*mep90*(3,13)	0 to 255	counts	table
1527	1	*mep90*(4,13)	0 to 255	counts	table
1528	1	*mep90*(5,13)	0 to 255	counts	table
1529	1	*mep90*(6,13)	0 to 255	counts	table
1530	1	*mep90*(7,13)	0 to 255	counts	table
1531	1	*mep90*(8,13)	0 to 255	counts	table
1532	1	*mep90*(9,13)	0 to 255	counts	table
1533	1	*mep90*(1,14)	0 to 255	counts	table
1534	1	*mep90*(2,14)	0 to 255	counts	table
1535	1	*mep90*(3,14)	0 to 255	counts	table
1536	1	*mep90*(4,14)	0 to 255	counts	table

Packed		Unpacked Parameter	Range	Units	Conversion Factor
Byte Number	Len				
1537	1	*mep90*(5,14)	0 to 255	counts	table
1538	1	*mep90*(6,14)	0 to 255	counts	table
1539	1	*mep90*(7,14)	0 to 255	counts	table
1540	1	*mep90*(8,14)	0 to 255	counts	table
1541	1	*mep90*(9,14)	0 to 255	counts	table
1542	1	*mep90*(1,15)	0 to 255	counts	table
1543	1	*mep90*(2,15)	0 to 255	counts	table
1544	1	*mep90*(3,15)	0 to 255	counts	table
1545	1	*mep90*(4,15)	0 to 255	counts	table
1546	1	*mep90*(5,15)	0 to 255	counts	table
1547	1	*mep90*(6,15)	0 to 255	counts	table
1548	1	*mep90*(7,15)	0 to 255	counts	table
1549	1	*mep90*(8,15)	0 to 255	counts	table
1550	1	*mep90*(9,15)	0 to 255	counts	table
1551	1	*mep90*(1,16)	0 to 255	counts	table
1552	1	*mep90*(2,16)	0 to 255	counts	table
1553	1	*mep90*(3,16)	0 to 255	counts	table
1554	1	*mep90*(4,16)	0 to 255	counts	table
1555	1	*mep90*(5,16)	0 to 255	counts	table
1556	1	*mep90*(6,16)	0 to 255	counts	table
1557	1	*mep90*(7,16)	0 to 255	counts	table
1558	1	*mep90*(8,16)	0 to 255	counts	table
1559	1	*mep90*(9,16)	0 to 255	counts	table
1560	1	*mepOmni*(1,13)	0 to 255	counts	table
1561	1	*mepOmni*(2,13)	0 to 255	counts	table
1562	1	*mepOmni*(3,13)	0 to 255	counts	table
1563	1	ignore entry			
1564	1	*mepOmni*(1,14)	0 to 255	counts	table
1565	1	*mepOmni*(2,14)	0 to 255	counts	table
1566	1	ignore entry			
1567	1	*mepOmni*(4,14)	0 to 255	counts	table
1568	1	*mepOmni*(1,15)	0 to 255	counts	table
1569	1	*mepOmni*(2,15)	0 to 255	counts	table
1570	1	*mepOmni*(3,15)	0 to 255	counts	table
1571	1	ignore entry			
1572	1	*mepOmni*(1,16)	0 to 255	counts	table
1573	1	*mepOmni*(2,16)	0 to 255	counts	table
1574	1	ignore entry			
1575	1	*mepOmni*(4,16)	0 to 255	counts	table
1576	1	*ted0*(1,13)	0 to 255	counts	table
1577	1	*ted0*(2,13)	0 to 255	counts	table
1578	1	*ted0*(3,13)	0 to 255	counts	table
1579	1	*ted0*(4,13)	0 to 255	counts	table
1580	1	*ted0*(1,14)	0 to 255	counts	table
1581	1	*ted0*(2,14)	0 to 255	counts	table
1582	1	*ted0*(3,14)	0 to 255	counts	table
1583	1	*ted0*(4,14)	0 to 255	counts	table
1584	1	*ted0*(1,15)	0 to 255	counts	table
1585	1	*ted0*(2,15)	0 to 255	counts	table
1586	1	*ted0*(3,15)	0 to 255	counts	table

Packed		Unpacked Parameter	Range	Units	Conversion Factor
Byte Number	Len				
1587	1	*ted0*(4,15)	0 to 255	counts	table
1588	1	*ted0*(1,16)	0 to 255	counts	table
1589	1	*ted0*(2,16)	0 to 255	counts	table
1590	1	*ted0*(3,16)	0 to 255	counts	table
1591	1	*ted0*(4,16)	0 to 255	counts	table
1592	1	*ted0*(5,13)	0 to 15	N/A	none
1593	1	*ted0*(6,13)	0 to 15	N/A	none
1594	1	*ted0*(7,13)	0 to 255	counts	table
1595	1	*ted0*(8,13)	0 to 255	counts	table
1596	1	*ted0*(5,14)	0 to 15	N/A	none
1597	1	*ted0*(6,14)	0 to 15	N/A	none
1598	1	*ted0*(7,14)	0 to 255	counts	table
1599	1	*ted0*(8,14)	0 to 255	counts	table
1600	1	*ted0*(5,15)	0 to 15	N/A	none
1601	1	*ted0*(6,15)	0 to 15	N/A	none
1602	1	*ted0*(7,15)	0 to 255	counts	table
1603	1	*ted0*(8,15)	0 to 255	counts	table
1604	1	*ted0*(5,16)	0 to 15	N/A	none
1605	1	*ted0*(6,16)	0 to 15	N/A	none
1606	1	*ted0*(7,16)	0 to 255	counts	table
1607	1	*ted0*(8,16)	0 to 255	counts	table
1608	1	*ted30*(1,13)	0 to 255	counts	table
1609	1	*ted30*(2,13)	0 to 255	counts	table
1610	1	*ted30*(3,13)	0 to 255	counts	table
1611	1	*ted30*(4,13)	0 to 255	counts	table
1612	1	*ted30*(1,14)	0 to 255	counts	table
1613	1	*ted30*(2,14)	0 to 255	counts	table
1614	1	*ted30*(3,14)	0 to 255	counts	table
1615	1	*ted30*(4,14)	0 to 255	counts	table
1616	1	*ted30*(1,15)	0 to 255	counts	table
1617	1	*ted30*(2,15)	0 to 255	counts	table
1618	1	*ted30*(3,15)	0 to 255	counts	table
1619	1	*ted30*(4,15)	0 to 255	counts	table
1620	1	*ted30*(1,16)	0 to 255	counts	table
1621	1	*ted30*(2,16)	0 to 255	counts	table
1622	1	*ted30*(3,16)	0 to 255	counts	table
1623	1	*ted30*(4,16)	0 to 255	counts	table
1624	1	*ted30*(5,13)	0 to 15	N/A	none
1625	1	*ted30*(6,13)	0 to 15	N/A	none
1626	1	*ted30*(7,13)	0 to 255	counts	table
1627	1	*ted30*(8,13)	0 to 255	counts	table
1628	1	*ted30*(5,14)	0 to 15	N/A	none
1629	1	*ted30*(6,14)	0 to 15	N/A	none
1630	1	*ted30*(7,14)	0 to 255	counts	table
1631	1	*ted30*(8,14)	0 to 255	counts	table
1632	1	*ted30*(5,15)	0 to 15	N/A	none
1633	1	*ted30*(6,15)	0 to 15	N/A	none
1634	1	*ted30*(7,15)	0 to 255	counts	table
1635	1	*ted30*(8,15)	0 to 255	counts	table
1636	1	*ted30*(5,16)	0 to 15	N/A	none

Packed		Unpacked Parameter	Range	Units	Conversion Factor
Byte Number	Len				
1637	1	*ted30*(6,16)	0 to 15	N/A	none
1638	1	*ted30*(7,16)	0 to 255	counts	table
1639	1	*ted30*(8,16)	0 to 255	counts	table
1640	4	*head(* 4,1)		nT	0.0001
1644	4	*head(* 5,1)		nT	0.0001
1648	4	*head(* 6,1)		nT	0.0001
1652	4	*head(* 7,1)		nT	0.0001
1656	4	*head(* 8,1)	0.0 to 180.0	degrees	0.0001
1660	4	*head(* 9,1)	0.0 to 180.0	degrees	0.0001
1664	4	*head(*10,1)	0.0 to 180.0	degrees	0.0001
1668	4	*head(*11,1)	0.0 to 180.0	degrees	0.0001
1672	4	*head(*12,1)		nT	0.0001
1676	4	*head(*13,1)		nT	0.0001
1680	4	*head(*14,1)		nT	0.0001
1684	4	*head(*15,1)		nT	0.0001
1688	4	*head(*16,1)	0.0 to 180.0	degrees	0.0001
1692	4	*head(*17,1)	0.0 to 180.0	degrees	0.0001
1696	4	*head(*18,1)	0.0 to 180.0	degrees	0.0001
1700	4	*head(*19,1)	0.0 to 180.0	degrees	0.0001
1704	4	*head(*20,1)	+90.0 to -90.0	degrees	0.0001
1708	4	*head(*21,1)	0.0 to 360.0	degrees	0.0001
1712	4	*head(*22,1)	+90.0 to -90.0	degrees	0.0001
1716	4	*head(*23,1)	0.0 to 360.0	degrees	0.0001
1720	4	*head(*24,1)	0.0 to 20.00	N/A	0.0001
1724	4	*head(*25,1)	+90.0 to -90.0	degrees	0.0001
1728	4	*head(*26,1)	0.0 to 360.0	degrees	0.0001
1732	4	*head(*27,1)	0.0 to 360.0	degrees	0.0001
1736	4	*head(* 4,2)		nT	0.0001
1740	4	*head(* 5,2)		nT	0.0001
1744	4	*head(* 6,2)		nT	0.0001
1748	4	*head(* 7,2)		nT	0.0001
1752	4	*head(* 8,2)	0.0 to 180.0	degrees	0.0001
1756	4	*head(* 9,2)	0.0 to 180.0	degrees	0.0001
1760	4	*head(*10,2)	0.0 to 180.0	degrees	0.0001
1764	4	*head(*11,2)	0.0 to 180.0	degrees	0.0001
1768	4	*head(*12,2)		nT	0.0001
1772	4	*head(*13,2)		nT	0.0001
1776	4	*head(*14,2)		nT	0.0001
1780	4	*head(*15,2)		nT	0.0001
1784	4	*head(*16,2)	0.0 to 180.0	degrees	0.0001
1788	4	*head(*17,2)	0.0 to 180.0	degrees	0.0001
1792	4	*head(*18,2)	0.0 to 180.0	degrees	0.0001
1796	4	*head(*19,2)	0.0 to 180.0	degrees	0.0001
1800	4	*head(*20,2)	+90.0 to -90.0	degrees	0.0001
1804	4	*head(*21,2)	0.0 to 360.0	degrees	0.0001
1808	4	*head(*22,2)	+90.0 to -90.0	degrees	0.0001
1812	4	*head(*23,2)	0.0 to 360.0	degrees	0.0001
1816	4	*head(*24,2)	0.0 to 20.00	N/A	0.0001
1820	4	*head(*25,2)	+90.0 to -90.0	degrees	0.0001
1824	4	*head(*26,2)	0.0 to 360.0	degrees	0.0001

Packed		Unpacked Parameter	Range	Units	Conversion Factor
Byte Number	Len				
1828	4	*head(*27,2)	0.0 to 360.0	degrees	0.0001
1832	4	*head(* 4,3)		nT	0.0001
1836	4	*head(* 5,3)		nT	0.0001
1840	4	*head(* 6,3)		nT	0.0001
1844	4	*head(* 7,3)		nT	0.0001
1848	4	*head(* 8,3)	0.0 to 180.0	degrees	0.0001
1852	4	*head(* 9,3)	0.0 to 180.0	degrees	0.0001
1856	4	*head(*10,3)	0.0 to 180.0	degrees	0.0001
1860	4	*head(*11,3)	0.0 to 180.0	degrees	0.0001
1864	4	*head(*12,3)		nT	0.0001
1868	4	*head(*13,3)		nT	0.0001
1872	4	*head(*14,3)		nT	0.0001
1876	4	*head(*15,3)		nT	0.0001
1880	4	*head(*16,3)	0.0 to 180.0	degrees	0.0001
1884	4	*head(*17,3)	0.0 to 180.0	degrees	0.0001
1888	4	*head(*18,3)	0.0 to 180.0	degrees	0.0001
1892	4	*head(*19,3)	0.0 to 180.0	degrees	0.0001
1896	4	*head(*20,3)	+90.0 to -90.0	degrees	0.0001
1900	4	*head(*21,3)	0.0 to 360.0	degrees	0.0001
1904	4	*head(*22,3)	+90.0 to -90.0	degrees	0.0001
1908	4	*head(*23,3)	0.0 to 360.0	degrees	0.0001
1912	4	*head(*24,3)	0.0 to 20.00	N/A	0.0001
1916	4	*head(*25,3)	+90.0 to -90.0	degrees	0.0001
1920	4	*head(*26,3)	0.0 to 360.0	degrees	0.0001
1924	4	*head(*27,3)	0.0 to 360.0	degrees	0.0001
1928	4	*head(* 4,4)		nT	0.0001
1932	4	*head(* 5,4)		nT	0.0001
1936	4	*head(* 6,4)		nT	0.0001
1940	4	*head(* 7,4)		nT	0.0001
1944	4	*head(* 8,4)	0.0 to 180.0	degrees	0.0001
1948	4	*head(* 9,4)	0.0 to 180.0	degrees	0.0001
1952	4	*head(*10,4)	0.0 to 180.0	degrees	0.0001
1956	4	*head(*11,4)	0.0 to 180.0	degrees	0.0001
1960	4	*head(*12,4)		nT	0.0001
1964	4	*head(*13,4)		nT	0.0001
1968	4	*head(*14,4)		nT	0.0001
1972	4	*head(*15,4)		nT	0.0001
1976	4	*head(*16,4)	0.0 to 180.0	degrees	0.0001
1980	4	*head(*17,4)	0.0 to 180.0	degrees	0.0001
1984	4	*head(*18,4)	0.0 to 180.0	degrees	0.0001
1988	4	*head(*19,4)	0.0 to 180.0	degrees	0.0001
1992	4	*head(*20,4)	+90.0 to -90.0	degrees	0.0001
1996	4	*head(*21,4)	0.0 to 360.0	degrees	0.0001
2000	4	*head(*22,4)	+90.0 to -90.0	degrees	0.0001
2004	4	*head(*23,4)	0.0 to 360.0	degrees	0.0001
2008	4	*head(*24,4)	0.0 to 20.00	N/A	0.0001
2012	4	*head(*25,4)	+90.0 to -90.0	degrees	0.0001
2016	4	*head(*26,4)	0.0 to 360.0	degrees	0.0001
2020	4	*head(*27,4)	0.0 to 360.0	degrees	0.0001
2024	1	*ted0s*(1,1)	0 to 255	counts	table

Packed		Unpacked Parameter	Range	Units	Conversion Factor
Byte Number	Len				
2025	1	*ted0s*(2,1)	0 to 255	counts	table
2026	1	*ted0s*(3,1)	0 to 255	counts	table
2027	1	*ted0s*(4,1)	0 to 255	counts	table
2028	1	*ted0s*(5,1)	0 to 255	counts	table
2029	1	*ted0s*(6,1)	0 to 255	counts	table
2030	1	*ted0s*(7,1)	0 to 255	counts	table
2031	1	*ted0s*(8,1)	0 to 255	counts	table
2032	1	*ted0s*(1,2)	0 to 255	counts	table
2033	1	*ted0s*(2,2)	0 to 255	counts	table
2034	1	*ted0s*(3,2)	0 to 255	counts	table
2035	1	*ted0s*(4,2)	0 to 255	counts	table
2036	1	*ted0s*(5,2)	0 to 255	counts	table
2037	1	*ted0s*(6,2)	0 to 255	counts	table
2038	1	*ted0s*(7,2)	0 to 255	counts	table
2039	1	*ted0s*(8,2)	0 to 255	counts	table
2040	1	*ted0s*(1,3)	0 to 255	counts	table
2041	1	*ted0s*(2,3)	0 to 255	counts	table
2042	1	*ted0s*(3,3)	0 to 255	counts	table
2043	1	*ted0s*(4,3)	0 to 255	counts	table
2044	1	*ted0s*(5,3)	0 to 255	counts	table
2045	1	*ted0s*(6,3)	0 to 255	counts	table
2046	1	*ted0s*(7,3)	0 to 255	counts	table
2047	1	*ted0s*(8,3)	0 to 255	counts	table
2048	1	*ted0s*(1,4)	0 to 255	counts	table
2049	1	*ted0s*(2,4)	0 to 255	counts	table
2050	1	*ted0s*(3,4)	0 to 255	counts	table
2051	1	*ted0s*(4,4)	0 to 255	counts	table
2052	1	ignore entry			
2053	1	ignore entry			
2054	1	ignore entry			
2055	1	ignore entry			
2056	1	*tedback*(1,1)	0 to 255	counts	table
2057	1	*tedback*(1,2)	0 to 255	counts	table
2058	1	*tedback*(1,3)	0 to 255	counts	table
2059	1	*tedback*(1,4)	0 to 255	counts	table
2060	1	*ted30s*(1,1)	0 to 255	counts	table
2061	1	*ted30s*(2,1)	0 to 255	counts	table
2062	1	*ted30s*(3,1)	0 to 255	counts	table
2063	1	*ted30s*(4,1)	0 to 255	counts	table
2064	1	*ted30s*(5,1)	0 to 255	counts	table
2065	1	*ted30s*(6,1)	0 to 255	counts	table
2066	1	*ted30s*(7,1)	0 to 255	counts	table
2067	1	*ted30s*(8,1)	0 to 255	counts	table
2068	1	*ted30s*(1,2)	0 to 255	counts	table
2069	1	*ted30s*(2,2)	0 to 255	counts	table
2070	1	*ted30s*(3,2)	0 to 255	counts	table
2071	1	*ted30s*(4,2)	0 to 255	counts	table
2072	1	*ted30s*(5,2)	0 to 255	counts	table
2073	1	*ted30s*(6,2)	0 to 255	counts	table
2074	1	*ted30s*(7,2)	0 to 255	counts	table

Packed		Unpacked Parameter	Range	Units	Conversion Factor
Byte Number	Len				
2075	1	*ted30s*(8,2)	0 to 255	counts	table
2076	1	*ted30s*(1,3)	0 to 255	counts	table
2077	1	*ted30s*(2,3)	0 to 255	counts	table
2078	1	*ted30s*(3,3)	0 to 255	counts	table
2079	1	*ted30s*(4,3)	0 to 255	counts	table
2080	1	*ted30s*(5,3)	0 to 255	counts	table
2081	1	*ted30s*(6,3)	0 to 255	counts	table
2082	1	*ted30s*(7,3)	0 to 255	counts	table
2083	1	*ted30s*(8,3)	0 to 255	counts	table
2084	1	*ted30s*(1,4)	0 to 255	counts	table
2085	1	*ted30s*(2,4)	0 to 255	counts	table
2086	1	*ted30s*(3,4)	0 to 255	counts	table
2087	1	*ted30s*(4,4)	0 to 255	counts	table
2088	1	ignore entry			
2089	1	ignore entry			
2090	1	ignore entry			
2091	1	ignore entry			
2092	1	*tedback*(2,1)	0 to 255	counts	table
2093	1	*tedback*(2,2)	0 to 255	counts	table
2094	1	*tedback*(2,3)	0 to 255	counts	table
2095	1	*tedback*(2,4)	0 to 255	counts	table
2096	4	*tedfx*(1, 1)	0.0 to ~ 20.	mW m^{-2}	0.0001
2100	4	*tedfx*(1, 2)	0.0 to ~ 20.	mW m^{-2}	0.0001
2104	4	*tedfx*(1, 3)	0.0 to ~ 20.	mW m^{-2}	0.0001
2108	4	*tedfx*(1, 4)	0.0 to ~ 20.	mW m^{-2}	0.0001
2112	4	*tedfx*(2, 1)	0.0 to ~ 300.	mW m^{-2}	0.0001
2116	4	*tedfx*(2, 2)	0.0 to ~ 300.	mW m^{-2}	0.0001
2120	4	*tedfx*(2, 3)	0.0 to ~ 300.	mW m^{-2}	0.0001
2124	4	*tedfx*(2, 4)	0.0 to ~ 300.	mW m^{-2}	0.0001
2128	4	*tedfx*(3, 1)	0.0 to ~ 20.	mW m^{-2}	0.0001
2132	4	*tedfx*(3, 2)	0.0 to ~ 20.	mW m^{-2}	0.0001
2136	4	*tedfx*(3, 3)	0.0 to ~ 20.	mW m^{-2}	0.0001
2140	4	*tedfx*(3, 4)	0.0 to ~ 20.	mW m^{-2}	0.0001
2144	4	*tedfx*(4, 1)	0.0 to ~ 300.	mW m^{-2}	0.0001
2148	4	*tedfx*(4, 2)	0.0 to ~ 300.	mW m^{-2}	0.0001
2152	4	*tedfx*(4, 3)	0.0 to ~ 300.	mW m^{-2}	0.0001
2156	4	*tedfx*(4, 4)	0.0 to ~ 300.	mW m^{-2}	0.0001
2160	4	*tedfx*(5, 1)	0.0 to ~ 300.	mW m^{-2}	0.0001
2164	4	*tedfx*(5, 2)	0.0 to ~ 300.	mW m^{-2}	0.0001
2168	4	*tedfx*(5, 3)	0.0 to ~ 300.	mW m^{-2}	0.0001
2172	4	*tedfx*(5, 4)	0.0 to ~ 300.	mW m^{-2}	0.0001
2176	4	*tedfx*(6, 1)	0.0 to ~ 300.	mW m^{-2}	0.0001
2180	4	*tedfx*(6, 2)	0.0 to ~ 300.	mW m^{-2}	0.0001
2184	4	*tedfx*(6, 3)	0.0 to ~ 300.	mW m^{-2}	0.0001
2188	4	*tedfx*(6, 4)	0.0 to ~ 300.	mW m^{-2}	0.0001
2192	4	*tedfx*(7, 1)	0.0 to ~ 300.	mW m^{-2}	0.0001
2196	4	*tedfx*(7, 2)	0.0 to ~ 300.	mW m^{-2}	0.0001
2200	4	*tedfx*(7, 3)	0.0 to ~ 300.	mW m^{-2}	0.0001
2204	4	*tedfx*(7, 4)	0.0 to ~ 300.	mW m^{-2}	0.0001
2208	4	*tedfx*(1, 5)	0.0 to ~ 20.	mW m^{-2}	0.0001

Packed		Unpacked Parameter	Range	Units	Conversion Factor
Byte Number	Len				
2212	4	*tedfx*(1, 6)	0.0 to ~ 20.	mW m^{-2}	0.0001
2216	4	*tedfx*(1, 7)	0.0 to ~ 20.	mW m^{-2}	0.0001
2220	4	*tedfx*(1, 8)	0.0 to ~ 20.	mW m^{-2}	0.0001
2224	4	*tedfx*(2, 5)	0.0 to ~ 300.	mW m^{-2}	0.0001
2228	4	*tedfx*(2, 6)	0.0 to ~ 300.	mW m^{-2}	0.0001
2322	4	*tedfx*(2, 7)	0.0 to ~ 300.	mW m^{-2}	0.0001
2236	4	*tedfx*(2, 8)	0.0 to ~ 300.	mW m^{-2}	0.0001
2240	4	*tedfx*(3, 5)	0.0 to ~ 20.	mW m^{-2}	0.0001
2244	4	*tedfx*(3, 6)	0.0 to ~ 20.	mW m^{-2}	0.0001
2248	4	*tedfx*(3, 7)	0.0 to ~ 20.	mW m^{-2}	0.0001
2252	4	*tedfx*(3, 8)	0.0 to ~ 20.	mW m^{-2}	0.0001
2256	4	*tedfx*(4, 5)	0.0 to ~ 300.	mW m^{-2}	0.0001
2260	4	*tedfx*(4, 6)	0.0 to ~ 300.	mW m^{-2}	0.0001
2264	4	*tedfx*(4, 7)	0.0 to ~ 300.	mW m^{-2}	0.0001
2268	4	*tedfx*(4, 8)	0.0 to ~ 300.	mW m^{-2}	0.0001
2272	4	*tedfx*(5, 5)	0.0 to ~ 300.	mW m^{-2}	0.0001
2276	4	*tedfx*(5, 6)	0.0 to ~ 300.	mW m^{-2}	0.0001
2280	4	*tedfx*(5, 7)	0.0 to ~ 300.	mW m^{-2}	0.0001
2284	4	*tedfx*(5, 8)	0.0 to ~ 300.	mW m^{-2}	0.0001
2288	4	*tedfx*(6, 5)	0.0 to ~ 300.	mW m^{-2}	0.0001
2292	4	*tedfx*(6, 6)	0.0 to ~ 300.	mW m^{-2}	0.0001
2296	4	*tedfx*(6, 7)	0.0 to ~ 300.	mW m^{-2}	0.0001
2300	4	*tedfx*(6, 8)	0.0 to ~ 300.	mW m^{-2}	0.0001
2304	4	*tedfx*(7, 5)	0.0 to ~ 300.	mW m^{-2}	0.0001
2308	4	*tedfx*(7, 6)	0.0 to ~ 300.	mW m^{-2}	0.0001
2312	4	*tedfx*(7, 7)	0.0 to ~ 300.	mW m^{-2}	0.0001
2316	4	*tedfx*(7, 8)	0.0 to ~ 300.	mW m^{-2}	0.0001
2320	4	*tedfx*(1, 9)	0.0 to ~ 20.	mW m^{-2}	0.0001
2324	4	*tedfx*(1,10)	0.0 to ~ 20.	mW m^{-2}	0.0001
2328	4	*tedfx*(1,11)	0.0 to ~ 20.	mW m^{-2}	0.0001
2332	4	*tedfx*(1,12)	0.0 to ~ 20.	mW m^{-2}	0.0001
2336	4	*tedfx*(2, 9)	0.0 to ~ 300.	mW m^{-2}	0.0001
2340	4	*tedfx*(2,10)	0.0 to ~ 300.	mW m^{-2}	0.0001
2344	4	*tedfx*(2,11)	0.0 to ~ 300.	mW m^{-2}	0.0001
2348	4	*tedfx*(2,12)	0.0 to ~ 300.	mW m^{-2}	0.0001
2352	4	*tedfx*(3, 9)	0.0 to ~ 20.	mW m^{-2}	0.0001
2356	4	*tedfx*(3,10)	0.0 to ~ 20.	mW m^{-2}	0.0001
2360	4	*tedfx*(3,11)	0.0 to ~ 20.	mW m^{-2}	0.0001
2364	4	*tedfx*(3,12)	0.0 to ~ 20.	mW m^{-2}	0.0001
2368	4	*tedfx*(4, 9)	0.0 to ~ 300.	mW m^{-2}	0.0001
2372	4	*tedfx*(4,10)	0.0 to ~ 300.	mW m^{-2}	0.0001
2376	4	*tedfx*(4,11)	0.0 to ~ 300.	mW m^{-2}	0.0001
2380	4	*tedfx*(4,12)	0.0 to ~ 300.	mW m^{-2}	0.0001
2384	4	*tedfx*(5, 9)	0.0 to ~ 300.	mW m^{-2}	0.0001
2388	4	*tedfx*(5,10)	0.0 to ~ 300.	mW m^{-2}	0.0001
2392	4	*tedfx*(5,11)	0.0 to ~ 300.	mW m^{-2}	0.0001
2396	4	*tedfx*(5,12)	0.0 to ~ 300.	mW m^{-2}	0.0001
2400	4	*tedfx*(6, 9)	0.0 to ~ 300.	mW m^{-2}	0.0001
2404	4	*tedfx*(6,10)	0.0 to ~ 300.	mW m^{-2}	0.0001
2408	4	*tedfx*(6,11)	0.0 to ~ 300.	mW m^{-2}	0.0001

Packed		Unpacked Parameter	Range	Units	Conversion Factor
Byte Number	Len				
2412	4	*tedfx*(6,12)	0.0 to ~ 300.	mW m^{-2}	0.0001
2416	4	*tedfx*(7, 9)	0.0 to ~ 300.	mW m^{-2}	0.0001
2420	4	*tedfx*(7,10)	0.0 to ~ 300.	mW m^{-2}	0.0001
2424	4	*tedfx*(7,11)	0.0 to ~ 300.	mW m^{-2}	0.0001
2428	4	*tedfx*(7,12)	0.0 to ~ 300.	mW m^{-2}	0.0001
2432	4	*tedfx*(1,13)	0.0 to ~ 20.	mW m^{-2}	0.0001
2436	4	*tedfx*(1,14)	0.0 to ~ 20.	mW m^{-2}	0.0001
2440	4	*tedfx*(1,15)	0.0 to ~ 20.	mW m^{-2}	0.0001
2444	4	*tedfx*(1,16)	0.0 to ~ 20.	mW m^{-2}	0.0001
2448	4	*tedfx*(2,13)	0.0 to ~ 300.	mW m^{-2}	0.0001
2452	4	*tedfx*(2,14)	0.0 to ~ 300.	mW m^{-2}	0.0001
2456	4	*tedfx*(2,15)	0.0 to ~ 300.	mW m^{-2}	0.0001
2460	4	*tedfx*(2,16)	0.0 to ~ 300.	mW m^{-2}	0.0001
2464	4	*tedfx*(3,13)	0.0 to ~ 20.	mW m^{-2}	0.0001
2468	4	*tedfx*(3,14)	0.0 to ~ 20.	mW m^{-2}	0.0001
2472	4	*tedfx*(3,15)	0.0 to ~ 20.	mW m^{-2}	0.0001
2476	4	*tedfx*(3,16)	0.0 to ~ 20.	mW m^{-2}	0.0001
2480	4	*tedfx*(4,13)	0.0 to ~ 300.	mW m^{-2}	0.0001
2484	4	*tedfx*(4,14)	0.0 to ~ 300.	mW m^{-2}	0.0001
2488	4	*tedfx*(4,15)	0.0 to ~ 300.	mW m^{-2}	0.0001
2492	4	*tedfx*(4,16)	0.0 to ~ 300.	mW m^{-2}	0.0001
2496	4	*tedfx*(5,13)	0.0 to ~ 300.	mW m^{-2}	0.0001
2500	4	*tedfx*(5,14)	0.0 to ~ 300.	mW m^{-2}	0.0001
2504	4	*tedfx*(5,15)	0.0 to ~ 300.	mW m^{-2}	0.0001
2508	4	*tedfx*(5,16)	0.0 to ~ 300.	mW m^{-2}	0.0001
2512	4	*tedfx*(6,13)	0.0 to ~ 300.	mW m^{-2}	0.0001
2516	4	*tedfx*(6,14)	0.0 to ~ 300.	mW m^{-2}	0.0001
2520	4	*tedfx*(6,15)	0.0 to ~ 300.	mW m^{-2}	0.0001
2524	4	*tedfx*(6,16)	0.0 to ~ 300.	mW m^{-2}	0.0001
2528	4	*tedfx*(7,13)	0.0 to ~ 300.	mW m^{-2}	0.0001
2532	4	*tedfx*(7,14)	0.0 to ~ 300.	mW m^{-2}	0.0001
2536	4	*tedfx*(7,15)	0.0 to ~ 300.	mW m^{-2}	0.0001
2540	4	*tedfx*(7,16)	0.0 to ~ 300.	mW m^{-2}	0.0001
2544		**TOTAL**			

* 0 = no errors
| 0x80 = missing value
| 0x10 lower channels have higher values than higher channels
| 0x20 = ted band is > maximum intensity
| 0x40 = sensor response energy flux integral

Appendix B. Conversion table for MEPED and TED counts

Raw Data Value	0	1	2	3	4	5	6	7	8	9
0	0.0	1.0	2.0	3.0	4.0	5.0	6.0	7.0	8.0	9.0
10	10.0	11.0	12.0	13.0	14.0	15.0	16.0	17.0	18.0	19.0
20	20.0	21.0	22.0	23.0	24.0	25.0	26.0	27.0	28.0	29.0
30	30.0	31.0	32.0	34.5	36.5	38.5	40.5	42.5	44.5	46.5
40	48.5	50.5	53.0	56.0	59.0	62.0	65.5	69.5	73.5	77.5
50	81.5	85.5	89.5	93.5	97.5	101.5	106.5	112.5	118.5	124.5
60	135.0	139.5	147.5	155.5	163.5	171.5	179.5	187.5	195.5	203.5
70	213.5	225.5	237.5	249.5	263.5	279.5	295.5	311.5	327.5	343.5
80	359.5	375.5	391.5	407.5	427.5	451.5	475.5	499.5	527.5	559.5
90	591.5	623.5	655.5	687.5	719.5	751.5	783.5	815.5	855.5	903.5
100	951.5	999.5	1055.5	1119.5	1183.5	1247.5	1311.5	1375.5	1439.5	1503.5
110	1567.5	1631.5	1711.5	1807.5	1903.5	1999.5	2111.5	2239.5	2367.5	2495.5
120	2623.5	2751.5	2879.5	3007.5	3135.5	3263.5	3423.5	3615.5	3807.5	3999.5
130	4223.5	4479.5	4735.5	4991.5	5247.5	5503.5	5759.5	6015.5	6271.5	6527.5
140	6847.5	7231.5	7615.5	7999.5	8447.5	8959.5	9471.5	9983.5	10495.5	11007.5
150	11519.5	12031.5	12543.5	13055.5	13695.5	14463.5	15231.5	15999.5	16895.5	17919.5
160	18943.5	19967.5	20991.5	22015.5	23039.5	24063.5	25087.5	26111.5	27391.5	28927.5
170	30463.5	31999.5	33791.5	35839.5	37887.5	39935.5	41983.5	44031.5	46079.5	48127.5
180	50175.5	52223.5	54783.5	57855.5	60927.5	63999.5	67583.5	71679.5	75775.5	79871.5
190	83967.5	88063.5	92159.5	96255.5	100351.5	104447.5	109567.5	115711.5	121855.5	127999.5
200	135167.5	143359.5	151551.5	159743.5	167935.5	176127.5	184319.5	192511.5	200703.5	208895.5
210	219135.5	231423.5	243711.5	255999.5	270335.5	286719.5	303103.5	319487.5	335871.5	352255.5
220	368639.5	385023.5	401407.5	417791.5	438271.5	462847.5	487423.5	511999.5	540671.5	573439.5
230	606207.5	638975.5	671743.5	704511.5	737279.5	770047.5	802815.5	835583.5	876543.5	925695.5
240	974847.5	1023999.5	1081343.5	1146879.5	1212415.5	1277951.5	1343487.5	1409023.5	1474559.5	1540095.5
250	1605631.5	1671167.5	1753087.5	1851391.5	1949695.5	1998848.0				

Appendix C. TED Sensor Data Grouped by Unit Serial Number

TED Serial Number 009 Sensor Data

TED Weighting Factors

0º electron low-energy band number	Particle energy weight	Detection efficiency weight	30º electron low-energy band number	Particle energy weight	Detection efficiency weight
1	1.0	1.0	1	1.0	1.0
2	1.5	1.0	2	1.5	1.0
3	2.0	1.0	3	2.0	1.0
4	3.0	1.0	4	3.0	1.0
5	4.0	1.0	5	4.0	1.0
6	6.0	1.0	6	6.0	1.0
7	8.0	1.0	7	8.0	1.0
8	12.0	1.0	8	12.0	1.0
0º electron high-energy band number	**Particle energy weight**	**Detection efficiency weight**	**30º electron high-energy band number**	**Particle energy weight**	**Detection efficiency weight**
9	1.0	1.0	9	1.0	1.0
10	1.5	1.0	10	1.5	1.0
11	3.0	1.0	11	3.0	1.0
12	4.0	1.0	12	4.0	1.0
13	8.0	0.667	13	8.0	0.667
14	16.0	0.667	14	16.0	0.667
15	24.0	0.667	15	24.0	0.667
16	48.0	0.667	16	48.0	0.667
0º proton low-energy band number	**Particle energy weight**	**Detection efficiency weight**	**30º proton low-energy band number**	**Particle energy weight**	**Detection efficiency weight**
1	1.0	1.0	1	1.0	1.0
2	1.5	1.0	2	1.5	1.0
3	2.0	1.0	3	2.0	1.0
4	2.0	1.0	4	2.0	1.0
5	3.0	1.0	5	3.0	1.0
6	4.0	1.0	6	4.0	1.0
7	6.0	1.0	7	6.0	1.0
8	8.0	1.0	8	8.0	1.0
0º proton high-energy band number	**Particle energy weight**	**Detection efficiency weight**	**30º proton high-energy band number**	**Particle energy weight**	**Detection efficiency weight**
9	3.0	1.0	9	3.0	1.0
10	4.0	1.0	10	4.0	1.0
11	4.0	1.0	11	4.0	1.0
12	6.0	1.0	12	6.0	1.0
13	8.0	1.0	13	8.0	1.0
14	12.0	1.0	14	12.0	1.0
15	12.0	1.0	15	12.0	1.0
16	16.0	1.0	16	16.0	1.0

Multiplicative Factors to Convert Actual Counts Within an Energy Band to Directional Energy Flux Contained Within that Energy Band

TED S/N 009 Electron Detector System

Energy band	Band center energy (eV)	0º electron sensor to convert counts to mW m^{-2} $ster^{-1}$	30º electron sensor to convert counts to mW m^{-2} $ster^{-1}$
1	61	1.519×10^{-6}	2.713×10^{-6}
2	89	2.290×10^{-6}	4.262×10^{-6}
3	130	3.386×10^{-6}	6.224×10^{-6}
4	189	5.061×10^{-6}	9.283×10^{-6}
5	274	7.504×10^{-6}	1.365×10^{-5}
6	399	1.078×10^{-5}	1.969×10^{-5}
7	580	1.579×10^{-5}	2.902×10^{-5}
8	844	2.302×10^{-5}	4.209×10^{-5}
9	1227	7.803×10^{-5}	7.494×10^{-5}
10	1784	1.251×10^{-4}	1.202×10^{-4}
11	2595	2.003×10^{-4}	1.930×10^{-4}
12	3774	3.192×10^{-4}	3.077×10^{-4}
13	5488	5.073×10^{-4}	4.897×10^{-4}
14	7980	8.027×10^{-4}	7.755×10^{-4}
15	11605	1.258×10^{-3}	1.215×10^{-3}
16	16877	1.946×10^{-3}	1.878×10^{-3}

TED S/N 009 Proton Detector System

Energy band	Band center energy (eV)	0º proton sensor to convert counts to mW m^{-2} $ster^{-1}$	30º proton sensor to convert counts to mW m^{-2} $ster^{-1}$
1	61	1.955×10^{-6}	2.125×10^{-6}
2	89	2.686×10^{-6}	2.961×10^{-6}
3	130	3.555×10^{-6}	3.319×10^{-6}
4	189	4.660×10^{-6}	5.156×10^{-6}
5	274	6.102×10^{-6}	6.802×10^{-6}
6	399	7.930×10^{-6}	8.810×10^{-6}
7	580	1.035×10^{-5}	1.155×10^{-5}
8	844	1.350×10^{-5}	1.504×10^{-5}
9	1227	1.485×10^{-4}	1.167×10^{-4}
10	1784	1.951×10^{-4}	1.535×10^{-4}
11	2595	2.566×10^{-4}	2.027×10^{-4}
12	3774	3.357×10^{-4}	2.662×10^{-4}
13	5488	4.400×10^{-4}	3.493×10^{-4}
14	7980	5.739×10^{-4}	4.565×10^{-4}
15	11605	7.451×10^{-4}	5.919×10^{-4}
16	16877	9.554×10^{-4}	7.568×10^{-4}

Multiplicative Factors to Convert From Actual Counts Within an Energy Band to Directional Number Flux at the Center Energy of that Band

TED S/N 009 Electron Detector System

Energy band	Band center energy (eV)	0º electron sensor to convert counts to particles m^{-2} sec^{-1} eV^{-1} $ster^{-1}$	30º electron sensor to convert counts to particles m^{-2} sec^{-1} eV^{-1} $ster^{-1}$
1	61	6.699×10^{6}	1.197×10^{7}
2	89	4.738×10^{6}	8.818×10^{6}
3	130	3.344×10^{6}	6.149×10^{6}
4	189	2.367×10^{6}	4.324×10^{6}
5	274	1.659×10^{6}	3.017×10^{6}
6	399	1.143×10^{6}	2.088×10^{6}
7	580	7.903×10^{5}	1.452×10^{6}
8	844	5.461×10^{5}	9.984×10^{5}
9	1227	8.740×10^{5}	8.394×10^{5}
10	1784	6.651×10^{5}	6.391×10^{5}
11	2595	5.047×10^{5}	4.863×10^{5}
12	3774	3.825×10^{5}	3.687×10^{5}
13	5488	2.901×10^{5}	2.801×10^{5}
14	7980	2.199×10^{5}	2.127×10^{5}
15	11605	1.663×10^{5}	1.610×10^{5}
16	16877	1.251×10^{5}	1.213×10^{5}

TED S/N 009 Proton Detector System

Energy band	Band center energy (eV)	0º proton sensor to convert counts to particles m^{-2} sec^{-1} eV^{-1} $ster^{-1}$	30º proton sensor to convert counts to particles m^{-2} sec^{-1} eV^{-1} $ster^{-1}$
1	61	8.623×10^{6}	9.379×10^{6}
2	89	5.559×10^{6}	6.129×10^{6}
3	130	3.514×10^{6}	3.873×10^{6}
4	189	2.181×10^{6}	2.414×10^{6}
5	274	1.350×10^{6}	1.505×10^{6}
6	399	8.424×10^{5}	9.358×10^{5}
7	580	5.187×10^{5}	5.786×10^{5}
8	844	3.206×10^{5}	3.573×10^{5}
9	1227	1.665×10^{6}	1.308×10^{6}
10	1784	1.035×10^{6}	8.145×10^{5}
11	2595	6.427×10^{5}	5.079×10^{5}
12	3774	3.977×10^{5}	3.157×10^{5}
13	5488	2.470×10^{5}	1.965×10^{5}
14	7980	1.531×10^{5}	1.223×10^{5}
15	11605	9.487×10^{4}	7.597×10^{4}
16	16877	5.854×10^{4}	4.701×10^{4}

TED Serial Number 009 Sensor Data
Conversion to Integrated Directional Energy Flux Moment

Sensor	Energy range eV	To convert decompressed counts to mW m^{-2} $ster^{-1}$ multiply by
0º low-energy electron	50 - 1000	1.902×10^{-6}
30º low-energy electron	50 - 1000	3.481×10^{-6}
0º high-energy electron	1000 - 20000	7.656×10^{-5}
30º high-energy electron	1000 - 20000	7.406×10^{-5}
0º low-energy proton	50 - 1000	1.775×10^{-6}
30º low-energy proton	50 - 1000	1.955×10^{-6}
0º high-energy proton	1000 - 20000	5.727×10^{-5}
30º high-energy proton	1000 - 20000	4.575×10^{-5}

TED Serial Number 010 Sensor Data

TED Weighting Factors

0º electron low-energy band number	Particle energy weight	Detection efficiency weight	30º electron low-energy band number	Particle energy weight	Detection efficiency weight
1	1.0	1.0	1	1.0	1.0
2	1.5	1.0	2	1.5	1.0
3	2.0	1.0	3	2.0	1.0
4	3.0	1.0	4	3.0	1.0
5	4.0	1.0	5	4.0	1.0
6	6.0	1.0	6	6.0	1.0
7	8.0	1.0	7	8.0	1.0
8	12.0	1.0	8	12.0	1.0
0º electron high-energy band number	**Particle energy weight**	**Detection efficiency weight**	**30º electron high-energy band number**	**Particle energy weight**	**Detection efficiency weight**
9	1.0	1.0	9	1.0	1.0
10	1.5	1.0	10	1.5	1.0
11	3.0	1.0	11	3.0	1.0
12	4.0	1.0	12	4.0	1.0
13	8.0	1.0	13	8.0	0.667
14	16.0	1.0	14	16.0	0.667
15	24.0	1.0	15	24.0	0.667
16	48.0	1.0	16	48.0	0.667
0º proton low-energy band number	**Particle energy weight**	**Detection efficiency weight**	**30º proton low-energy band number**	**Particle energy weight**	**Detection efficiency weight**
1	1.0	1.0	1	1.0	1.0
2	1.5	1.0	2	1.5	1.0
3	2.0	1.0	3	2.0	1.0
4	2.0	1.0	4	2.0	1.0
5	3.0	1.0	5	3.0	1.0
6	4.0	1.0	6	4.0	1.0
7	6.0	1.0	7	6.0	1.0
8	8.0	1.0	8	8.0	1.0
0º proton high-energy band number	**Particle energy weight**	**Detection efficiency weight**	**30º proton high-energy band number**	**Particle energy weight**	**Detection efficiency weight**
9	3.0	1.0	9	3.0	1.0
10	4.0	1.0	10	4.0	1.0
11	4.0	1.0	11	4.0	1.0
12	6.0	1.0	12	6.0	1.0
13	8.0	1.0	13	8.0	1.0
14	12.0	1.0	14	12.0	1.0
15	12.0	1.0	15	12.0	1.0
16	16.0	1.0	16	16.0	1.0

Multiplicative Factors to Convert Actual Counts Within an Energy Band to Directional Energy Flux Contained Within that Energy Band

TED S/N 010 Electron Detector System

Energy band	Band center energy (eV)	0º electron sensor to convert counts to mW m^{-2} $ster^{-1}$	30º electron sensor to convert counts to mW m^{-2} $ster^{-1}$
1	61	2.387×10^{-6}	2.724×10^{-6}
2	89	3.455×10^{-6}	4.223×10^{-6}
3	130	5.155×10^{-6}	6.209×10^{-6}
4	189	7.628×10^{-6}	9.243×10^{-6}
5	274	1.122×10^{-5}	1.362×10^{-5}
6	399	1.627×10^{-5}	1.964×10^{-5}
7	580	2.385×10^{-5}	2.889×10^{-5}
8	844	3.469×10^{-5}	4.202×10^{-5}
9	1227	5.665×10^{-5}	5.277×10^{-5}
10	1784	9.543×10^{-5}	8.655×10^{-5}
11	2595	1.602×10^{-4}	1.423×10^{-4}
12	3774	2.679×10^{-4}	2.324×10^{-4}
13	5488	4.463×10^{-4}	3.786×10^{-4}
14	7980	7.398×10^{-4}	6.130×10^{-4}
15	11605	1.213×10^{-3}	9.823×10^{-4}
16	16877	1.960×10^{-3}	1.549×10^{-3}

TED S/N 010 Proton Detector System

Energy band	Band center energy (eV)	0º proton sensor to convert counts to mW m^{-2} $ster^{-1}$	30º proton sensor to convert counts to mW m^{-2} $ster^{-1}$
1	61	1.013×10^{-6}	1.439×10^{-6}
2	89	1.455×10^{-6}	2.102×10^{-6}
3	130	1.936×10^{-6}	2.912×10^{-6}
4	189	2.602×10^{-6}	4.016×10^{-6}
5	274	3.528×10^{-6}	5.511×10^{-6}
6	399	4.588×10^{-6}	7.471×10^{-6}
7	580	6.098×10^{-6}	1.029×10^{-5}
8	844	8.027×10^{-6}	1.391×10^{-5}
9	1227	1.315×10^{-4}	1.001×10^{-4}
10	1784	1.705×10^{-4}	1.318×10^{-4}
11	2595	2.206×10^{-4}	1.735×10^{-4}
12	3774	2.850×10^{-4}	2.279×10^{-4}
13	5488	3.676×10^{-4}	2.981×10^{-4}
14	7980	4.733×10^{-4}	3.893×10^{-4}
15	11605	6.055×10^{-4}	5.042×10^{-4}
16	16877	7.658×10^{-4}	6.452×10^{-4}

Multiplicative Factors to Convert From Actual Counts Within an Energy Band to Directional Number Flux at the Center Energy of that Band

TED S/N 010 Electron Detector System

Energy band	Band center energy (eV)	0º electron sensor to convert counts to particles m^{-2} sec^{-1} eV^{-1} $ster^{-1}$	30º electron sensor to convert counts to particles m^{-2} sec^{-1} eV^{-1} $ster^{-1}$
1	61	1.052×10^{7}	1.202×10^{7}
2	89	7.148×10^{6}	8.738×10^{6}
3	130	5.093×10^{6}	6.134×10^{6}
4	189	3.568×10^{6}	4.323×10^{6}
5	274	2.480×10^{6}	3.010×10^{6}
6	399	1.726×10^{6}	2.084×10^{6}
7	580	1.193×10^{6}	1.446×10^{6}
8	844	8.229×10^{5}	9.969×10^{5}
9	1227	6.345×10^{5}	5.911×10^{5}
10	1784	5.075×10^{5}	4.602×10^{5}
11	2595	4.043×10^{5}	3.589×10^{5}
12	3774	3.219×10^{5}	2.790×10^{5}
13	5488	2.564×10^{5}	2.172×10^{5}
14	7980	2.041×10^{5}	1.690×10^{5}
15	11605	1.620×10^{5}	1.310×10^{5}
16	16877	1.279×10^{5}	1.011×10^{5}

TED S/N 010 Proton Detector System

Energy band	Band center energy (eV)	0º proton sensor to convert counts to particles m^{-2} sec^{-1} eV^{-1} $ster^{-1}$	30º proton sensor to convert counts to particles m^{-2} sec^{-1} eV^{-1} $ster^{-1}$
1	61	4.472×10^{6}	6.349×10^{6}
2	89	3.013×10^{6}	4.351×10^{6}
3	130	1.913×10^{6}	2.878×10^{6}
4	189	1.218×10^{6}	1.880×10^{6}
5	274	7.808×10^{5}	1.219×10^{6}
6	399	4.874×10^{5}	7.932×10^{5}
7	580	3.055×10^{5}	5.156×10^{5}
8	844	1.907×10^{5}	3.304×10^{5}
9	1227	1.475×10^{6}	1.122×10^{6}
10	1784	9.042×10^{5}	6.994×10^{5}
11	2595	5.524×10^{5}	4.347×10^{5}
12	3774	3.373×10^{5}	2.701×10^{5}
13	5488	2.061×10^{5}	1.676×10^{5}
14	7980	1.260×10^{5}	1.041×10^{5}
15	11605	7.685×10^{4}	6.459×10^{4}
16	16877	4.671×10^{4}	3.991×10^{4}

TED Serial Number 010 Sensor Data
Conversion to Integrated Directional Energy Flux Moment

Sensor	Energy range eV	To convert decompressed counts to mW m^{-2} $ster^{-1}$ multiply by
0º low-energy electron	50 - 1000	2.868×10^{-6}
30º low-energy electron	50 - 1000	3.473×10^{-6}
0º high-energy electron	1000 - 20000	5.112×10^{-5}
30º high-energy electron	1000 - 20000	5.932×10^{-5}
0º low-energy proton	50 - 1000	1.034×10^{-6}
30º low-energy proton	50 - 1000	1.751×10^{-6}
0º high-energy proton	1000 - 20000	4.691×10^{-5}
30º high-energy proton	1000 - 20000	3.895×10^{-5}

TED Serial Number 012 Sensor Data

TED Weighting Factors

0º electron low-energy band number	Particle energy weight	Detection efficiency weight	30º electron low-energy band number	Particle energy weight	Detection efficiency weight
1	1.0	1.0	1	1.0	1.0
2	1.5	1.0	2	1.5	1.0
3	2.0	1.0	3	2.0	1.0
4	3.0	1.0	4	3.0	1.0
5	4.0	1.0	5	4.0	1.0
6	6.0	1.0	6	6.0	1.0
7	8.0	1.0	7	8.0	1.0
8	12.0	1.0	8	12.0	1.0
0º electron high-energy band number	**Particle energy weight**	**Detection efficiency weight**	**30º electron high-energy band number**	**Particle energy weight**	**Detection efficiency weight**
9	1.0	1.0	9	1.0	1.0
10	1.5	1.0	10	1.5	1.0
11	3.0	1.0	11	3.0	1.0
12	4.0	1.0	12	4.0	1.0
13	8.0	0.667	13	8.0	0.667
14	16.0	0.667	14	16.0	0.667
15	24.0	0.667	15	24.0	0.667
16	48.0	0.667	16	48.0	0.667
0º proton low-energy band number	**Particle energy weight**	**Detection efficiency weight**	**30º proton low-energy band number**	**Particle energy weight**	**Detection efficiency weight**
1	1.0	1.0	1	1.0	1.0
2	1.5	1.0	2	1.5	1.0
3	2.0	1.0	3	2.0	1.0
4	2.0	1.0	4	2.0	1.0
5	3.0	1.0	5	3.0	1.5
6	4.0	1.0	6	4.0	1.5
7	6.0	1.0	7	6.0	1.5
8	8.0	1.0	8	8.0	1.5
0º proton high-energy band number	**Particle energy weight**	**Detection efficiency weight**	**30º proton high-energy band number**	**Particle energy weight**	**Detection efficiency weight**
9	3.0	1.0	9	3.0	1.0
10	4.0	1.0	10	4.0	1.0
11	4.0	1.0	11	4.0	1.0
12	6.0	1.0	12	6.0	1.0
13	8.0	1.0	13	8.0	1.0
14	12.0	1.0	14	12.0	1.0
15	12.0	1.0	15	12.0	1.0
16	16.0	1.0	16	16.0	1.0

Multiplicative Factors to Convert Actual Counts Within an Energy Band to Directional Energy Flux Contained Within that Energy Band

TED S/N 012 Electron Detector System

Energy band	Band center energy (eV)	0º electron sensor to convert counts to mW m^{-2} $ster^{-1}$	30º electron sensor to convert counts to mW m^{-2} $ster^{-1}$
1	61	1.454×10^{-6}	1.889×10^{-6}
2	89	2.284×10^{-6}	2.954×10^{-6}
3	130	3.335×10^{-6}	4.378×10^{-6}
4	189	4.975×10^{-6}	6.460×10^{-6}
5	274	7.312×10^{-6}	9.484×10^{-6}
6	399	1.055×10^{-5}	1.375×10^{-5}
7	580	1.555×10^{-5}	2.027×10^{-5}
8	844	2.264×10^{-5}	2.942×10^{-5}
9	1227	6.343×10^{-5}	8.033×10^{-5}
10	1784	1.021×10^{-4}	1.265×10^{-4}
11	2595	1.645×10^{-4}	1.993×10^{-4}
12	3774	2.634×10^{-4}	3.122×10^{-4}
13	5488	4.207×10^{-4}	4.879×10^{-4}
14	7980	6.685×10^{-4}	7.586×10^{-4}
15	11605	1.051×10^{-3}	1.167×10^{-3}
16	16877	1.630×10^{-3}	1.772×10^{-3}

TED S/N 012 Proton Detector System

Energy band	Band center energy (eV)	0º proton sensor to convert counts to mW m^{-2} $ster^{-1}$	30º proton sensor to convert counts to mW m^{-2} $ster^{-1}$
1	61	9.360×10^{-7}	8.898×10^{-7}
2	89	1.365×10^{-6}	1.337×10^{-6}
3	130	1.876×10^{-6}	1.929×10^{-6}
4	189	2.576×10^{-6}	2.757×10^{-6}
5	274	3.565×10^{-6}	3.931×10^{-6}
6	399	4.744×10^{-6}	5.488×10^{-6}
7	580	6.508×10^{-6}	7.795×10^{-6}
8	844	8.787×10^{-6}	1.102×10^{-5}
9	1227	1.469×10^{-4}	1.091×10^{-4}
10	1784	1.897×10^{-4}	1.394×10^{-4}
11	2595	2.456×10^{-4}	1.781×10^{-4}
12	3774	3.161×10^{-4}	2.271×10^{-4}
13	5488	4.074×10^{-4}	2.889×10^{-4}
14	7980	5.227×10^{-4}	3.662×10^{-4}
15	11605	6.662×10^{-4}	4.598×10^{-4}
16	16877	8.390×10^{-4}	5.695×10^{-4}

Multiplicative Factors to Convert From Actual Counts Within an Energy Band to Directional Number Flux at the Center Energy of that Band

TED S/N 012 Electron Detector System

Energy band	Band center energy (eV)	0º electron sensor to convert counts to particles m^{-2} sec^{-1} eV^{-1} $ster^{-1}$	30º electron sensor to convert counts to particles m^{-2} sec^{-1} eV^{-1} $ster^{-1}$
1	61	6.416×10^{6}	8.332×10^{6}
2	89	4.725×10^{6}	6.111×10^{6}
3	130	3.295×10^{6}	4.325×10^{6}
4	189	2.327×10^{6}	3.022×10^{6}
5	274	1.617×10^{6}	2.096×10^{6}
6	399	1.119×10^{6}	1.459×10^{6}
7	580	7.781×10^{5}	1.014×10^{6}
8	844	5.350×10^{5}	6.951×10^{5}
9	1227	7.105×10^{5}	8.999×10^{5}
10	1784	5.429×10^{5}	6.724×10^{5}
11	2595	4.147×10^{5}	5.022×10^{5}
12	3774	3.157×10^{5}	3.738×10^{5}
13	5488	2.407×10^{5}	2.787×10^{5}
14	7980	1.834×10^{5}	2.077×10^{5}
15	11605	1.393×10^{5}	1.542×10^{5}
16	16877	1.054×10^{5}	1.141×10^{5}

TED S/N 012 Proton Detector System

Energy band	Band center energy (eV)	0º proton sensor to convert counts to particles m^{-2} sec^{-1} eV^{-1} $ster^{-1}$	30º proton sensor to convert counts to particles m^{-2} sec^{-1} eV^{-1} $ster^{-1}$
1	61	4.130×10^{6}	3.926×10^{6}
2	89	2.826×10^{6}	2.767×10^{6}
3	130	1.854×10^{6}	1.906×10^{6}
4	189	1.206×10^{6}	1.290×10^{6}
5	274	7.890×10^{5}	8.693×10^{5}
6	399	5.036×10^{5}	5.824×10^{5}
7	580	3.260×10^{5}	3.902×10^{5}
8	844	2.078×10^{5}	2.605×10^{5}
9	1227	1.647×10^{6}	1.224×10^{6}
10	1784	1.006×10^{6}	7.392×10^{5}
11	2595	6.150×10^{5}	4.460×10^{5}
12	3774	3.742×10^{5}	2.690×10^{5}
13	5488	2.286×10^{5}	1.623×10^{5}
14	7980	1.394×10^{5}	9.793×10^{4}
15	11605	8.493×10^{4}	5.898×10^{4}
16	16877	5.155×10^{4}	3.540×10^{4}

TED Serial Number 012 Sensor Data
Conversion to Integrated Directional Energy Flux Moment

Sensor	Energy range eV	To convert decompressed counts to mW m^{-2} $ster^{-1}$ multiply by
0º low-energy electron	50 - 1000	1.865×10^{-6}
30º low-energy electron	50 - 1000	2.427×10^{-6}
0º high-energy electron	1000 - 20000	6.394×10^{-5}
30º high-energy electron	1000 - 20000	7.183×10^{-5}
0º low-energy proton	50 - 1000	1.107×10^{-6}
30º low-energy proton	50 - 1000	9.042×10^{-7}
0º high-energy proton	1000 - 20000	5.191×10^{-5}
30º high-energy proton	1000 - 20000	3.634×10^{-5}

TED Serial Number 014 Sensor Data

TED Weighting Factors

0º electron low-energy band number	Particle energy weight	Detection efficiency weight	30º electron low-energy band number	Particle energy weight	Detection efficiency weight
1	1.0	1.0	1	1.0	1.0
2	1.5	1.0	2	1.5	1.0
3	2.0	1.0	3	2.0	1.0
4	3.0	1.0	4	3.0	1.0
5	4.0	1.0	5	4.0	1.0
6	6.0	1.0	6	6.0	1.0
7	8.0	1.0	7	8.0	1.0
8	12.0	1.0	8	12.0	1.0
0º electron high-energy band number	**Particle energy weight**	**Detection efficiency weight**	**30º electron high-energy band number**	**Particle energy weight**	**Detection efficiency weight**
9	1.0	1.0	9	1.0	1.0
10	1.5	1.0	10	1.5	1.0
11	3.0	1.0	11	3.0	1.0
12	4.0	1.0	12	4.0	1.0
13	8.0	0.667	13	8.0	0.667
14	16.0	0.667	14	16.0	0.667
15	24.0	0.667	15	24.0	0.667
16	48.0	0.667	16	48.0	0.667
0º proton low-energy band number	**Particle energy weight**	**Detection efficiency weight**	**30º proton low-energy band number**	**Particle energy weight**	**Detection efficiency weight**
1	1.0	1.0	1	1.0	1.0
2	1.5	1.0	2	1.5	1.0
3	2.0	1.0	3	2.0	1.0
4	2.0	1.0	4	2.0	1.0
5	3.0	1.0	5	3.0	1.0
6	4.0	1.0	6	4.0	1.0
7	6.0	1.0	7	6.0	1.0
8	8.0	1.0	8	8.0	1.0
0º proton high-energy band number	**Particle energy weight**	**Detection efficiency weight**	**30º proton high-energy band number**	**Particle energy weight**	**Detection efficiency weight**
9	3.0	1.0	9	3.0	1.0
10	4.0	1.0	10	4.0	1.0
11	4.0	1.0	11	4.0	1.0
12	6.0	1.0	12	6.0	1.0
13	8.0	0.667	13	8.0	0.667
14	12.0	0.667	14	12.0	0.667
15	12.0	0.667	15	12.0	0.667
16	16.0	0.667	16	16.0	0.667

Multiplicative Factors to Convert Actual Counts Within an Energy Band to Directional Energy Flux Contained Within that Energy Band

TED S/N 014 Electron Detector System

Energy band	Band center energy (eV)	0º electron sensor to convert counts to mW m^{-2} $ster^{-1}$	30º electron sensor to convert counts to mW m^{-2} $ster^{-1}$
1	61	2.500×10^{-6}	2.750×10^{-6}
2	89	3.863×10^{-6}	3.786×10^{-6}
3	130	5.550×10^{-6}	5.305×10^{-6}
4	189	8.142×10^{-6}	7.429×10^{-6}
5	274	1.177×10^{-5}	1.041×10^{-5}
6	399	1.671×10^{-5}	1.431×10^{-5}
7	580	2.423×10^{-5}	1.991×10^{-5}
8	844	3.457×10^{-5}	2.747×10^{-5}
9	1227	7.754×10^{-5}	6.114×10^{-5}
10	1784	1.279×10^{-4}	1.005×10^{-4}
11	2595	2.104×10^{-4}	1.646×10^{-4}
12	3774	3.448×10^{-4}	2.686×10^{-4}
13	5488	5.629×10^{-4}	4.368×10^{-4}
14	7980	9.144×10^{-4}	7.056×10^{-4}
15	11605	1.469×10^{-3}	1.128×10^{-3}
16	16877	2.327×10^{-3}	1.774×10^{-3}

TED S/N 014 Proton Detector System

Energy band	Band center energy (eV)	0º proton sensor to convert counts to mW m^{-2} $ster^{-1}$	30º proton sensor to convert counts to mW m^{-2} $ster^{-1}$
1	61	1.698×10^{-6}	2.657×10^{-6}
2	89	2.212×10^{-6}	3.334×10^{-6}
3	130	3.033×10^{-6}	4.405×10^{-6}
4	189	4.093×10^{-6}	5.726×10^{-6}
5	274	5.573×10^{-6}	7.511×10^{-6}
6	399	7.346×10^{-6}	9.539×10^{-6}
7	580	9.892×10^{-6}	1.238×10^{-5}
8	844	1.320×10^{-5}	1.591×10^{-5}
9	1227	2.150×10^{-4}	1.705×10^{-4}
10	1784	2.624×10^{-4}	2.076×10^{-4}
11	2595	3.200×10^{-4}	2.537×10^{-4}
12	3774	3.897×10^{-4}	3.092×10^{-4}
13	5488	4.740×10^{-4}	3.762×10^{-4}
14	7980	5.757×10^{-4}	4.557×10^{-4}
15	11605	6.947×10^{-4}	5.467×10^{-4}
16	16877	8.290×10^{-4}	6.455×10^{-4}

Multiplicative Factors to Convert From Actual Counts Within an Energy Band to Directional Number Flux at the Center Energy of that Band

TED S/N 014 Electron Detector System

Energy band	Band center energy (eV)	0º electron sensor to convert counts to particles m^{-2} sec^{-1} eV^{-1} $ster^{-1}$	30º electron sensor to convert counts to particles m^{-2} sec^{-1} eV^{-1} $ster^{-1}$
1	61	1.103×10^{7}	1.213×10^{7}
2	89	7.993×10^{6}	7.833×10^{6}
3	130	5.483×10^{6}	5.242×10^{6}
4	189	3.809×10^{6}	3.477×10^{6}
5	274	2.603×10^{6}	2.301×10^{6}
6	399	1.773×10^{6}	1.519×10^{6}
7	580	1.213×10^{6}	9.969×10^{5}
8	844	8.202×10^{5}	6.521×10^{5}
9	1227	8.685×10^{5}	6.847×10^{5}
10	1784	6.803×10^{5}	5.345×10^{5}
11	2595	5.307×10^{5}	4.152×10^{5}
12	3774	4.139×10^{5}	3.225×10^{5}
13	5488	3.229×10^{5}	2.507×10^{5}
14	7980	2.518×10^{5}	1.946×10^{5}
15	11605	1.957×10^{5}	1.506×10^{5}
16	16877	1.514×10^{5}	1.160×10^{5}

TED S/N 014 Proton Detector System

Energy band	Band center energy (eV)	0º proton sensor to convert counts to particles m^{-2} sec^{-1} eV^{-1} $ster^{-1}$	30º proton sensor to convert counts to particles m^{-2} sec^{-1} eV^{-1} $ster^{-1}$
1	61	7.492×10^{6}	1.172×10^{7}
2	89	4.578×10^{6}	6.902×10^{6}
3	130	2.998×10^{6}	4.354×10^{6}
4	189	1.916×10^{6}	2.681×10^{6}
5	274	1.233×10^{6}	1.663×10^{6}
6	399	7.800×10^{5}	1.013×10^{6}
7	580	4.995×10^{5}	6.203×10^{5}
8	844	3.134×10^{5}	3.780×10^{5}
9	1227	2.410×10^{6}	1.912×10^{6}
10	1784	1.391×10^{6}	1.101×10^{6}
11	2595	7.998×10^{5}	6.345×10^{5}
12	3774	4.597×10^{5}	3.655×10^{5}
13	5488	2.644×10^{5}	2.107×10^{5}
14	7980	1.521×10^{5}	1.215×10^{5}
15	11605	8.741×10^{4}	6.999×10^{4}
16	16877	5.005×10^{4}	4.015×10^{4}

TED Serial Number 014 Sensor Data
Conversion to Integrated Directional Energy Flux Moment

Sensor	Energy range eV	To convert decompressed counts to mW m^{-2} $ster^{-1}$ multiply by
0º low-energy electron	50 - 1000	2.899×10^{-6}
30º low-energy electron	50 - 1000	2.370×10^{-6}
0º high-energy electron	1000 - 20000	8.846×10^{-5}
30º high-energy electron	1000 - 20000	6.826×10^{-5}
0º low-energy proton	50 - 1000	1.684×10^{-6}
30º low-energy proton	50 - 1000	2.088×10^{-6}
0º high-energy proton	1000 - 20000	7.865×10^{-5}
30º high-energy proton	1000 - 20000	6.287×10^{-5}

TED Serial Number 015 Sensor Data

TED Weighting Factors

0º electron low-energy band number	Particle energy weight	Detection efficiency weight	30º electron low-energy band number	Particle energy weight	Detection efficiency weight
1	1.0	1.0	1	1.0	1.0
2	1.5	1.0	2	1.5	1.0
3	2.0	1.0	3	2.0	1.0
4	3.0	1.0	4	3.0	1.0
5	4.0	1.0	5	4.0	1.0
6	6.0	1.0	6	6.0	1.0
7	8.0	1.0	7	8.0	1.0
8	12.0	1.0	8	12.0	1.0
0º electron high-energy band number	**Particle energy weight**	**Detection efficiency weight**	**30º electron high-energy band number**	**Particle energy weight**	**Detection efficiency weight**
9	1.0	1.0	9	1.0	1.0
10	1.5	1.0	10	1.5	1.0
11	3.0	1.0	11	3.0	1.0
12	4.0	1.0	12	4.0	1.0
13	8.0	1.0	13	8.0	0.667
14	16.0	1.0	14	16.0	0.667
15	24.0	1.0	15	24.0	0.667
16	48.0	1.0	16	48.0	0.667
0º proton low-energy band number	**Particle energy weight**	**Detection efficiency weight**	**30º proton low-energy band number**	**Particle energy weight**	**Detection efficiency weight**
1	1.0	1.0	1	1.0	1.0
2	1.5	1.0	2	1.5	1.0
3	2.0	1.0	3	2.0	1.0
4	2.0	1.0	4	2.0	1.0
5	3.0	1.0	5	3.0	1.0
6	4.0	1.0	6	4.0	1.0
7	6.0	1.0	7	6.0	1.0
8	8.0	1.0	8	8.0	1.0
0º proton high-energy band number	**Particle energy weight**	**Detection efficiency weight**	**30º proton high-energy band number**	**Particle energy weight**	**Detection efficiency weight**
9	3.0	1.0	9	3.0	1.0
10	4.0	1.0	10	4.0	1.0
11	4.0	1.0	11	4.0	1.0
12	6.0	1.0	12	6.0	1.0
13	8.0	0.667	13	8.0	0.667
14	12.0	0.667	14	12.0	0.667
15	12.0	0.667	15	12.0	0.667
16	16.0	0.667	16	16.0	0.667

Multiplicative Factors to Convert Actual Counts Within an Energy Band to Directional Energy Flux Contained Within that Energy Band

TED S/N 015 Electron Detector System

Energy band	Band center energy (eV)	0º electron sensor to convert counts to mW m^{-2} $ster^{-1}$	30º electron sensor to convert counts to mW m^{-2} $ster^{-1}$
1	61	1.560×10^{-6}	2.386×10^{-6}
2	89	3.895×10^{-6}	3.445×10^{-6}
3	130	5.662×10^{-6}	4.761×10^{-6}
4	189	8.088×10^{-6}	6.620×10^{-6}
5	274	1.175×10^{-5}	9.103×10^{-6}
6	399	1.658×10^{-5}	1.241×10^{-5}
7	580	2.367×10^{-5}	1.170×10^{-5}
8	844	3.371×10^{-5}	2.339×10^{-5}
9	1227	7.770×10^{-5}	5.833×10^{-5}
10	1784	1.309×10^{-4}	9.674×10^{-5}
11	2595	2.199×10^{-4}	1.608×10^{-4}
12	3774	3.676×10^{-4}	2.656×10^{-4}
13	5488	6.131×10^{-4}	4.375×10^{-4}
14	7980	1.018×10^{-3}	7.161×10^{-4}
15	11605	1.674×10^{-3}	1.160×10^{-3}
16	16877	2.712×10^{-3}	1.849×10^{-3}

TED S/N 015 Proton Detector System

Energy band	Band center energy (eV)	0º proton sensor to convert counts to mW m^{-2} $ster^{-1}$	30º proton sensor to convert counts to mW m^{-2} $ster^{-1}$
1	61	1.421×10^{-6}	3.426×10^{-6}
2	89	1.910×10^{-6}	4.477×10^{-6}
3	130	2.642×10^{-6}	5.804×10^{-6}
4	189	3.635×10^{-6}	7.510×10^{-6}
5	274	4.967×10^{-6}	9.689×10^{-6}
6	399	6.744×10^{-6}	1.229×10^{-5}
7	580	9.179×10^{-6}	1.548×10^{-5}
8	844	1.245×10^{-5}	2.017×10^{-5}
9	1227	1.946×10^{-4}	1.556×10^{-4}
10	1784	2.369×10^{-4}	1.912×10^{-4}
11	2595	2.900×10^{-4}	2.360×10^{-4}
12	3774	3.536×10^{-4}	2.900×10^{-4}
13	5488	4.309×10^{-4}	3.559×10^{-4}
14	7980	5.425×10^{-4}	4.345×10^{-4}
15	11605	6.341×10^{-4}	5.253×10^{-4}
16	16877	7.590×10^{-4}	6.250×10^{-4}

Multiplicative Factors to Convert From Actual Counts Within an Energy Band to Directional Number Flux at the Center Energy of that Band

TED S/N 015 Electron Detector System

Energy band	Band center energy (eV)	0º electron sensor to convert counts to particles m^{-2} sec^{-1} eV^{-1} $ster^{-1}$	30º electron sensor to convert counts to particles m^{-2} sec^{-1} eV^{-1} $ster^{-1}$
1	61	1.129×10^{7}	1.053×10^{7}
2	89	8.061×10^{6}	7.129×10^{6}
3	130	5.595×10^{6}	4.705×10^{6}
4	189	3.785×10^{6}	3.097×10^{6}
5	274	2.599×10^{6}	2.014×10^{6}
6	399	1.760×10^{6}	1.318×10^{6}
7	580	1.185×10^{6}	8.561×10^{5}
8	844	8.001×10^{5}	5.553×10^{5}
9	1227	8.720×10^{5}	6.532×10^{5}
10	1784	6.958×10^{5}	5.144×10^{5}
11	2595	5.548×10^{5}	4.057×10^{5}
12	3774	4.416×10^{5}	3.191×10^{5}
13	5488	3.519×10^{5}	2.512×10^{5}
14	7980	2.803×10^{5}	1.976×10^{5}
15	11605	2.225×10^{5}	1.550×10^{5}
16	16877	1.758×10^{5}	1.210×10^{5}

TED S/N 015 Proton Detector System

Energy band	Band center energy (eV)	0º proton sensor to convert counts to particles m^{-2} sec^{-1} eV^{-1} $ster^{-1}$	30º proton sensor to convert counts to particles m^{-2} sec^{-1} eV^{-1} $ster^{-1}$
1	61	6.268×10^{6}	1.511×10^{7}
2	89	3.952×10^{6}	9.266×10^{6}
3	130	2.611×10^{6}	5.737×10^{6}
4	189	1.701×10^{6}	3.516×10^{6}
5	274	1.099×10^{6}	2.145×10^{6}
6	399	7.161×10^{5}	1.305×10^{6}
7	580	4.597×10^{5}	7.942×10^{5}
8	844	2.955×10^{5}	4.793×10^{5}
9	1227	2.181×10^{6}	1.744×10^{6}
10	1784	1.255×10^{6}	1.014×10^{6}
11	2595	7.247×10^{5}	5.906×10^{5}
12	3774	4.170×10^{5}	3.430×10^{5}
13	5488	2.403×10^{5}	1.995×10^{5}
14	7980	1.386×10^{5}	1.161×10^{5}
15	11605	7.976×10^{4}	6.741×10^{4}
16	16877	4.576×10^{4}	3.901×10^{4}

TED Serial Number 015 Sensor Data
Conversion to Integrated Directional Energy Flux Moment

Sensor	Energy range eV	To convert decompressed counts to mW m^{-2} $ster^{-1}$ multiply by
0º low-energy electron	50 - 1000	2.841×10^{-6}
30º low-energy electron	50 - 1000	2.032×10^{-6}
0º high-energy electron	1000 - 20000	7.020×10^{-5}
30º high-energy electron	1000 - 20000	6.963×10^{-5}
0º low-energy proton	50 - 1000	1.568×10^{-6}
30º low-energy proton	50 - 1000	2.664×10^{-6}
0º high-energy proton	1000 - 20000	7.167×10^{-5}
30º high-energy proton	1000 - 20000	6.017×10^{-5}

TED Serial Number 016 Sensor Data

TED Weighting Factors

0º electron low-energy band number	Particle energy weight	Detection efficiency weight	30º electron low-energy band number	Particle energy weight	Detection efficiency weight
1	1.0	1.0	1	1.0	1.0
2	1.5	1.0	2	1.5	1.0
3	2.0	1.0	3	2.0	1.0
4	3.0	1.0	4	3.0	1.0
5	4.0	1.0	5	4.0	1.0
6	6.0	1.0	6	6.0	1.0
7	8.0	1.0	7	8.0	1.0
8	12.0	1.0	8	12.0	1.0
0º electron high-energy band number	**Particle energy weight**	**Detection efficiency weight**	**30º electron high-energy band number**	**Particle energy weight**	**Detection efficiency weight**
9	1.0	1.0	9	1.0	1.0
10	1.5	1.0	10	1.5	1.0
11	3.0	1.0	11	3.0	1.0
12	4.0	1.0	12	4.0	1.0
13	8.0	0.667	13	8.0	0.667
14	16.0	0.667	14	16.0	0.667
15	24.0	0.667	15	24.0	0.667
16	48.0	0.667	16	48.0	0.667
0º proton low-energy band number	**Particle energy weight**	**Detection efficiency weight**	**30º proton low-energy band number**	**Particle energy weight**	**Detection efficiency weight**
1	1.0	1.0	1	1.0	1.0
2	1.5	1.0	2	1.5	1.0
3	2.0	1.0	3	2.0	1.0
4	2.0	1.0	4	2.0	1.0
5	3.0	1.0	5	3.0	0.667
6	4.0	1.0	6	4.0	0.667
7	6.0	1.0	7	6.0	0.667
8	8.0	1.0	8	8.0	0.667
0º proton high-energy band number	**Particle energy weight**	**Detection efficiency weight**	**30º proton high-energy band number**	**Particle energy weight**	**Detection efficiency weight**
9	3.0	1.0	9	3.0	1.0
10	4.0	1.0	10	4.0	1.0
11	4.0	1.0	11	4.0	1.0
12	6.0	1.0	12	6.0	1.0
13	8.0	1.0	13	8.0	1.0
14	12.0	1.0	14	12.0	1.0
15	12.0	1.0	15	12.0	1.0
16	16.0	1.0	16	16.0	1.0

Multiplicative Factors to Convert Actual Counts Within an Energy Band to Directional Energy Flux Contained Within that Energy Band

TED S/N 016 Electron Detector System

Energy band	Band center energy (eV)	0º electron sensor to convert counts to mW m^{-2} $ster^{-1}$	30º electron sensor to convert counts to mW m^{-2} $ster^{-1}$
1	61	2.029×10^{-6}	2.642×10^{-6}
2	89	3.032×10^{-6}	3.762×10^{-6}
3	130	4.516×10^{-6}	5.127×10^{-6}
4	189	6.642×10^{-6}	7.030×10^{-6}
5	274	9.722×10^{-6}	9.531×10^{-6}
6	399	1.404×10^{-5}	1.282×10^{-5}
7	580	2.064×10^{-5}	1.741×10^{-5}
8	844	2.991×10^{-5}	2.349×10^{-5}
9	1227	7.233×10^{-5}	7.145×10^{-5}
10	1784	1.190×10^{-4}	1.161×10^{-4}
11	2595	1.963×10^{-4}	1.881×10^{-4}
12	3774	3.223×10^{-4}	3.037×10^{-4}
13	5488	5.276×10^{-4}	4.886×10^{-4}
14	7980	8.587×10^{-4}	7.821×10^{-4}
15	11605	1.383×10^{-3}	1.239×10^{-3}
16	16877	2.192×10^{-3}	1.932×10^{-3}

TED S/N 016 Proton Detector System

Energy band	Band center energy (eV)	0º proton sensor to convert counts to mW m^{-2} $ster^{-1}$	30º proton sensor to convert counts to mW m^{-2} $ster^{-1}$
1	61	1.494×10^{-6}	2.854×10^{-6}
2	89	1.904×10^{-6}	3.627×10^{-6}
3	130	2.500×10^{-6}	4.479×10^{-6}
4	189	3.257×10^{-6}	5.586×10^{-6}
5	274	4.218×10^{-6}	6.856×10^{-6}
6	399	5.387×10^{-6}	8.334×10^{-6}
7	580	6.953×10^{-6}	1.032×10^{-5}
8	844	8.910×10^{-6}	1.266×10^{-5}
9	1227	1.333×10^{-4}	1.118×10^{-4}
10	1784	1.716×10^{-4}	1.422×10^{-4}
11	2595	2.209×10^{-4}	1.815×10^{-4}
12	3774	2.846×10^{-4}	2.310×10^{-4}
13	5488	3.653×10^{-4}	2.935×10^{-4}
14	7980	4.678×10^{-4}	3.712×10^{-4}
15	11605	5.948×10^{-4}	4.464×10^{-4}
16	16877	7.478×10^{-4}	5.725×10^{-4}

Multiplicative Factors to Convert From Actual Counts Within an Energy Band to Directional Number Flux at the Center Energy of that Band

TED S/N 016 Electron Detector System

Energy band	Band center energy (eV)	0º electron sensor to convert counts to particles m^{-2} sec^{-1} eV^{-1} $ster^{-1}$	30º electron sensor to convert counts to particles m^{-2} sec^{-1} eV^{-1} $ster^{-1}$
1	61	8.951×10^{6}	1.166×10^{7}
2	89	6.273×10^{6}	7.786×10^{6}
3	130	4.461×10^{6}	5.067×10^{6}
4	189	3.107×10^{6}	3.289×10^{6}
5	274	2.149×10^{6}	2.109×10^{6}
6	399	1.490×10^{6}	1.361×10^{6}
7	580	1.033×10^{6}	8.718×10^{5}
8	844	7.096×10^{5}	5.577×10^{5}
9	1227	8.102×10^{5}	8.003×10^{5}
10	1784	6.330×10^{5}	6.174×10^{5}
11	2595	4.952×10^{5}	4.744×10^{5}
12	3774	3.870×10^{5}	3.642×10^{5}
13	5488	3.027×10^{5}	2.800×10^{5}
14	7980	2.366×10^{5}	2.150×10^{5}
15	11605	1.844×10^{5}	1.646×10^{5}
16	16877	1.430×10^{5}	1.255×10^{5}

TED S/N 016 Proton Detector System

Energy band	Band center energy (eV)	0º proton sensor to convert counts to particles m^{-2} sec^{-1} eV^{-1} $ster^{-1}$	30º proton sensor to convert counts to particles m^{-2} sec^{-1} eV^{-1} $ster^{-1}$
1	61	6.589×10^{6}	1.259×10^{7}
2	89	3.940×10^{6}	7.512×10^{6}
3	130	2.472×10^{6}	4.428×10^{6}
4	189	1.525×10^{6}	2.617×10^{6}
5	274	9.336×10^{5}	1.518×10^{6}
6	399	5.723×10^{5}	8.859×10^{5}
7	580	3.485×10^{5}	5.176×10^{5}
8	844	2.117×10^{5}	3.009×10^{5}
9	1227	1.494×10^{6}	1.254×10^{6}
10	1784	9.101×10^{5}	7.545×10^{5}
11	2595	5.529×10^{5}	4.547×10^{5}
12	3774	3.368×10^{5}	2.737×10^{5}
13	5488	2.047×10^{5}	1.650×10^{5}
14	7980	1.246×10^{5}	9.949×10^{4}
15	11605	7.562×10^{4}	5.984×10^{4}
16	16877	4.575×10^{4}	3.588×10^{4}

TED Serial Number 016 Sensor Data
Conversion to Integrated Directional Energy Flux Moment

Sensor	Energy range eV	To convert decompressed counts to mW m^{-2} $ster^{-1}$ multiply by
0º low-energy electron	50 - 1000	2.477×10^{-6}
30º low-energy electron	50 - 1000	2.063×10^{-6}
0º high-energy electron	1000 - 20000	8.320×10^{-5}
30º high-energy electron	1000 - 20000	7.517×10^{-5}
0º low-energy proton	50 - 1000	1.172×10^{-6}
30º low-energy proton	50 - 1000	2.551×10^{-6}
0º high-energy proton	1000 - 20000	4.632×10^{-5}
30º high-energy proton	1000 - 20000	3.690×10^{-5}

Appendix D. C Language Program to Read an Archive Record
Revised 2005-08-16

```
/*

It has been brought to our attention by a user of POES SEM-2 data that
the C language archive unpacking routine returns anomalous sensor
values during periods where there are data missing as flagged by 999.
We have examined that code and uncovered two significant
errors in the C version of the code that have existed since 2000.

Both errors involve the way the C unpacker implements missing data flags.
The first error centered around the fact that missing data flags associated
with sensor data from the second half of the 32-second archive record were
being improperly unpacked from the binary archive record.  The consequences
of that error were that TED and MEPED sensor values during periods when
data were missing were often improperly flagged with valid data being set
to -999. indicating missing data, while entries that should have been flagged
as missing data were given count values of 19988488, the highest count
value possible.

The second error also involved the implementation of missing data flags
and impacted P8 and P9 omni-directional detector data throughout an
entire 32-second archive record.  The P8 and P9 data share the same data
word in the TIROS data format and readouts alternate between the two.
In the archive record the data listing for P8 alternates between valid data
readouts and values set to 0 in the archive format while the P9 data alternates
in the same fashion but with valid readouts when the P8 value is zero. T
he existing documentation explains this and a user is expected to extract
only the appropiate entries when using P8 and P9 data.
During instances when data were missing, the C unpacker assigned the
missing data flag (-999.), in both the P8 and P9 data, to the entry appropriate
to 'no data' while the entries appropriate to valid data were given count
values of 19988488.  This count value is unphysical for P8 and P9 data.

Both these errors would have impact upon any analysis that had not
recognized these unphysical sensor count.

The FORTRAN version of the archive record unpacker did not have
either of these problems.

David S Evans <David.S.Evans@noaa.gov>

Corrected sofware (filename: unpackSem2_v2.c) is now available for distribution.
*/

/* Function: unpackSem2.c
```

unpackSem2.c returns a NOAA POES SEM2 data record from an
already opened file in packed binary format.

Calling from Fortran: It is recommended that Fortran users use the
Fortran 77 subroutine: readArcSub.f instead.

Compilation: c89 -c unpackSem2.c

Programmer: Sue Greer

Note: variables of type long are 4-byte integers, short are 2-byte integers.

*/

```
#include <stdio.h>
#include <string.h>

void open_archive(char *);
void close_archive(void);
void unpackSem2(short *);

void main (int argc, char *argv[]){

    FILE *fout;
    char arcfile[80],outfile[80];
    short iend = 0;
    short i,j,rnum;
    extern struct archive_rec {
        long cSum;
        long ihd[4][6];
        short cSumFlag;
        short major;
        short status[10];
        short qual[16];
        short minor[16];
        short mdf[16][40];
        float analog[17];
        float head[4][27];
        float ssLoc[16][2];
        float mep0[16][9];
        float mep90[16][9];
        float mepOmni[16][4];
        float ted0[16][8];
        float ted30[16][8];
        float ted0s[4][8];
        float ted30s[4][8];
```

```
        float tedback[4][2];
        float tedfx[16][7];
    } rec;

    if (argc < 3) {
        printf("Arguments: 1) Input archive file name\n");
        printf("           2) Output file name\n");
        exit(0);
    }

    strcpy(arcfile,argv[1]);
    strcpy(outfile,argv[2]);

    /* printf("Archive file = %s\n",arcfile); */

    /* Open the output file */

    if (( fout = fopen(outfile,"w"))==NULL) {
        printf("Cannot open %s -- aborting.\n",outfile);
        exit(0);
    }


    /* Open the archive file */

    open_archive(arcfile);
    rnum = 0;

 /* Daily POES archive data file has 2700 32-second records
if
    it has a complete day */

 while((rnum < 3000) && (iend == 0)){

    unpackSem2(&iend);

    if(iend == 0) {

    fprintf(fout,"ihd:\n");
    for(i=0; i<4; i++) {
        fprintf(fout,"%d %d %4d %3d %8ld %4d %5d\n",
           i,rec.ihd[i][0],rec.ihd[i][1],rec.ihd[i][2],
           rec.ihd[i][3],rec.ihd[i][4],rec.ihd[i][5]);

    }
    fprintf(fout,"ssLoc:\n");
    for(i=0; i<16; i++) {
```

```
        fprintf(fout,"%d %6.2f
%6.2f\n",i,rec.ssLoc[i][0],rec.ssLoc[i][1]);
    }

    fprintf(fout,"status:\n");
    for(i=0; i<10; i++) fprintf(fout,"%4d ",rec.status[i]);
    fprintf(fout,"\n");
    fprintf(fout,"qual:\n");
    for(i=0; i<16; i++) fprintf(fout,"%3d ",rec.qual[i]);
    fprintf(fout,"\n");
    fprintf(fout,"minor:\n");
    for(i=0; i<16; i++) fprintf(fout,"%4d ",rec.minor[i]);
    fprintf(fout,"\n");
    fprintf(fout,"mdf:\n");
    for(i=0; i<40; i++) {
        fprintf(fout,"%3d ",i);
        for(j=0; j<16; j++)
            fprintf(fout,"%2d ",rec.mdf[j][i]);
        fprintf(fout,"\n");
    }
    fprintf(fout,"analog:\n");
    for(i=0; i<8; i++) fprintf(fout,"%8.2f ",rec.analog[i]);
    fprintf(fout,"\n");
    for(i=8; i<16; i++) fprintf(fout,"%8.2f
",rec.analog[i]);
    fprintf(fout,"\n");
    fprintf(fout,"head:\n");
    for(j=0; j<27; j++)
        fprintf(fout,"%3d %10.2f %10.2f %10.2f %10.2f\n",
            j,rec.head[0][j],rec.head[1][j],rec.head[2][j],
            rec.head[3][j]);

    fprintf(fout,"mep0:\n");
    for(j=0; j<16; j++) {
        fprintf(fout,"%2d ",j);
        for(i=0; i<9; i++) fprintf(fout,"%8.2f
",rec.mep0[j][i]);
        fprintf(fout,"\n");
    }
    fprintf(fout,"mep90:\n");
    for(j=0; j<16; j++) {
        fprintf(fout,"%2d ",j);
        for(i=0; i<9; i++) fprintf(fout,"%8.2f
",rec.mep90[j][i]);
        fprintf(fout,"\n");
    }
    fprintf(fout,"mepOmni:\n");
```

```
    for(j=0; j<16; j++) {
        fprintf(fout,"%2d %10.2f %10.2f %10.2f %10.2f\n",
            j,rec.mepOmni[j][0],rec.mepOmni[j][1],
            rec.mepOmni[j][2],rec.mepOmni[j][3]);
    }

    fprintf(fout,"ted0:\n");
    for(j=0; j<16; j++) {
        fprintf(fout,"%2d ",j);
        for(i=0; i<8; i++) fprintf(fout,"%8.2f
",rec.ted0[j][i]);
        fprintf(fout,"\n");
    }
    fprintf(fout,"ted30:\n");
    for(j=0; j<16; j++) {
        fprintf(fout,"%2d ",j);
        for(i=0; i<8; i++) fprintf(fout,"%8.2f
",rec.ted30[j][i]);
        fprintf(fout,"\n");
    }

    fprintf(fout,"ted0s:\n");
    for(j=0; j<4; j++) {
        fprintf(fout,"%2d ",j);
        for(i=0; i<8; i++) fprintf(fout,"%8.2f
",rec.ted0s[j][i]);
        fprintf(fout,"\n");
    }
    fprintf(fout,"ted30s:\n");
    for(j=0; j<4; j++) {
        fprintf(fout,"%2d ",j);
        for(i=0; i<8; i++) fprintf(fout,"%8.2f
",rec.ted30s[j][i]);
        fprintf(fout,"\n");
    }
    fprintf(fout,"tedback:\n");
    for(j=0; j<4; j++) {
        fprintf(fout,"%2d ",j);
        for(i=0; i<2; i++) fprintf(fout,"%8.2f
",rec.tedback[j][i]);
        fprintf(fout,"\n");
    }
     fprintf(fout,"tedfx:\n");
    for(j=0; j<16; j++) {
        fprintf(fout,"%2d ",j);
        for(i=0; i<7; i++) fprintf(fout,"%8.2f
",rec.tedfx[j][i]);
```

```
        fprintf(fout,"\n");
    }


fprintf(fout,"=========================================\n");
    rnum = rnum+1;

    } /* End if */

} /* End do */
    printf("Records read: %d\n",rnum--);
    close_archive();
    close(fout);
    printf("Done\n");

}




/* Function: unpackSem2.c

    unpackSem2.c returns a NOAA POES SEM2 data record from
an
                already opened file in packed binary format.

    Calling from Fortran:  It is recommended that Fortran
users use the
                           Fortran 77 subroutine:
readArcSub.f instead.

    Compilation: c89 -c unpackSem2.c

    Programmer:  Sue Greer

    Note: variables of type long are 4-byte integers, short
are 2-byte
          integers.

*/

#include <stdio.h>
#include <string.h>
#include <sys/types.h>
#include <netinet/in.h>

static FILE *fp;
```

```
struct archive_rec {
    long cSum;
    long ihd[4][6];
    short cSumFlag;
    short major;
    short status[10];
    short qual[16];
    short minor[16];
    short mdf[16][40];
    float analog[17];
    float head[4][27];
    float ssLoc[16][2];
    float mep0[16][9];
    float mep90[16][9];
    float mepOmni[16][4];
    float ted0[16][8];
    float ted30[16][8];
    float ted0s[4][8];
    float ted30s[4][8];
    float tedback[4][2];
    float tedfx[16][7];
} rec;

void unpackSem2 (short *IEND) {

    extern FILE *fp;
    unsigned char arc[2544];
    long i,j,jj,k,m,n,mf,mo,mp0,mp90,qf,tf;
    long b1,b2,b3;
    float cf = .0001;
    float cnvrt[] = {
  0.0,1.0,2.0,3.0,4.0,5.0,6.0,7.0,8.0,9.0,10.0,11.0,
12.0,13.0,14.0,15.0,16.0,17.0,18.0,19.0,20.0,21.0,22.0,23.0,
24.0,25.0,
26.0,27.0,28.0,29.0,30.0,31.0,32.0,34.5,36.5,38.5,40.5,42.5,
44.5,
46.5,48.5,50.5,53.0,56.0,59.0,62.0,65.5,69.5,73.5,77.5,81.5,
85.5,
89.5,93.5,97.5,101.5,106.5,112.5,118.5,124.5,131.5,139.5,147
.5,155.5,
163.5,171.5,179.5,187.5,195.5,203.5,213.5,225.5,237.5,249.5,
263.5,
279.5,295.5,311.5,327.5,343.5,359.5,375.5,391.5,407.5,427.5,
451.5,
475.5,499.5,527.5,559.5,591.5,623.5,655.5,687.5,719.5,751.5,
783.5,
```

```
815.5,855.5,903.5,951.5,999.5,1055.5,1119.5,1183.5,1247.5,13
11.5,
1375.5,1439.5,1503.5,1567.5,1631.5,1711.5,1807.5,1903.5,1999
.5,2111.5,
2239.5,2367.5,2495.5,2623.5,2751.5,2879.5,3007.5,3135.5,3263
.5,3423.5,
3615.5,3807.5,3999.5,4223.5,4479.5,4735.5,4991.5,5247.5,5503
.5,5759.5,
6015.5,6271.5,6527.5,6847.5,7231.5,7615.5,7999.5,8447.5,8959
.5,9471.5,
9983.5,10495.5,11007.5,11519.5,12031.5,12543.5,13055.5,13695
.5,14463.5,
15231.5,15999.5,16895.5,17919.5,18943.5,19967.5,20991.5,2201
5.5,23039.5,
24063.5,25087.5,26111.5,27391.5,28927.5,30463.5,31999.5,3379
1.5,35839.5,
37887.5,39935.5,41983.5,44031.5,46079.5,48127.5,50175.5,5222
3.5,54783.5,
57855.5,60927.5,63999.5,67583.5,71679.5,75775.5,79871.5,8396
7.5,88063.5,
92159.5,96255.5,100351.5,104447.5,109567.5,115711.5,121855.5
,127999.5,
135167.5,143359.5,151551.5,159743.5,167935.5,176127.5,184319
.5,192511.5,
200703.5,208895.5,219135.5,231423.5,243711.5,255999.5,270335
.5,286719.5,
303103.5,319487.5,335871.5,352255.5,368639.5,385023.5,401407
.5,417791.5,
438271.5,462847.5,487423.5,511999.5,540671.5,573439.5,606207
.5,638975.5,
671743.5,704511.5,737279.5,770047.5,802815.5,835583.5,876543
.5,925695.5,
974847.5,1023999.5,1081343.5,1146879.5,1212415.5,1277951.5,1
343487.5,
1409023.5,1474559.5,1540095.5,1605631.5,1671167.5,1753087.5,
1851391.5,
    1949695.5,1998848.0
    };

    b1 = 256*256*256;
    b2 = 256*256;
    b3 = 256;

    fread(arc, sizeof(unsigned char),2544,fp);
    if(feof(fp)) {
        printf("End of file\n");
        *IEND = 1;
```

```
    }
    if(ferror(fp)) {
        printf("File read error\n");
        *IEND = 2;
    }

    /* A 32-second record was read, now unpack it*/

    /*for(i=0; i<215; i++)
        printf ("%d = %d\n",i,arc[i]); */

    /* Checksum flag */
    rec.cSumFlag = arc[0]*b1 + arc[1]*b2 + arc[2]*b3 +
arc[3];
    /* Checksum */
    rec.cSum = arc[4]*b1 + arc[5]*b2 + arc[6]*b3 + arc[7];
    /* Major Frame Number */
    rec.major = arc[8]*b3 + arc[9];
    /* Status: instrument on/off, etc. */
    for(i=0; i<10; i++) rec.status[i] = arc[i+10];
    /* Analog data, etc. */
    for(i=0; i<68; i+=4) {
        k = (i+1)/4;
        rec.analog[k] = (arc[i+20]*b1 + arc[i+21]*b2 +
arc[i+22]*b3
            + arc[i+23])*cf;
    }

    /* Sub-satellite location */

    rec.ssLoc[0][0] = (arc[88]*b1 + arc[89]*b2 + arc[90]*b3
+
                       arc[91]) * cf;
    rec.ssLoc[1][0] = (arc[92]*b1 + arc[93]*b2 + arc[94]*b3
+
                       arc[95]) * cf;
    rec.ssLoc[2][0] = (arc[96]*b1 + arc[97]*b2 + arc[98]*b3
+
                       arc[99]) * cf;
    rec.ssLoc[3][0] = (arc[100]*b1 + arc[101]*b2 +
arc[102]*b3 +
                       arc[103]) * cf;
    rec.ssLoc[0][1] = (arc[104]*b1 + arc[105]*b2 +
arc[106]*b3 +
                       arc[107]) * cf;
    rec.ssLoc[1][1] = (arc[108]*b1 + arc[109]*b2 +
arc[110]*b3 +
```

```
                        arc[111]) * cf;
    rec.ssLoc[2][1] = (arc[112]*b1 + arc[113]*b2 +
arc[114]*b3 +
                        arc[115]) * cf;
    rec.ssLoc[3][1] = (arc[116]*b1 + arc[117]*b2 +
arc[118]*b3 +
                        arc[119]) * cf;
    rec.ssLoc[4][0] = (arc[120]*b1 + arc[121]*b2 +
arc[122]*b3 +
                        arc[123]) * cf;
    rec.ssLoc[5][0] = (arc[124]*b1 + arc[125]*b2 +
arc[126]*b3 +
                        arc[127]) * cf;
    rec.ssLoc[6][0] = (arc[128]*b1 + arc[129]*b2 +
arc[130]*b3 +
                        arc[131]) * cf;
    rec.ssLoc[7][0] = (arc[132]*b1 + arc[133]*b2 +
arc[134]*b3 +
                        arc[135]) * cf;
    rec.ssLoc[4][1] = (arc[136]*b1 + arc[137]*b2 +
arc[138]*b3 +
                        arc[139]) * cf;
    rec.ssLoc[5][1] = (arc[140]*b1 + arc[141]*b2 +
arc[142]*b3 +
                        arc[143]) * cf;
    rec.ssLoc[6][1] = (arc[144]*b1 + arc[145]*b2 +
arc[146]*b3 +
                        arc[147]) * cf;
    rec.ssLoc[7][1] = (arc[148]*b1 + arc[149]*b2 +
arc[150]*b3 +
                        arc[151]) * cf;
    rec.ssLoc[8][0] = (arc[152]*b1 + arc[153]*b2 +
arc[154]*b3 +
                        arc[155]) * cf;
    rec.ssLoc[9][0] = (arc[156]*b1 + arc[157]*b2 +
arc[158]*b3 +
                        arc[159]) * cf;
    rec.ssLoc[10][0] = (arc[160]*b1 + arc[161]*b2 +
arc[162]*b3 +
                        arc[163]) * cf;
    rec.ssLoc[11][0] = (arc[164]*b1 + arc[165]*b2 +
arc[166]*b3 +
                        arc[167]) * cf;
    rec.ssLoc[8][1] = (arc[168]*b1 + arc[169]*b2 +
arc[170]*b3 +
                        arc[171]) * cf;
```

```
    rec.ssLoc[9][1] = (arc[172]*b1 + arc[173]*b2 +
arc[174]*b3 +
                      arc[175]) * cf;
    rec.ssLoc[10][1] = (arc[176]*b1 + arc[177]*b2 +
arc[178]*b3 +
                      arc[179]) * cf;
    rec.ssLoc[11][1] = (arc[180]*b1 + arc[181]*b2 +
arc[182]*b3 +
                      arc[183]) * cf;
    rec.ssLoc[12][0] = (arc[184]*b1 + arc[185]*b2 +
arc[186]*b3 +
                      arc[187]) * cf;
    rec.ssLoc[13][0] = (arc[188]*b1 + arc[189]*b2 +
arc[190]*b3 +
                      arc[191]) * cf;
    rec.ssLoc[14][0] = (arc[192]*b1 + arc[193]*b2 +
arc[194]*b3 +
                      arc[195]) * cf;
    rec.ssLoc[15][0] = (arc[196]*b1 + arc[197]*b2 +
arc[198]*b3 +
                      arc[199]) * cf;
    rec.ssLoc[12][1] = (arc[200]*b1 + arc[201]*b2 +
arc[202]*b3 +
                      arc[203]) * cf;
    rec.ssLoc[13][1] = (arc[204]*b1 + arc[205]*b2 +
arc[206]*b3 +
                      arc[207]) * cf;
    rec.ssLoc[14][1] = (arc[208]*b1 + arc[209]*b2 +
arc[210]*b3 +
                      arc[211]) * cf;
    rec.ssLoc[15][1] = (arc[212]*b1 + arc[213]*b2 +
arc[214]*b3 +
                      arc[215]) * cf;

    /* Header information */

    rec.head[0][1] = rec.ssLoc[0][0];
    rec.head[1][1] = rec.ssLoc[4][0];
    rec.head[2][1] = rec.ssLoc[8][0];
    rec.head[3][1] = rec.ssLoc[12][0];
    rec.head[0][2] = rec.ssLoc[0][1];
    rec.head[1][2] = rec.ssLoc[4][1];
    rec.head[2][2] = rec.ssLoc[8][1];
    rec.head[3][2] = rec.ssLoc[12][1];

    for(j=0; j<4; j++) {
        m = 2;
```

```
        i = 1640+j*96;
        for(k = 3;k<96; k+=4){
            m++;
            rec.head[j][m] = (arc[i+1+k-4]*b1 + arc[i+2+k-
4]*b2
                + arc[i+3+k-4]*b3 + arc[i+4+k-4]) * cf;
        }
    }


/*=====================================================*/
    /* Each 32-second record contains four 8-second records
*/

/*=====================================================*/

    j = 0;    /* Index for 8-sec records */
    /* --- ihd info, 4-byte integers, ihd[j][0..4] --- */
    for(i=0; i<20; i+=4) {
        k = (i+1)/4;
        rec.ihd[j][k] = arc[i+216]*b1 + arc[i+217]*b2
                + arc[i+218]*b3 + arc[i+219];
    }
    /* --- Satellite orbital inclination, head[j][0] --- */
    rec.head[j][0] = (arc[236]*b1 + arc[237]*b2 +
arc[238]*b3 +
        arc[239])*cf/10.;
    /* --- Orbit number, ihd[j][5] --- */
    rec.ihd[j][5] = arc[240]*b1 + arc[241]*b2 + arc[242]*b3
+
        arc[243];
    /* --- Quality flag, 2-byte integer, qual[0..3] --- */
    qf = 0;
    for(i=0; i<7; i+=2){
        rec.qual[qf] = arc[i+244]*b3 + arc[i+245];
        qf++;
    }
    /* --- Minor frame numbers, 2-byte integer, minor[0..3]
--- */
    mf = 0;
    for(i=0; i<7; i+=2){
        rec.minor[mf] = arc[i+252]*b3 + arc[i+253];
        mf++;
    }
    /* --- Missing data flags, 1-byte integer,
mdf[0..3][0..39] --- */
    for(i=0; i<4; i++) {
```

```
        for(n=0; n<39; n++) {
            rec.mdf[i][n] = arc[n+40*i+260];
        }
    }

    j = 1;    /* Index for 8-sec records */
    /* --- ihd info, 4-byte integers, ihd[j][0..4] --- */
    for(i=0; i<20; i+=4) {
        k = (i+1)/4;
        rec.ihd[j][k] = arc[i+420]*b1 + arc[i+421]*b2
                + arc[i+422]*b3 + arc[i+423];
    }
    /* --- Satellite orbital inclination, head[j][0] --- */
    rec.head[j][0] = (arc[440]*b1 + arc[441]*b2 +
arc[442]*b3 +
        arc[443])*cf/10.;
    /* --- Orbit number, ihd[j][5] --- */
    rec.ihd[j][5] = arc[444]*b1 + arc[445]*b2 + arc[446]*b3
+
        arc[447];
    /* --- Quality flag, 2-byte integer, qual[4..7] --- */
    for(i=0; i<7; i+=2){
        rec.qual[qf] = arc[i+448]*b3 + arc[i+449];
        qf++;
    }
    /* --- Minor frame numbers, 2-byte integer, minor[4..7]
--- */
    for(i=0; i<7; i+=2){
        rec.minor[mf] = arc[i+456]*b3 + arc[i+457];
        mf++;
    }
    /* --- Missing data flags, 1-byte integer,
mdf[4..7][0..39] --- */
    for(i=4; i<8; i++) {
        for(n=0; n<39; n++) {
            rec.mdf[i][n] = arc[n+40*(i-4)+464];
        }
    }

    j = 2;    /* Index for 8-sec records */
    /* --- ihd info, 4-byte integers, ihd[j][0..4] --- */
    for(i=0; i<20; i+=4) {
        k = (i+1)/4;
        rec.ihd[j][k] = arc[i+624]*b1 + arc[i+625]*b2
                + arc[i+626]*b3 + arc[i+627];
    }
    /* --- Satellite orbital inclination, head[j][0] --- */
```

```
    rec.head[j][0] = (arc[644]*b1 + arc[645]*b2 +
arc[646]*b3 +
        arc[647])*cf/10.;
    /* --- Orbit number, ihd[j][5] --- */
    rec.ihd[j][5] = arc[648]*b1 + arc[649]*b2 + arc[650]*b3
+
        arc[651];
    /* --- Quality flag, 2-byte integer, qual[8..11] --- */
    for(i=0; i<7; i+=2){
        rec.qual[qf] = arc[i+652]*b3 + arc[i+652];
        qf++;
    }
    /* --- Minor frame numbers, 2-byte integer, minor[8..11]
--- */
    for(i=0; i<7; i+=2){
        rec.minor[mf] = arc[i+660]*b3 + arc[i+661];
        mf++;
    }
    /* --- Missing data flags, 1-byte integer,
mdf[8..11][0..39] --- */
    for(i=8; i<12; i++) {
        for(n=0; n<39; n++) {
            rec.mdf[i][n] = arc[n+40*(i-8)+668];
        }
    }

    j = 3;    /* Index for 8-sec records */
    /* --- ihd info, 4-byte integers, ihd[j][0..4] --- */
    for(i=0; i<20; i+=4) {
        k = (i+1)/4;
        rec.ihd[j][k] = arc[i+828]*b1 + arc[i+829]*b2
                + arc[i+830]*b3 + arc[i+831];
    }
    /* --- Satellite orbital inclination, head[j][0] --- */
    rec.head[j][0] = (arc[848]*b1 + arc[849]*b2 +
arc[850]*b3 +
        arc[851])*cf/10.;
    /* --- Orbit number, ihd[j][5] --- */
    rec.ihd[j][5] = arc[852]*b1 + arc[853]*b2 + arc[854]*b3
+
        arc[855];
    /* --- Quality flag, 2-byte integer, qual[12..15] --- */
    for(i=0; i<7; i+=2){
        rec.qual[qf] = arc[i+856]*b3 + arc[i+857];
        qf++;
    }
```

```
    /* --- Minor frame numbers, 2-byte integer,
minor[12..15] --- */
    for(i=0; i<7; i+=2){
        rec.minor[mf] = arc[i+864]*b3 + arc[i+865];
        mf++;
    }
    /* --- Missing data flags, 1-byte integer,
mdf[12..15][0..39] --- */
    for(i=12; i<16; i++) {
        for(n=0; n<39; n++) {
            rec.mdf[i][n] = arc[n+40*(i-12)+872];
        }
    }

    /*-----------------------------------------------------*/
    /*                  MEPED Sensor Data                  */
    /*-----------------------------------------------------*/

    j = mp0 = mp90 = mo = 0;

    /* MEPED 0-deg telescope mep0[0..3][0..8]  */
    for(i=0; i<4; i++) {
        jj = j*4+i;
        for(k=0; k<9; k++) {
            if(rec.mdf[jj][k+1] == 1) {
                rec.mep0[jj][k] = -999.;
            } else {
                rec.mep0[jj][k] = cnvrt[arc[mp0+1032]];
            }
            mp0++;
        }
    }
    /* MEPED 90-deg telescope mep0[0..3][0..8]  */
    for(i=0; i<4; i++) {
        jj = j*4+i;
        for(k=0; k<9; k++) {
            if(rec.mdf[jj][k+10] == 1) {
                rec.mep90[jj][k] = -999.;
            } else {
                rec.mep90[jj][k] = cnvrt[arc[mp90+1068]];
            }
            mp90++;
        }
    }
    /* MEPED Omnidirectional [0..3][0..3]  */
    for(i=0; i<4; i++) {
        jj = j*4+i;
```

```
    for(k=0; k<4; k++) {
        rec.mepOmni[jj][k] = cnvrt[arc[mo+1104]];
        mo++;
    }
    if(rec.mdf[jj][19] == 1) rec.mepOmni[jj][0] = -999.;
    if(rec.mdf[jj][20] == 1) rec.mepOmni[jj][1] = -999.;
    if((jj % 2 == 1) && (rec.mdf[jj][21] == 1))
        rec.mepOmni[jj][3] = -999.;
    if((jj % 2 == 0) && (rec.mdf[jj][21] == 1))
        rec.mepOmni[jj][2] = -999.;
}

j = 1;
mp0 = mp90 = mo = 0;
/* MEPED 0-deg telescope mep0[4..7][0..8]  */
for(i=0; i<4; i++) {
    jj = j*4+i;
    for(k=0; k<9; k++) {
        if(rec.mdf[jj][k+1] == 1) {
            rec.mep0[jj][k] = -999.;
        } else {
            rec.mep0[jj][k] = cnvrt[arc[mp0+1184]];
        }
        mp0++;
    }
}
/* MEPED 90-deg telescope mep0[4..7][0..8]  */
for(i=0; i<4; i++) {
    jj = j*4+i;
    for(k=0; k<9; k++) {
        if(rec.mdf[jj][k+10] == 1) {
            rec.mep90[jj][k] = -999.;
        } else {
            rec.mep90[jj][k] = cnvrt[arc[mp90+1220]];
        }
        mp90++;
    }
}
/* MEPED Omnidirectional [4..7][0..3]  */
for(i=0; i<4; i++) {
    jj = j*4+i;
    for(k=0; k<4; k++) {
        rec.mepOmni[jj][k] = cnvrt[arc[mo+1256]];
        mo++;
    }
    if(rec.mdf[jj][19] == 1) rec.mepOmni[jj][0] = -999.;
    if(rec.mdf[jj][20] == 1) rec.mepOmni[jj][1] = -999.;
```

```
    if((jj % 2 == 1) && (rec.mdf[jj][21] == 1))
        rec.mepOmni[jj][3] = -999.;
    if((jj % 2 == 0) && (rec.mdf[jj][21] == 1))
        rec.mepOmni[jj][2] = -999.;
}

j = 2;
mp0 = mp90 = mo = 0;
/* MEPED 0-deg telescope mep0[8..11][0..8]  */
for(i=0; i<4; i++) {
    jj = j*4+i;
    for(k=0; k<9; k++) {
        if(rec.mdf[jj][k+1] == 1) {
            rec.mep0[jj][k] = -999.;
        } else {
            rec.mep0[jj][k] = cnvrt[arc[mp0+1336]];
        }
        mp0++;
    }
}
/* MEPED 90-deg telescope mep0[8..11][0..8]  */
for(i=0; i<4; i++) {
    jj = j*4+i;
    for(k=0; k<9; k++) {
        if(rec.mdf[jj][k+10] == 1) {
            rec.mep90[jj][k] = -999.;
        } else {
            rec.mep90[jj][k] = cnvrt[arc[mp90+1372]];
        }
        mp90++;
    }
}
/* MEPED Omnidirectional [8..11][0..3]  */
for(i=0; i<4; i++) {
    jj = j*4+i;
    for(k=0; k<4; k++) {
        rec.mepOmni[jj][k] = cnvrt[arc[mo+1408]];
        mo++;
    }
    if(rec.mdf[jj][19] == 1) rec.mepOmni[jj][0] = -999.;
    if(rec.mdf[jj][20] == 1) rec.mepOmni[jj][1] = -999.;
    if((jj % 2 == 1) && (rec.mdf[jj][21] == 1))
        rec.mepOmni[jj][3] = -999.;
    if((jj % 2 == 0) && (rec.mdf[jj][21] == 1))
        rec.mepOmni[jj][2] = -999.;
}
```

```
j = 3;
mp0 = mp90 = mo = 0;
/* MEPED 0-deg telescope mep0[12..15][0..8]  */
for(i=0; i<4; i++) {
    jj = j*4+i;
    for(k=0; k<9; k++) {
        if(rec.mdf[jj][k+1] == 1) {
            rec.mep0[jj][k] = -999.;
        } else {
            rec.mep0[jj][k] = cnvrt[arc[mp0+1488]];
        }
        mp0++;
    }
}
/* MEPED 90-deg telescope mep0[12..15][0..8]  */
for(i=0; i<4; i++) {
    jj = j*4+i;
    for(k=0; k<9; k++) {
        if(rec.mdf[jj][k+10] == 1) {
            rec.mep90[jj][k] = -999.;
        } else {
            rec.mep90[jj][k] = cnvrt[arc[mp90+1524]];
        }
        mp90++;
    }
}
/* MEPED Omnidirectional [12..15][0..3]  */
for(i=0; i<4; i++) {
    jj = j*4+i;
    for(k=0; k<4; k++) {
        rec.mepOmni[jj][k] = cnvrt[arc[mo+1560]];
        mo++;
    }
    if(rec.mdf[jj][19] == 1) rec.mepOmni[jj][0] = -999.;
    if(rec.mdf[jj][20] == 1) rec.mepOmni[jj][1] = -999.;
    if((jj % 2 == 1) && (rec.mdf[jj][21] == 1))
        rec.mepOmni[jj][3] = -999.;
    if((jj % 2 == 0) && (rec.mdf[jj][21] == 1))
        rec.mepOmni[jj][2] = -999.;
}

/*-------------------------------------------------*/
/*     TED uncalibrated energy flux, max channel     */
/*          response, and max channel                */
/*-------------------------------------------------*/

/* TED 0-deg and 30-deg uncalibrated energy flux */
```

```
for(k=0; k<4; k++) {
    for(i=0; i<4; i++) {
        j = k*4 + i;    /* 0..15 */
        rec.ted0[j][0] = cnvrt[arc[1120+i*4+k*152]];
        if(rec.mdf[j][26] == 1) rec.ted0[j][0] = -999.;
        rec.ted0[j][1] = cnvrt[arc[1121+i*4+k*152]];
        if(rec.mdf[j][28] == 1) rec.ted0[j][1] = -999.;
        rec.ted0[j][2] = cnvrt[arc[1122+i*4+k*152]];
        if(rec.mdf[j][30] == 1) rec.ted0[j][2] = -999.;
        rec.ted0[j][3] = cnvrt[arc[1123+i*4+k*152]];
        if(rec.mdf[j][32] == 1) rec.ted0[j][3] = -999.;
        rec.ted0[j][4] = arc[1136+i*4+k*152];
        rec.ted0[j][5] = arc[1137+i*4+k*152];
        if(rec.mdf[j][34] == 1) {
            rec.ted0[j][4] = -999.;
            rec.ted0[j][5] = -999.;
        }
        rec.ted0[j][6] = cnvrt[arc[1138+i*4+k*152]];
        if(rec.mdf[j][35] == 1) rec.ted0[j][6] = -999.;
        rec.ted0[j][7] = cnvrt[arc[1139+i*4+k*152]];
        if(rec.mdf[j][36] == 1) rec.ted0[j][7] = -999.;

        rec.ted30[j][0] = cnvrt[arc[1152+i*4+k*152]];
        if(rec.mdf[j][27] == 1) rec.ted30[j][0] = -999.;
        rec.ted30[j][1] = cnvrt[arc[1153+i*4+k*152]];
        if(rec.mdf[j][29] == 1) rec.ted30[j][1] = -999.;
        rec.ted30[j][2] = cnvrt[arc[1154+i*4+k*152]];
        if(rec.mdf[j][31] == 1) rec.ted30[j][2] = -999.;
        rec.ted30[j][3] = cnvrt[arc[1155+i*4+k*152]];
        if(rec.mdf[j][33] == 1) rec.ted30[j][3] = -999.;
        rec.ted30[j][4] = arc[1168+i*4+k*152];
        rec.ted30[j][5] = arc[1169+i*4+k*152];
        if(rec.mdf[j][34] == 1) {
            rec.ted30[j][4] = -999.;
            rec.ted30[j][5] = -999.;
        }
        rec.ted30[j][6] = cnvrt[arc[1170+i*4+k*152]];
        if(rec.mdf[j][35] == 1) rec.ted30[j][6] = -999.;
        rec.ted30[j][7] = cnvrt[arc[1171+i*4+k*152]];
        if(rec.mdf[j][36] == 1) rec.ted30[j][7] = -999.;
    }
}

/*-----------------------------------------------------*/
/*          TED spectra and background                 */
/*-----------------------------------------------------*/
```

```
for(j=0; j<4; j++) {
    for(i=0; i<8; i++) {
        rec.ted0s[j][i] = cnvrt[arc[i+j*8+2024]];
        rec.ted30s[j][i] = cnvrt[arc[i+j*8+2060]];
    }
    rec.tedback[j][0] = cnvrt[arc[j+2056]];
    rec.tedback[j][1] = cnvrt[arc[j+2092]];
}
for(j=0; j<16; j++) {
    if(j==0 || j==4 || j==8 || j==12) {
        for(i=0; i<4; i++) {
            if(rec.mdf[j][i+22] == 1) {
                for(k=0; k<4; k++) {
                    rec.ted0s[k][i] = -999.;
                }
            }
        }
    }
    if(j==2 || j==6 || j==10) {
        for(i=4; i<8; i++) {
            if(rec.mdf[j][i+18] == 1) {
                for(k=0; k<4; k++) {
                    rec.ted0s[k][i] = -999.;
                }
            }
        }
    }
    if(j==1 || j==5 || j==9 || j==13) {
        for(i=0; i<4; i++) {
            if(rec.mdf[j][i+22] == 1) {
                for(k=0; k<4; k++) {
                    rec.ted30s[k][i] = -999.;
                }
            }
        }
    }
    if(j==3 || j==7 || j==11) {
        for(i=4; i<8; i++) {
            if(rec.mdf[j][i+18] == 1) {
                for(k=0; k<4; k++) {
                    rec.ted30s[k][i] = -999.;
                }
            }
        }
    }
    if(j == 14) {
```

```
            if(rec.mdf[j][0] == 1) rec.tedback[0][0] = -
999.;
            if(rec.mdf[j][22] == 1) rec.tedback[1][0] = -
999.;
            if(rec.mdf[j][25] == 1) rec.tedback[2][0] = -
999.;
            if(rec.mdf[j][24] == 1) rec.tedback[3][0] = -
999.;
            if(rec.mdf[j][23] == 1) rec.tedback[1][1] = -
999.;
        }
        if(j == 15) {
            if(rec.mdf[j][0] == 1) rec.tedback[0][1] = -
999.;
            if(rec.mdf[j][25] == 1) rec.tedback[2][1] = -
999.;
            if(rec.mdf[j][23] == 1) rec.tedback[3][1] = -
999.;
        }
    }

    /*-----------------------------------------------------*/
    /*                    TED flux                         */
    /*-----------------------------------------------------*/
    tf = 0;
    for(i=0; i<4; i++) {
        for(n=0; n<7; n++) {
            for(j=0; j<4; j++) {
                k = i*4+j;
                rec.tedfx[k][n] = (arc[tf+2096]*b1 +
                    arc[tf+2097]*b2 + arc[tf+2098]*b3 +
                    arc[tf+2099]) * cf;
                tf+=4;
            }
        }
    }

} /* End of unpackSem2 */

void open_archive(char *filename) {
    extern FILE *fp;
    short i;
    size_t len;
    len = strlen(filename);

     /* printf("In open: archive file = *%s*\n",filename);
*/
```

```
    for (i=0; i<=len; i++) {
        if (filename[i] == ' ') {
            filename[i] = '\0';
            break;
        }
    }

    if((fp = fopen(filename, "rb")) == NULL) {
        printf("Cannot open packed archive file
%s.\n",filename);
        fclose(fp);
        exit(1);
    } else {
        printf("Opened packed archive file %s.\n",filename);
    }

}

void close_archive(void) {
    extern FILE *fp;
    fclose(fp);
}
```

Appendix E. FORTRAN Language Program To Read an Archive Record

```
program testRead(arcfile,outfile)

      ! The program takes two arguments, specifying the
input
      ! filename and the output filename (including paths.)
      ! The output file is written in the current working
directory
      ! unless a path is included as part of the filename.

      integer*2 j
      integer*4 rec,eof,hr,min,sec
      character*80 arcfile,outfile

      ! Common block /rec/ variables:
      integer*4 cSum,ihd(6,4)
      integer*2
cSumFlag,major,status(10),qual(16),minor(16),mdf(40,16)
      real*4
analog(17),head(27,4),ssLoc(2,16),mep0(9,16),mep90(9,16),
     +
mepOmni(4,16),ted0(8,16),ted30(8,16),ted0s(8,4),ted30s(8,4),
     +    tedback(2,4),tedfx(7,16)

      common /rec/cSum,ihd,cSumFlag,major,status,qual,minor,
     +
mdf,analog,head,ssLoc,mep0,mep90,mepOmni,ted0,ted30,
     +    ted0s,ted30s,tedback,tedfx

      eof = 0
      open(unit=7,access='direct',recl=2544,file =
arcfile,status='old')
      open(unit=11,access='sequential',file = outfile,
     +     status='unknown',form='formatted')

      do rec = 1,3
          call readArcSub(7,rec,eof)
          if(eof.eq.1) goto 100
          do j=1,4
              hr = ihd(4,j)/3600000
              min = (ihd(4,j) - hr*3600000)/60000
              sec = (ihd(4,j) - hr*3600000 - min*60000)/1000
              write(11,200),ihd(2,j),ihd(3,j),hr,min,sec,
     +                  head(2,j),head(3,j),ihd(6,j)
          enddo
          write(11,300)"mep0:"
```

```
          do j=1,16

write(11,220)j,mep0(1,j),mep0(2,j),mep0(3,j),mep0(4,j),
     +
mep0(5,j),mep0(6,j),mep0(7,j),mep0(8,j),mep0(9,j)
          enddo
          write(11,300)"mep90:"
          do j=1,16

write(11,220)j,mep90(1,j),mep90(2,j),mep90(3,j),
     +
mep90(4,j),mep90(5,j),mep90(6,j),mep90(7,j),mep90(8,j),
     +          mep90(9,j)
          enddo
          write(11,300)"mepOmni:"
          do j=1,16

write(11,220)j,mepOmni(1,j),mepOmni(2,j),mepOmni(3,j),
     +       mepOmni(4,j)
          enddo
          write(11,300)"ted0:"
          do j=1,16

write(11,220)j,ted0(1,j),ted0(2,j),ted0(3,j),ted0(4,j),
     +          ted0(5,j),ted0(6,j),ted0(7,j),ted0(8,j)
          enddo
          write(11,300)"ted30:"
          do j=1,16

write(11,220)j,ted30(1,j),ted30(2,j),ted30(3,j),
     +          ted30(4,j),ted30(5,j),ted30(6,j),ted30(7,j),
     +          ted30(8,j)
          enddo
          write(11,300)"ted0s:"
          do j=1,4

write(11,220)j,ted0s(1,j),ted0s(2,j),ted0s(3,j),
     +
ted0s(4,j),ted0s(5,j),ted0s(6,j),ted0s(7,j),ted0s(8,j)
          enddo
          write(11,300)"ted30s:"
          do j=1,4

write(11,220)j,ted30s(1,j),ted30s(2,j),ted30s(3,j),
     +
ted30s(4,j),ted30s(5,j),ted30s(6,j),ted30s(7,j),
     +          ted30s(8,j)
```

```
          enddo
          write(11,300)"tedback:"
          do j=1,4
              write(11,220)j,tedback(1,j),tedback(2,j)
          enddo
          write(11,300)"tedfx:"
          do j=1,16

write(11,220)j,tedfx(1,j),tedfx(2,j),tedfx(3,j),
     +           tedfx(4,j),tedfx(5,j),tedfx(6,j),tedfx(7,j)
          enddo

          write(11,300)"-----------------------------------
----------"

       enddo

  200 format(i4,1x,i3,3(1x,i2),1x,f8.3,1x,f8.3,1x,i7)
  220 format(i4,9(1x,f8.2))
  300 format(A)
  100 close(7)
      close(11)
      end


subroutine readArcSub (unit,rnum,eof)

      ! ------------------------------------------------
-------
      !   readArcSub.f returns a NOAA POES SEM2 data record
from an
      !               already opened file in packed binary
format.
      !
      !   Calling from C:  It is recommended that C users
use the
      !                    C routine: unpackSem2.c instead.
      !
      !   Compilation: f77 -c readArcSub.f
      !
      !
      !   Programmer:  Sue Greer
      !
      ! ------------------------------------------------
-------
      byte arcBytes(2544)
      integer*4 unit,rnum,eof,ios
```

```
      integer*4 arc(2544),i,j,jj,k,m,mf,mo,mp0,mp90,qf,tf
      integer*4 b1,b2,b3,b4
      integer*2 onebyte
      real*4 cf ! Conversion factor (.0001)
      real*4 cnvrt(256)

      ! Common block /rec/ variables:
      integer*4 cSum,ihd(6,4)
      integer*2
cSumFlag,major,status(10),qual(16),minor(16),mdf(40,16)
      real*4
analog(17),head(27,4),ssLoc(2,16),mep0(9,16),mep90(9,16),
     +
mepOmni(4,16),ted0(8,16),ted30(8,16),ted0s(8,4),ted30s(8,4),
     +    tedback(2,4),tedfx(7,16)

      common /rec/cSum,ihd,cSumFlag,major,status,qual,minor,
     +
mdf,analog,head,ssLoc,mep0,mep90,mepOmni,ted0,ted30,
     +    ted0s,ted30s,tedback,tedfx

      cf = 0.0001
      b1=256*256*256
      b2=256*256
      b3=256
      b4=1

      data cnvrt
/0.0,1.0,2.0,3.0,4.0,5.0,6.0,7.0,8.0,9.0,10.0,11.0,

+12.0,13.0,14.0,15.0,16.0,17.0,18.0,19.0,20.0,21.0,22.0,23.0
,24.0,

+25.0,26.0,27.0,28.0,29.0,30.0,31.0,32.0,34.5,36.5,38.5,40.5
,42.5,

+44.5,46.5,48.5,50.5,53.0,56.0,59.0,62.0,65.5,69.5,73.5,77.5
,81.5,

+85.5,89.5,93.5,97.5,101.5,106.5,112.5,118.5,124.5,131.5,139
.5,

+147.5,155.5,163.5,171.5,179.5,187.5,195.5,203.5,213.5,225.5
,

+237.5,249.5,263.5,279.5,295.5,311.5,327.5,343.5,359.5,375.5
,
```

```
+391.5,407.5,427.5,451.5,475.5,499.5,527.5,559.5,591.5,623.5
,

+655.5,687.5,719.5,751.5,783.5,815.5,855.5,903.5,951.5,999.5
,

+1055.5,1119.5,1183.5,1247.5,1311.5,1375.5,1439.5,1503.5,156
7.5,

+1631.5,1711.5,1807.5,1903.5,1999.5,2111.5,2239.5,2367.5,249
5.5,

+2623.5,2751.5,2879.5,3007.5,3135.5,3263.5,3423.5,3615.5,380
7.5,

+3999.5,4223.5,4479.5,4735.5,4991.5,5247.5,5503.5,5759.5,601
5.5,

+6271.5,6527.5,6847.5,7231.5,7615.5,7999.5,8447.5,8959.5,947
1.5,

+9983.5,10495.5,11007.5,11519.5,12031.5,12543.5,13055.5,1369
5.5,

+14463.5,15231.5,15999.5,16895.5,17919.5,18943.5,19967.5,209
91.5,

+22015.5,23039.5,24063.5,25087.5,26111.5,27391.5,28927.5,304
63.5,

+31999.5,33791.5,35839.5,37887.5,39935.5,41983.5,44031.5,460
79.5,

+48127.5,50175.5,52223.5,54783.5,57855.5,60927.5,63999.5,675
83.5,

+71679.5,75775.5,79871.5,83967.5,88063.5,92159.5,96255.5,100
351.5,

+104447.5,109567.5,115711.5,121855.5,127999.5,135167.5,14335
9.5,

+151551.5,159743.5,167935.5,176127.5,184319.5,192511.5,20070
3.5,
```

```
+208895.5,219135.5,231423.5,243711.5,255999.5,270335.5,28671
9.5,

+303103.5,319487.5,335871.5,352255.5,368639.5,385023.5,40140
7.5,

+417791.5,438271.5,462847.5,487423.5,511999.5,540671.5,57343
9.5,

+606207.5,638975.5,671743.5,704511.5,737279.5,770047.5,80281
5.5,

+835583.5,876543.5,925695.5,974847.5,1023999.5,1081343.5,

+1146879.5,1212415.5,1277951.5,1343487.5,1409023.5,1474559.5
,

+1540095.5,1605631.5,1671167.5,1753087.5,1851391.5,1949695.5
,
     +1998848.0/

      eof = 0
      if (rnum.lt.1) goto 100

   10 read(unit,rec=rnum,iostat=ios) arcBytes
      if(ios.ne.0) then
          eof = 1
          goto 100
      endif
      do i=1,2544
          ! Byte type goes from -128 to +127
          ! Convert to 8-bit integer
          onebyte = arcBytes(i)
          arc(i) = onebyte
          if(onebyte.lt.0) arc(i) = onebyte+256
      enddo

* ------------------------------------------------------------
--------
*     ! Parse the data in arc()
* ------------------------------------------------------------
--------

      ! Checksum flag
      cSumFlag = arc(1)*b1 + arc(2)*b2 + arc(3)*b3 + arc(4)
      ! Checksum
```

```
      cSum = arc(5)*b1 + arc(6)*b2 + arc(7)*b3 + arc(8)
      ! Major frame number
      major = arc(9)*b3 + arc(10)*b4
      !print *,'cSumFlag, cSum, MF ',cSumFlag,cSum,major

      ! Status: instrument on/off, ifc, etc.
      do i = 1,10
          status(i) = arc(i+10)
          !print *,i,status(i)
      enddo

      ! Analog data, etc. 4-byte integers converted to reals

      do i = 1,68,4
          k = (i+1)/4 + 1
          analog(k) =
(arc(i+20)*b1+arc(i+21)*b2+arc(i+22)*b3+
     +         arc(i+23))*cf
          !print *,k,analog(k)
      enddo

      ! Sub-satellite location, 4-byte integers converted to
reals
      k = 1
      ssLoc(1,1) = (arc(k+88)*b1+arc(k+89)*b2+arc(k+90)*b3+
     +         arc(k+91))*cf
      ssLoc(1,2) = (arc(k+92)*b1+arc(k+93)*b2+arc(k+94)*b3+
     +         arc(k+95))*cf
      ssLoc(1,3) = (arc(k+96)*b1+arc(k+97)*b2+arc(k+98)*b3+
     +         arc(k+99))*cf
      ssLoc(1,4) =
(arc(k+100)*b1+arc(k+101)*b2+arc(k+102)*b3+
     +         arc(k+103))*cf
      ssLoc(2,1)
=(arc(k+104)*b1+arc(k+105)*b2+arc(k+106)*b3+
     +         arc(k+107))*cf
      ssLoc(2,2)
=(arc(k+108)*b1+arc(k+109)*b2+arc(k+110)*b3+
     +         arc(k+111))*cf
      ssLoc(2,3)
=(arc(k+112)*b1+arc(k+113)*b2+arc(k+114)*b3+
     +         arc(k+115))*cf
      ssLoc(2,4)
=(arc(k+116)*b1+arc(k+117)*b2+arc(k+118)*b3+
     +         arc(k+119))*cf
      ssLoc(1,5) =
(arc(k+120)*b1+arc(k+121)*b2+arc(k+122)*b3+
```

```
     +         arc(k+123))*cf
      ssLoc(1,6) =
(arc(k+124)*b1+arc(k+125)*b2+arc(k+126)*b3+
     +         arc(k+127))*cf
      ssLoc(1,7) =
(arc(k+128)*b1+arc(k+129)*b2+arc(k+130)*b3+
     +         arc(k+131))*cf
      ssLoc(1,8) =
(arc(k+132)*b1+arc(k+133)*b2+arc(k+134)*b3+
     +         arc(k+135))*cf
      ssLoc(2,5)
=(arc(k+136)*b1+arc(k+137)*b2+arc(k+138)*b3+
     +         arc(k+139))*cf
      ssLoc(2,6)
=(arc(k+140)*b1+arc(k+141)*b2+arc(k+142)*b3+
     +         arc(k+143))*cf
      ssLoc(2,7)
=(arc(k+144)*b1+arc(k+145)*b2+arc(k+146)*b3+
     +         arc(k+147))*cf
      ssLoc(2,8)
=(arc(k+148)*b1+arc(k+149)*b2+arc(k+150)*b3+
     +         arc(k+151))*cf
      ssLoc(1,9) =
(arc(k+152)*b1+arc(k+153)*b2+arc(k+154)*b3+
     +         arc(k+155))*cf
      ssLoc(1,10) =
(arc(k+156)*b1+arc(k+157)*b2+arc(k+158)*b3+
     +         arc(k+159))*cf
      ssLoc(1,11) =
(arc(k+160)*b1+arc(k+161)*b2+arc(k+162)*b3+
     +         arc(k+163))*cf
      ssLoc(1,12) =
(arc(k+164)*b1+arc(k+165)*b2+arc(k+166)*b3+
     +         arc(k+167))*cf
      ssLoc(2,9)
=(arc(k+168)*b1+arc(k+169)*b2+arc(k+170)*b3+
     +         arc(k+171))*cf
      ssLoc(2,10)
=(arc(k+172)*b1+arc(k+173)*b2+arc(k+174)*b3+
     +         arc(k+175))*cf
      ssLoc(2,11)
=(arc(k+176)*b1+arc(k+177)*b2+arc(k+178)*b3+
     +         arc(k+179))*cf
      ssLoc(2,12)
=(arc(k+180)*b1+arc(k+181)*b2+arc(k+182)*b3+
     +         arc(k+183))*cf
```

```
      ssLoc(1,13) =
(arc(k+184)*b1+arc(k+185)*b2+arc(k+186)*b3+
     +         arc(k+187))*cf
      ssLoc(1,14) =
(arc(k+188)*b1+arc(k+189)*b2+arc(k+190)*b3+
     +         arc(k+191))*cf
      ssLoc(1,15) =
(arc(k+192)*b1+arc(k+193)*b2+arc(k+194)*b3+
     +         arc(k+195))*cf
      ssLoc(1,16) =
(arc(k+196)*b1+arc(k+197)*b2+arc(k+198)*b3+
     +         arc(k+199))*cf
      ssLoc(2,13)
=(arc(k+200)*b1+arc(k+201)*b2+arc(k+202)*b3+
     +         arc(k+203))*cf
      ssLoc(2,14)
=(arc(k+204)*b1+arc(k+205)*b2+arc(k+206)*b3+
     +         arc(k+207))*cf
      ssLoc(2,15)
=(arc(k+208)*b1+arc(k+209)*b2+arc(k+210)*b3+
     +         arc(k+211))*cf
      ssLoc(2,16)
=(arc(k+212)*b1+arc(k+213)*b2+arc(k+214)*b3+
     +         arc(k+215))*cf


* -------------------------------------------------------
*      ! Header information
* -------------------------------------------------------
      ! Subsatellite latitude and longitude
      head(2,1) = ssLoc(1,1)
      head(2,2) = ssLoc(1,5)
      head(2,3) = ssLoc(1,9)
      head(2,4) = ssLoc(1,13)
      head(3,1) = ssLoc(2,1)
      head(3,2) = ssLoc(2,5)
      head(3,3) = ssLoc(2,9)
      head(3,4) = ssLoc(2,13)

      do j = 1,4
          m = 3
          i = 1640+(j-1)*96
          do k = 4,96,4
              m = m+1
              head(m,j) = (arc(i+1+k-4)*b1 + arc(i+2+k-4)*b2
+
     +            arc(i+3+k-4)*b3 + arc(i+4+k-4))*cf
```

```
          enddo
       enddo

       j = 1    ! Index for 8-second records
       ! ihd info, 4-byte integers  (1..5,1)
       do i=1,20,4
           k = (i+1)/4 +1
           ihd(k,j) =
(arc(i+216)*b1+arc(i+217)*b2+arc(i+218)*b3+
     +         arc(i+219))
       enddo
       ! Inclination (head(1,1))
       head(1,j) =  (arc(237)*b1+arc(238)*b2+arc(239)*b3+
     +         arc(240))*cf/10.
       ! Orbit number (6,1)
       ihd(6,j) = (arc(241)*b1+arc(242)*b2+arc(243)*b3+
     +         arc(244))
       ! Quality, 2-byte integer (1..4)
       qf = 1
       do i=1,7,2
           qual(qf) = arc(i+244)*b3+arc(i+245)
           qf = qf + 1
       enddo
       ! Minor frame numbers (1..4)
       mf = 1
       do i = 1,7,2
           minor(mf) = arc(i+252)*b3+arc(i+253)
           mf = mf+1
       enddo
       ! Missing data flags (1..40,1..4)
       do i = 1,4
         do n = 1,40
               mdf(n,i) = arc(n-1+40*(i-1)+261)
         enddo
       enddo

       j = 2
       ! ihd info, 4-byte integers (1..5,2)
       do i=1,20,4
           k = (i+1)/4 +1
           ihd(k,j) =
(arc(i+420)*b1+arc(i+421)*b2+arc(i+422)*b3+
     +         arc(i+423))
       enddo
       ! Inclination (head(1,2))
       head(1,j) =  (arc(441)*b1+arc(442)*b2+arc(443)*b3+
     +         arc(444))*cf/10.
```

```
       ! Orbit number  (ihd(6,2))
       ihd(6,j) = (arc(445)*b1+arc(446)*b2+arc(447)*b3+
      +         arc(448))
       ! Quality, 2-byte integer (5..8)
       do i=1,7,2
           qual(qf) = arc(i+448)*b3+arc(i+449)
           qf = qf + 1
       enddo
       ! Minor frame numbers (5..8)
       do i = 1,7,2
           minor(mf) = arc(i+456)*b3+arc(i+457)
           mf = mf+1
       enddo
       ! Missing data flags (1..40,5..8)
       do i = 5,8
           do n = 1,40
               mdf(n,i) = arc(n-1+40*(i-5)+465)
           enddo
       enddo

       j = 3
       ! ihd info, 4-byte integers (1..5,3)
       do i=1,20,4
           k = (i+1)/4 +1
           ihd(k,j) =
  (arc(i+624)*b1+arc(i+625)*b2+arc(i+626)*b3+
      +         arc(i+627))
       enddo
       ! Inclination (head(1,3))
       head(1,j) =  (arc(645)*b1+arc(646)*b2+arc(647)*b3+
      +         arc(648))*cf/10.
       ! Orbit number  (ihd(6,3))
       ihd(6,j) = (arc(649)*b1+arc(650)*b2+arc(651)*b3+
      +         arc(652))
       ! Quality, 2-byte integer (9..12)
       do i=1,7,2
           qual(qf) = arc(i+652)*b3+arc(i+653)
           qf = qf + 1
       enddo
       ! Minor frame numbers (9..12)
       do i = 1,7,2
           minor(mf) = arc(i+660)*b3+arc(i+661)
           mf = mf+1
       enddo
       ! Missing data flags (1..40,9..12)
       do i = 9,12
           do n = 1,40
```

```
              mdf(n,i) = arc(n-1+40*(i-9)+669)
            enddo
         enddo

         j = 4
         ! ihd info, 4-byte integers (1..5,4)
         do i=1,20,4
             k = (i+1)/4 +1
             ihd(k,j) =
(arc(i+828)*b1+arc(i+829)*b2+arc(i+830)*b3+
     +         arc(i+831))
         enddo
         ! Inclination (head(1,4))
         head(1,j) =  (arc(849)*b1+arc(850)*b2+arc(851)*b3+
     +         arc(852))*cf/10.
         ! Orbit number (ihd(6,4))
         ihd(6,j) = (arc(853)*b1+arc(854)*b2+arc(855)*b3+
     +         arc(856))
         ! Quality, 2-byte integer (13..16)
         do i=1,7,2
             qual(qf) = arc(i+856)*b3+arc(i+857)
             qf = qf + 1
         enddo
         ! Minor frame numbers (13..16)
         do i = 1,7,2
             minor(mf) = arc(i+864)*b3+arc(i+865)
             mf = mf+1
         enddo
         ! Missing data flags (1..40,13..16)
         do i = 13,16
             do n = 1,40
                 mdf(n,i) = arc(n-1+40*(i-13)+873)
             enddo
         enddo

* -------------------------------------------------------
*      ! MEPED sensor data
* -------------------------------------------------------
         j = 1
         mp0 = 1
         ! Meped 0-deg telescope (1..9,1..4)
         do i = 1,4
             jj = (j-1)*4+i
             do k = 1,9
                 if(mdf(k+1,jj).eq.1) then
                     mep0(k,jj) = -999.
                 else
```

```
                mep0(k,jj) = cnvrt(1+arc(mp0+1032))
            endif
            mp0 = mp0+1
        enddo
    enddo
    ! Meped 90-deg telescope (1..9,1..4)
    mp90 = 1
    do i = 1,4
        jj = (j-1)*4+i
        do k = 1,9
            if(mdf(k+10,jj).eq.1) then
                mep90(k,jj) = -999.
            else
                mep90(k,jj) = cnvrt(1+arc(mp90+1068))
            endif
            mp90 = mp90+1
        enddo
    enddo
    ! Meped omnidirectional (1..4,1..4)
    mo = 1
    do i = 1,4
        jj = (j-1)*4+i
        do k = 1,4
            mepOmni(k,jj) = cnvrt(1+arc(mo+1104))
            mo = mo+1
        enddo
        if(mdf(20,jj).eq.1) mepOmni(1,jj) = -999.
        if(mdf(21,jj).eq.1) mepOmni(2,jj) = -999.
        if(mod(jj,2).eq.1.AND.mdf(22,jj).eq.1)
mepOmni(3,jj) = -999.
        if(mod(jj,2).eq.0.AND.mdf(22,jj).eq.1)
mepOmni(4,jj) = -999.
    enddo

    j = 2
    mp0 = 1
    ! Meped 0-deg telescope (1..9,5..8)
    do i = 1,4
        jj = (j-1)*4+i
        do k = 1,9
            if(mdf(k+1,jj).eq.1) then
                mep0(k,jj) = -999.
            else
                mep0(k,jj) = cnvrt(1+arc(mp0+1184))
            endif
            mp0 = mp0+1
        enddo
```

```
      enddo
      ! Meped 90-deg telescope (1..9,5..8)
      mp90 = 1
      do i = 1,4
          jj = (j-1)*4+i
          do k = 1,9
              if(mdf(k+10,jj).eq.1) then
                  mep90(k,jj) = -999.
              else
                  mep90(k,jj) = cnvrt(1+arc(mp90+1220))
              endif
              mp90 = mp90+1
          enddo
      enddo
      ! Meped omnidirectional (1..4,5..8)
      mo = 1
      do i = 1,4
          jj = (j-1)*4+i
          do k = 1,4
              mepOmni(k,jj) = cnvrt(1+arc(mo+1256))
              mo = mo+1
          enddo
          if(mdf(20,jj).eq.1) mepOmni(1,jj) = -999.
          if(mdf(21,jj).eq.1) mepOmni(2,jj) = -999.
          if(mod(jj,2).eq.1.AND.mdf(22,jj).eq.1)
mepOmni(3,jj) = -999.
          if(mod(jj,2).eq.0.AND.mdf(22,jj).eq.1)
mepOmni(4,jj) = -999.
      enddo

      j = 3
      mp0 = 1
      ! Meped 0-deg telescope (1..9,9..12)
      do i = 1,4
          jj = (j-1)*4+i
          do k = 1,9
              if(mdf(k+1,jj).eq.1) then
                  mep0(k,jj) = -999.
              else
                  mep0(k,jj) = cnvrt(1+arc(mp0+1336))
              endif
              mp0 = mp0+1
          enddo
      enddo
      ! Meped 90-deg telescope (1..9,9..12)
      mp90 = 1
      do i = 1,4
```

```
            jj = (j-1)*4+i
            do k = 1,9
                if(mdf(k+10,jj).eq.1) then
                    mep90(k,jj) = -999.
                else
                    mep90(k,jj) = cnvrt(1+arc(mp90+1372))
                endif
                mp90 = mp90+1
            enddo
        enddo
        ! Meped omnidirectional (1..4,9..12)
        mo = 1
        do i = 1,4
            jj = (j-1)*4+i
            do k = 1,4
                mepOmni(k,jj) = cnvrt(1+arc(mo+1408))
                mo = mo+1
            enddo
            if(mdf(20,jj).eq.1) mepOmni(1,jj) = -999.
            if(mdf(21,jj).eq.1) mepOmni(2,jj) = -999.
            if(mod(jj,2).eq.1.AND.mdf(22,jj).eq.1)
mepOmni(3,jj) = -999.
            if(mod(jj,2).eq.0.AND.mdf(22,jj).eq.1)
mepOmni(4,jj) = -999.
        enddo

        j = 4
        mp0 = 1
        ! Meped 0-deg telescope (1..9,13..16)
        do i = 1,4
            jj = (j-1)*4+i
            do k = 1,9
                if(mdf(k+1,jj).eq.1) then
                    mep0(k,jj) = -999.
                else
                    mep0(k,jj) = cnvrt(1+arc(mp0+1488))
                endif
                mp0 = mp0+1
            enddo
        enddo
        ! Meped 90-deg telescope (1..9,13..16)
        mp90 = 1
        do i = 1,4
            jj = (j-1)*4+i
            do k = 1,9
                if(mdf(k+10,jj).eq.1) then
                    mep90(k,jj) = -999.
```

```
            else
                mep90(k,jj) = cnvrt(1+arc(mp90+1524))
            endif
            mp90 = mp90+1
        enddo
    enddo
    ! Meped omnidirectional (1..4,13..16)
    mo = 1
    do i = 1,4
        jj = (j-1)*4+i
        do k = 1,4
            mepOmni(k,jj) = cnvrt(1+arc(mo+1560))
            mo = mo+1
        enddo
        if(mdf(20,jj).eq.1) mepOmni(1,jj) = -999.
        if(mdf(21,jj).eq.1) mepOmni(2,jj) = -999.
        if(mod(jj,2).eq.1.AND.mdf(22,jj).eq.1)
mepOmni(3,jj) = -999.
        if(mod(jj,2).eq.0.AND.mdf(22,jj).eq.1)
mepOmni(4,jj) = -999.
    enddo

* ------------------------------------------------------
*       TED uncalibrated energy flux, max channel
*       response, and max channel
* ------------------------------------------------------

    ! TED 0-deg and 30-deg uncalibrated energy flux
    do k=1,4
        do i = 1,4
            j = (k-1)*4 + i  !(1..16)
            ted0(1,j) = cnvrt(1+arc(1121+(i-1)*4+(k-
1)*152))
            if(mdf(27,j).eq.1) ted0(1,j) = -999.
            ted0(2,j) = cnvrt(1+arc(1122+(i-1)*4+(k-
1)*152))
            if(mdf(29,j).eq.1) ted0(2,j) = -999.
            ted0(3,j) = cnvrt(1+arc(1123+(i-1)*4+(k-
1)*152))
            if(mdf(31,j).eq.1) ted0(3,j) = -999.
            ted0(4,j) = cnvrt(1+arc(1124+(i-1)*4+(k-
1)*152))
            if(mdf(33,j).eq.1) ted0(4,j) = -999.
            ted0(5,j) = 1+arc(1137+(i-1)*4+(k-1)*152)
            ted0(6,j) = 1+arc(1138+(i-1)*4+(k-1)*152)

            if(mdf(35,j).eq.1) then
```

```
                ted0(5,j) = -999.
                ted0(6,j) = -999.
            endif
            ted0(7,j) = cnvrt(1+arc(1139+(i-1)*4+(k-
1)*152))
            if(mdf(36,j).eq.1) ted0(7,j) = -999.
            ted0(8,j) = cnvrt(1+arc(1140+(i-1)*4+(k-
1)*152))
            if(mdf(37,j).eq.1) ted0(8,j) = -999.

            ted30(1,j) = cnvrt(1+arc(1153+(i-1)*4+(k-
1)*152))
            if(mdf(28,j).eq.1) ted30(1,j) = -999.
            ted30(2,j) = cnvrt(1+arc(1154+(i-1)*4+(k-
1)*152))
            if(mdf(30,j).eq.1) ted30(2,j) = -999.
            ted30(3,j) = cnvrt(1+arc(1155+(i-1)*4+(k-
1)*152))
            if(mdf(32,j).eq.1) ted30(3,j) = -999.
            ted30(4,j) = cnvrt(1+arc(1156+(i-1)*4+(k-
1)*152))
            if(mdf(34,j).eq.1) ted30(4,j) = -999.
            ted30(5,j) = 1+arc(1169+(i-1)*4+(k-1)*152)
            ted30(6,j) = 1+arc(1170+(i-1)*4+(k-1)*152)
            if(mdf(38,j).eq.1) then
                ted30(5,j) = -999.
                ted30(6,j) = -999.
            endif
            ted30(7,j) = cnvrt(1+arc(1171+(i-1)*4+(k-
1)*152))
            if(mdf(39,j).eq.1) ted30(7,j) = -999.
            ted30(8,j) = cnvrt(1+arc(1172+(i-1)*4+(k-
1)*152))
            if(mdf(40,j).eq.1) ted30(8,j) = -999.
        enddo
    enddo

* ------------------------------------------------
*     ! Ted spectra and background
* ------------------------------------------------
    do j = 1,4
        do i=1,8
            ted0s(i,j) = cnvrt(1+arc(i+(j-1)*8+2024))
            ted30s(i,j) = cnvrt(1+arc(i+(j-1)*8+2060))
        enddo
        tedback(1,j) = cnvrt(1+arc(j+2056))
        tedback(2,j) = cnvrt(1+arc(j+2092))
```

```
enddo
do j=1,16
    if(j.eq.1.OR.j.eq.5.OR.j.eq.9.OR.j.eq.13) then
        do i=1,4
            if(mdf(22+i,j).eq.1) then
                do k=1,4
                    ted0s(i,k) = -999.
                enddo
            endif
        enddo
    endif
    if(j.eq.3.OR.j.eq.7.OR.j.eq.11) then
        do i=5,8
            if(mdf(18+i,j).eq.1)then
                do k=1,4
                    ted0s(i,k) = -999.
                enddo
            endif
        enddo
    endif
    if(j.eq.2.OR.j.eq.6.OR.j.eq.10.OR.j.eq.14) then
        do i=1,4
            if(mdf(22+i,j).eq.1)then
                do k=1,4
                    ted30s(i,k) = -999.
                enddo
            endif
        enddo
    endif
    if(j.eq.4.OR.j.eq.8.OR.j.eq.12) then
        do i=5,8
            if(mdf(18+i,j).eq.1)then
                do k=1,4
                    ted30s(i,k) = -999.
                enddo
            endif
        enddo
    endif
    if(j.eq.15) then
        if(mdf(1,j).eq.1) tedback(1,1) = -999.
        if(mdf(23,j).eq.1) tedback(1,2) = -999.
        if(mdf(26,j).eq.1) tedback(1,3) = -999.
        if(mdf(25,j).eq.1) tedback(1,4) = -999.
        if(mdf(24,j).eq.1) tedback(2,2) = -999.
    endif
    if(j.eq.16) then
        if(mdf(1,j).eq.1) tedback(2,1) = -999.
```

```
              if(mdf(2,3).eq.1) tedback(2,3) = -999.
              if(mdf(24,j).eq.1) tedback(2,4) = -999.
          endif
      enddo
* ------------------------------------------------------
*      ! Ted flux
* ------------------------------------------------------
      tf = 1
      do i=1,4
          do n = 1,7
              do j = 1,4
                  k = (i-1)*4 + j
                  tedfx(n,k) = (arc(tf+2096)*b1 +
     +                          arc(tf+2097)*b2 +
     +                          arc(tf+2098)*b3 +
     +                          arc(tf+2099))*cf
                  tf = tf + 4
      !print *,n,k,tf+2096
              enddo
          enddo
      enddo
* ------------------------------------------------------
*      ! Check missing data flags
* ------------------------------------------------------

  100 continue
      return
      end
```

Appendix F

Procedures to recover energetic proton number fluxes from the Omnidirectional detector responses.

Figure F.1 shows the omnidirectional detector configuration. The detector itself is a right cylinder, 0.3 cm high with front and back surface areas of 0.5 cm^2. The diameter of the detector is 0.798 cm, the circumference of the cylinder is 2.507 cm, and the area of the cylinder side is 0.752 cm^2. The 60º reference angle refers to the half-angle subtended by the spherical shell absorbers in detectors P6 and P7.

Energetic particles may enter the front face of the solid-state detector at an angle ϑ to the central axis of the detector system and, should the Tungsten absorber surrounding the detector permit, a normal angle γ to the side of the cylinder. Particles energetic enough to penetrate the Tungsten shielding, and incident at a ϑ angle greater than 90º, may enter the solid-state detector through the back face.

For a given angular distribution of protons incident upon the detector system, the number of particles passing into the detector, which is the detector count rate, may be computed. In this way a relationship, unique to that angular distribution, can be established to relate the detector count rate to the directional number flux of protons within specific energy ranges.

The fundamental equation that relates the directional number flux of particles within a specified energy range, $J(\Phi,\vartheta)$ incident from a polar angle ϑ and an azimuthal angle Φ to the number flux through an elemental area dA on the surface of a detector is

Equation F.1 $$\text{Number flux} = J(\Phi,\vartheta)\, sin\vartheta\, cos\vartheta\, d\vartheta\, d\Phi\, dA$$

The integration of this equation over all angles Φ and ϑ and the entire surface of the detector yields the sensor count rate due to particles within the specified energy range.

The procedure to accomplish this for two specific proton angular distributions follows.

The first case is for a totally isotropic particle distribution. That is, the directional flux of protons in units of particles cm^{-2} sec^{-1} $ster^{-1}$ is constant from all directions. This proton angular distribution might be encountered at the magnetic equator in the inner radiation belt, but it is not likely to be encountered at the rather low altitude of the POES satellites.

The second case treated is for a proton angular distribution that is constant over all angles ϑ up to 105º but has zero intensity at ϑ between 105º and 180º. This proton angular distribution might be encountered by the NOAA/POES satellite at polar latitudes during energetic solar particle events. At these locations the central axis of the omnidirectional detectors is nearly parallel to the magnetic field. During such events the solar protons are often isotropic over the upper hemisphere and those protons incident downwards at ϑ angles between 75º and 90º are magnetically mirrored at altitudes below the satellite and appear as upward going protons at ϑ angles between 90º and 105º.

The analysis in both cases begins with the count rates registered by the P6, P7, P8, and P9 detectors, with the count rate determined from the telemetered count value divided by the accumulation period. These values are CR_6 CR_7, CR_8 and CR_9. The analysis is designed to return directional number fluxes within 4 energy ranges, J_6(16-35 MeV), J_7(35-70 MeV), J_8(70-140 MeV) and J_9(140-500 MeV).

Case 1. Completely Isotropic Angular Distribution

Step 1 is the calculation of the P9 sensor count rate from protons over the energy range 140 to 500 MeV. There are three parts to this calculation. The first is the contribution from protons entering the front face of the detector, the second from protons entering the side of the detector, and the third from particles entering the back face of the detector.

For a directional number flux J_9 the number of particles entering the front face of the detector is given by

Equation F.2 $$N_1 = \iiint J_9 \sin\vartheta \cos\vartheta \, d\vartheta \, d\Phi \, dA$$

Because J_9 is independent of ϑ and Φ, it may be moved outside the integral. Particles of energies greater than 140 MeV incident from all ϑ angles between 0º and 90º and from all Φ angles from 0º to 360º, reach the detector so that the integration of angle yields

Equation F.3 $$N_1 = \pi J_9 \int dA$$

The integration over the area of the detector is 0.5 cm^2 so the final contribution to the sensor count rate from particles entering the front face of the detector is

Equation F.3 $$N_1 = 0.5 \pi J_9 .$$

Since the particle population is assumed completely isotropic, the number of particles entering the detector through the back face is the same as through the front and their contribution to N_3 is

Equation F.4 $N_3 = 0.5 \pi J_9$.

Similarly, the contribution from particles entering the detector side is

Equation F.5 $N_2 = .752 \pi J_9$, and

the total number of particles entering the detector $N_1 + N_2 + N_3$, which is the count rate, is,

Equation F.6 $CR_9 = 1.752 \pi J_9 = 5.504 J_9$.

The geometric factor for the P9 detector for the case of a totally isotropic proton distribution is 5.504 cm^2 ster.

The directional number flux of protons in the energy range 140 to 500 MeV may then be calculated from the P9 sensor count rate CR_9 from

Equation F.7 $\mathbf{J_9 = 0.182\ CR_9}$ (J_9 in units of particles cm^{-2} sec^{-1} $ster^{-1}$)

Step 2 is the calculation of the P8 sensor count rate from protons over the energy range 70 to 500 MeV.

The design of the P8 omnidirectional detector is similar to the P9 in that the detector shielding is the same in all directions. Using the same procedure outlined for P9, the count rate in detector P8 due to an isotropic flux of protons over the energy range 70 to 500 MeV is

Equation F.7 $CR_8 = 5.504(J_8 + J_9)$.

The directional number flux of protons in the energy range 70 to 140 MeV may then be calculated from the P8 and P9 sensor count rates, CR_8 and CR_9 from

Equation F.8 $\mathbf{J_8 = 0.182(CR_8 - CR_9)}$ (units of particles cm^{-2} sec^{-1} $ster^{-1}$)

Step *3* is the calculation of the P7 sensor count rate from protons over the energy range 35 to 500 MeV.

The P7 detector design allows protons of energies greater than 70 MeV access to the solid-state detector from all directions, but access of protons between 35 and 70 MeV is permitted only through the hemispherical shell absorber which subtends approximately a 60º half-angle as viewed from the center of the detector. The P7 sensor count rate will have contributions, first from protons between 70 and 500 MeV entering from all directions, and second from protons between 35 and 70 MeV which enter through the dome. The latter contribution is calculated from the fundamental equation above, where the limits on the Φ integration remain 0º to 360º but the ϑ integration is now 0º to 60º. Protons entering through the dome have no access to either the sides or the back face of the detector, so using the procedure outlined above

Equation F.9 $CR_7 = 0.375\ \pi J_7 + 5.504(J_8 + J_9)$ or

Equation F.10 $CR_7 = 1.178\ J_7 + 5.504(J_8 + J_9)$.

The directional number flux of protons in the energy range 35 to 70 MeV may then be calculated from the P7 and P8 sensor count rates, CR_7 and CR_8 , from

Equation F.11 $\mathbf{J_7 = 0.849(CR_7 - CR_8)}$ (units of particles cm^{-2} sec^{-1} $ster^{-1}$)

Step 4 is the calculation of the P6 sensor count rate from protons over the energy range 16 to 500 MeV.

The design of the P6 omnidirectional detector is similar to the P7, except for the thickness and material used in the dome detector. Following the procedure outlined in step 3, the calculated P6 count rate is

Equation F.12 $CR_6 = 0.375\ \pi\ J_6 + 0.375\ \pi\ J_7 + 5.504(J_8 + J_9)$ or

Equation F.13 $CR_6 = 0.375\ \pi\ J_6 + CR_7$.

The directional number flux of protons in the energy range 16 to 35 MeV may then be calculated from the P6 and P7 sensor count rates, CR_6 and CR_7, from

Equation F.14 $\mathbf{J_6 = 0.849(CR_6 - CR_7)}$ (units of particles cm^{-2} sec^{-1} $ster^{-1}$)

Case 2. An Angular Distribution Isotropic to 105º Polar Angle and Empty Between 105º and 180º

A procedure similar to Case 1 is followed for computing particles entering the detectors through the front face of the detector. The ϑ integration for the back face of the detector is carried out only from 90º to 105º. The contribution from particles entering the side of the detector is obtained by using a full azimuthal (0º to 360º) integration for polar angles, γ, between 0º and 15º, but only a one-half azimuthal (0º to 180º) integration for polar angles between 15º and 90º to reflect the absence of particles arriving from below at angles greater than 105º.

Step 1. Following the earlier case,

Equation F.15 $N_1 = 0.5\ \pi J_9$

Equation F.16 $N_2 = 0.033\ \pi J_9$ reflecting the integration of ϑ from 90º to 105º, and

Equation F.17 $N_3 = 0.752\ \pi (0.067+0.467)\ J_9$

the first term from the 0º to 15º integration and the second the 15º to 90º integration over the angle γ.

The sum $N_1 + N_2 + N_3$, which is the count rate, is then determined by:

Equation F.18 $CR_9 = 0.934\ \pi J_9 = 2.935\ J_9$

The directional number flux of protons in the energy range 140 to 500 MeV may then be calculated from the P9 sensor count rate, CR_9, from

Equation F.19 $\mathbf{J_9 = 0.341\ CR_9}$ (units of particles cm^{-2} sec^{-1} $ster^{-1}$)

Step 2, following the above procedure, yields the directional number flux of protons in the energy range 70 to 140 MeV calculated from the P8 and P9 sensor count rates, CR_8 and CR_9, as

Equation F.20 $\mathbf{J_8 = 0.341(CR_8 - CR_9)}$ (units of particles cm^{-2} sec^{-1} $ster^{-1}$)

The expressions for J_6 and J_7 in case 2 are the same as in case 1 because the protons between 15 and 70 MeV are isotropic over the 60º angle subtended by the hemispherical shell absorber.

Equation F.21 $\mathbf{J_7 = 0.849(CR_7 - CR_8)}$ (units of particles cm^{-2} sec^{-1} $ster^{-1}$)

Equation F.22 $\mathbf{J_6 = 0.849(CR_6 - CR_7)}$ (units of particles cm^{-2} sec^{-1} $ster^{-1}$)

Similar procedures may be followed to obtain the conversion between sensor count rates and proton directional number fluxes in the four energy ranges for more complicated particle angular distributions.

It should be noted that these procedures neglect the increased shielding provided by the satellite structure and material (circuit boards, brackets, etc.) in the MEPED unit, that for some arrival angles, may increase the proton energy needed to reach the detector.

5 Appendix G

The First SEM-2 was launched on the NOAA-15 satellite on May 13, 1998. The TED unit in this SEM-2 was Serial Number 011 and the MEPED unit was Serial Number 010. Archived data from NOAA-15 are available from July 19, 1998 until the present. Both the TED and MEPED instruments on NOAA-15 are operating well, and there have been no technical difficulties.

An error in the archive processing of data from NOAA-15 was detected in late 1999. This error occurred on rare occasions when the sub-satellite geographic latitude location, either in the northern or southern hemisphere, exceeded by a small amount the maximum latitude that would have been determined from the satellite orbital inclination for that day's ephemeris. Under these circumstances, which generally lasted no more than 32 seconds at the very highest latitudes during the NOAA-15 orbit, the archive program miscalculated the pitch angles of the particles detected by the 30º TED, and the 0º and the 90º MEPED instruments. The omnidirectional energy fluxes calculated from the TED data depend upon knowledge of the particle pitch angles and during these short periods of time they will be slightly in error.

The error was corrected for all archive processing beginning on Jan 1, 2000. Prior to the correction being implemented, this error arises whenever the absolute value of the sub-satellite geographic latitude exceeds the value of the supplement of the satellite inclination. For example, if the satellite inclination in the archive record were 98.715º, the pitch angle error would occur whenever the absolute value of the sub-satellite latitude exceeded 81.285º. In these cases the correct pitch angles can be determined to within less than 1º by averaging the correct pitch angles on either side of the incorrect ones.

The second SEM-2 was successfully launched on NOAA-16 on September 21, 2000. This SEM-2 contains TED Serial Number 010 and MEPED Serial Number 011. With one exception, all SEM-2 instruments are operating properly and returning good data.

The sole exception is episodes of anomalous high background rates recorded by the 0º and 30º, TED high-energy proton sensors. This high background appears to be associated with spacecraft charging that accelerates positive ions into the electrostatic analyzers of these two sensors. Because there is a very low residue voltage between the analyzer plates during the background accumulation periods, these low energy ions pass through the analyzer and are counted by the channeltron detector. The periods of anomalous high background from these two sensors occurs when the satellite is in sunlight, not in darkness, strengthening the hypothesis that spacecraft charging is playing a role.

Fortunately, data taken from these two sensor systems during the energy sweep do not exhibit any indication of spurious counts. Both the sensor responses within specific energy bands and the integrated sensor responses, that provide the measure of the directional energy fluxes carried by ions between 1000 and 20,000 eV, are unaffected. The method for correcting sensor responses for penetrating radiation has been modified for NOAA-16 so that the corrected high-energy auroral ion energy flux values are not affected by anomalous background.

The third SEM-2 was successfully launched on NOAA-17 on June 24, 2002 and the SEM put into operation on July 12. This SEM-2 contains TED Serial Number 012 and MEPED Serial Number 012.

The NOAA-17 TED experiences the same anomalous high background rates as does the TED on NOAA-16, and for the same reason. The modification for correcting sensor responses that was implemented for the NOAA-16 TED data was used also for processing NOAA-17 data.

Beginning on November 25, 2002 the processing of NOAA SEM data to create the archive output was upgraded to new software. The new software is designed to better handle housekeeping information from these instruments and to provide better data quality control. The structure of the archive data was not affected by this upgrade and the material in this document remains valid.

Corrections included as of Version 1.2 of this document as per Dr. Dave Evans, SEC

In Appendix C. TED Sensor Data Grouped by Unit Serial Number

For TED S/N 009 Electron Detector System,
Column headed: 0º electron sensor to convert counts to mW m^{-2} $ster^{-1}$
Energy band 11, 2.003×10^{-4} REPLACES 2.033×10^{-4}

Column headed: 30º electron sensor to convert counts to mW m^{-2} $ster^{-1}$
Energy band 5, 1.365×10^{-5} REPLACES 1.365×10^{-6}

For TED S/N 010 Electron Detector System on NOAA-16
Column headed: 30º electron sensor to convert counts to mW m^{-2} $ster^{-1}$
Energy band 4, 9.243×10^{-6} REPLACES 9.234×10^{-6}

Column headed: 0º electron sensor to convert counts to
particles m^{-2} sec^{-1} eV^{-1} $ster^{-1}$
Energy band 6, 1.726×10^{6} REPLACES 1.193×10^{6}

For TED S/N 010 Proton Detector System on NOAA-16
Column headed: 30º proton sensor to convert counts to mW m^{-2} $ster^{-1}$
Energy band 16, 6.452×10^{-4} REPLACES 7.452×10^{-4}

For TED S/N 014 Electron Detector
Column headed: 0º electron sensor to convert counts to mW m^{-2} $ster^{-1}$
Energy band 1, 2.500×10^{-6} REPLACES 2.400×10^{-6}

Column headed: 30º proton sensor to convert counts to mW m^{-2} $ster^{-1}$
Energy band 6, 9.539×10^{-6} REPLACES 9.529×10^{-6}

In the main body of the text, Table 2.5.3 (page 14)
For TED S/N 011 Electron Detector System on NOAA-15
Column headed: 30º electron sensor to convert counts to
particles m^{-2} sec^{-1} eV^{-1} $ster^{-1}$
Energy band 2, 5.842×10^{6} REPLACES 5.824×10^{6}

On page 21 in the main body of the text the thickness of the Nickel foil is mistakenly given as 76 microns. The correct value is 0.76 microns. The mass thickness of 678 μg cm^{-2} is correct.

On pages 45 and 45, in the description of the archive file variables cSum and cSumFlag. Additional text has been inserted in the interest of clarification.

The material in Appendix C has been extended to include data for TED Serial Numbers 015 and 016 that are scheduled for flight on future satellites.

Appendix G has been amended to include the launch of NOAA-17.

Several misspellings and typographical errors have been corrected.

An additional errata:

In Appendix F, equation F.7 should be $CR_8=5.504(J_8+J_9)$
In keeping with the notation adopted in the discussion of Case 1, the following corrections should be made
In Appendix F, equation F.16 should be $N_3 = 0.033 \pi J_9$
In Appendix F, equation F.17 should be $N_2=.752\pi(0.067+0.467)J_9$

In the final paragraph of Appendix F the word bounds should be boards.

Corrections included as of Version 1.3 of this document as per Dr. Dave Evans, SEC

Further errata as of 15 October, 2003
In the archive document main text, Section 4.5, the material dealing with the cSumFlag should be updated to read:

cSumFlag=0,	telemetered and calculated check sums agree, no bit errors present,
cSumFlag=1,	telemetered and calculated check sums agree, bit errors likely,
cSumFlag=2,	a comparison could not be made because the necessary telemetered check sum had a missing data flag. The data in this 32-second record may be valid but should be treated with caution.
cSumFlag=3,	a comparison could not be made because a subsequent data gap meant the necessary telemetered check sum was not available. The data in this 32-second record may be valid but should be treated with caution.

Comments on Altitudes
It has been brought to our attention that the POES altitude (Table 4.2.1, element 5 in array ihd) occasionally has a zero value. In the course of SOCC processing of POES data there are instances when the satellite position cannot be located with normal precision. In those cases SOCC sets a geo-location quality flag and also sets the sub-satellite latitude, sub-satellite longitude, and satellite altitude above Earth to zero. In the course of processing to create the POES archive, those instances of zero sub-satellite latitudes and longitudes are interpolated to values that are correct to within 0.01 degree by a cubic fit to the nearby valid latitude and longitude entries. However, this fitting routine was not applied to the satellite altitude values and a zero entry was carried into the final archive record. Because the POES satellite orbits are near-circular and the satellite altitude

changes slowly during an orbit, users who are require the satellite altitude in these cases may obtain a valid altitude by linear interpolation using adjacent non-zero satellite altitude entries.

Comments on Omni-Directional Dome Sheilding

It has also been brought to our attention that there is a thermal cover over the four omni-directional (dome) detectors that are described in Section 3.4. This cover is Al and approximately 0.13 mm thick and so will have little impact on the proton energy required to reach the solid state detector. However, to compensate for that additional mass, the thickness of the four energy absorbing shells has been reduced by an equivalent mass so that the actual dimensions are slightly smaller than those given in Figures 3.4.1 and 3.4.2.

Further errata as of January 6, 2004

A minor error in the archive data processing was uncovered in early January, 2004 that had impacted 4 entries in the array status of the archive file for all SEM-2 instruments. This error was introduced beginning on November, 25, 2002 and was corrected in SEM-2 archive data beginning on Jan 6, 2004.

- The error interchanged element 5 with element 6 and interchanged element 7 with element 8 in the status array.

- Element 5 in array status is supposed to be the TED electron discriminator level (see Table 4.1.1), but during the time the error existed, element 5 was the TED proton discriminator level.

- Element 6 in array status is supposed to be the TED proton discriminator level (see Table 4.1.1), but during the time the error existed, element 6 was the TED electron discriminator level.

- The discriminator level setting on all SEM-2 TED discriminators has been at level 0 since launch, and so, fortuitously, this error has had no impact on the content of the archive files.

- Element 7 in array status is supposed to be the TED electron channeltron bias level setting (see Table 4.1.1), but during the time the error existed, element 7 was the TED proton channeltron bias level setting.

- Element 8 in array status is supposed to be the TED proton channeltron bias level setting (see Table 4.1.1), but during the time the error existed, element 8 was the TED electron channeltron bias level setting.

Corrections included as of Version 1.4 of this document as per Dr. Dave Evans, SEC

Further errata as of January 6, 2004

A minor error in the archive data processing was uncovered in early January, 2004 that had impacted 4 entries in the array status of the archive file for all SEM-2 instruments. This error was introduced beginning on November, 25, 2002 and was corrected in SEM-2 archive data beginning on Jan 6, 2004.

- The error interchanged element 5 with element 6 and interchanged element 7 with element 8 in the status array.

- Element 5 in array status is supposed to be the TED electron discriminator level (see Table 4.1.1), but during the time the error existed, element 5 was the TED proton discriminator level.

- Element 6 in array status is supposed to be the TED proton discriminator level (see Table 4.1.1), but during the time the error existed, element 6 was the TED electron discriminator level.

- The discriminator level setting on all SEM-2 TED discriminators has been at level 0 since launch, and so, fortuitously, this error has had no impact on the content of the archive files.

- Element 7 in array status is supposed to be the TED electron channeltron bias level setting (see Table 4.1.1), but during the time the error existed, element 7 was the TED proton channeltron bias level setting.

- Element 8 in array status is supposed to be the TED proton channeltron bias level setting (see Table 4.1.1), but during the time the error existed, element 8 was the TED electron channeltron bias level setting.